Université de Montréal

Hedgehog Interacting Protein (Hhip) Regulates Both Pancreatic and Renal Dysfunction in High Fat Diet-Induced Obese Mouse Model

Henry Nchienzia

Programme de Science Biomédicales
Faculté de Médecine

Thèse présentée à la faculté des études supérieures
en vue de l'obtention du grade de docteur en philosophie (Ph.D) en Science Biomédicales

Avril 2019

Université de Montréal

Hedgehog Interacting Protein (Hhip) Regulates Both Pancreatic and Renal Dysfunction in High Fat Diet-Induced Obese Mouse Model

par Henry Nchienzia

a été évaluée par un jury composé des personnes suivantes :

Dr. Ashok Srivastava

Président rapporteur

Dre. Shao-Ling Zhang

Directrice de recherche

Dr. John S. D. Chan

Codirecteur de recherche

Dre. Jennifer Estall

Membre du jury

Dr. Jun-Li Liu

Examinateur Externe

Dre. Jolanta Gutkowska

Représentante de la doyenne

Résumé

Hhip (Hedgehog interacting protein), un antagoniste de la voie de signalisation Hegehog (Hh) a était devouverte comme un antagoniste des 3 ligands Hh, soit Sonic (Shh), Indian (Ihh) et Desert (Dhh). La protéines Hhip régularise la fonction cellulaire autant par voie (Hh) canonique que non-canonique. Elle est formée de 700 acides aminés et est fortement exprimée dans les tissus riches en cellules endothéliales, comme les reins et le pancréas. Toutefois, son rôle dans le fonctionnement des cellules bêta matures soit en condition de bonne santé ou de maladie comme dans des conditions d'obésité provoquée par une diète riche en gras ainsi que son role dans les maladies chronique du rein et la dysfonction rénale. Les souris en déficience de Hhip ($Hhip^{-/-}$) ont une malformation des ilots pancréatiques (une diminution de 45% des ilots et de 40% de la prolifération des cellules beta) et un problème pulmonaire qui cause la mort post-natale.

L'objectif de notre étude initiale était de démontrer le role de Hhip dans le pancréas, en utilisant un KO corporel entier en réponse à une diète riche en gras (HFD) et la dysfonction des cellules beta in vivo et ex vivo sur des souris hétérozygotes pour Hhip ($Hhip^{+/-}$) et des souris contrôles ($Hhip^{+/+)}$

Suite à une HFD, toutefois, les souris mâles et femelles HFD-$Hhip^{+/+}$ ont développé une intolérance sévère au glucose (IPGTT) et cette intolérance a été améliorée chez les souris HFD-$Hhip^{+/-}$. Associé a cette intolérance, les males HFD-$Hhip^{+/-}$ démontraient une hyperinsulinémie et leur taux d'insuline plasmatique (phase 1 et 2), contrairement aux souris males HFD-$Hhip^{+/+}$, augmentait de façon significative. Dans les îlots de souris $Hhip^{+/+}$, l'augmentation de Hhip induite par une HFD a été observée principalement dans les cellules

bêta mais aucunement dans les cellules alpha. Sans varier le nombre total d'îlots et la quantité de cellules bêta, les souris mâles HFD-Hhip$^{+/+}$ avaient un nombre supérieur de gros îlots dans lesquels le taux d'insuline était diminué. La structure de ces îlots était désorganisée, démontrant une évidente invasion des cellules alpha au coeur des îlots bêta, le stress oxidatif (8-OHdG et NADPH oxidase 2 (Nox 2)) est aussi augmentée. En revanche, chez les souris mâles HFD-Hhip$^{+/-}$, il a été possible d'observer une augmentation du nombre de petits îlots, de la prolifération des cellules bêta, et aussi de la sécrétion d'insuline stimulée par le glucose (GSIS), une amélioration du stress oxidatif et un maintien de l'intégrité des îlots ont été démontré. In vitro, la protéine recombinante Hhip (rHhip) a accentué le stress oxidatif (Nox2 et l'activité de NADPH oxidase 2) et a causé une diminution du nombre de cellules bêta ; par contre, le siRNA-Hhip augmente le GSIS et abolit la stimulation de l'expression du gène Nox2 induite par le palmitate de sodium (PA)-BSA. Grace a ces observations, il est démontré que les genes Hhip pancréatiques inhibe la sécrétion d'insuline en altérant la structure des ilots et en favorisant l'expression du gene Nox2 dans les ilots en réponse à la dysfonction des cellules beta suite a une diète riche en gras HFD.

Le diabète engendre des risques élevés de complication tel que des problèmes chroniques des reins caractérisés par une perte graduelle des fonctions rénales. Cette situation a été récemment reliée au taux élevé d'obésité. On a aussi démontré dans notre modèle de diabète gestationnel que l'augmentation de Hhip causait des irrégularités durant la néphrogénèse des rejetons [127]. Ensuite, nos données récentes démontrent que, chez les souris adultes, l'hyperglycémie a provoqué une forte expression du gene Hhip rénales causant ainsi l'apoptose des cellules épithéliales des glomérules et la transition endothéliale à mésenchymateuse (EndoMT) - liée à fibrose rénale [128].

Dans l'étude présente, on a établi que la surexpression de Hhip dans les cellules des tubules proximaux rénaux contribuait au développement initial des problèmes chroniques des reins suite a une HFD de 14 semaines. Un gain de poids significatif a été observé chez les souris du groupe HFD comparativement aux groupes ND. Les souris du groupe HFD ont développé une intolérance au glucose mais sans changement apparent à la sensibilité à l'insuline ni à l'hypertension (pression arterielle) même si ces souris mâles avaient des légers dépôts du gras périrénal. Les fonctions rénales telle que mesurées par le taux de filtration glomérulaire restaient normales dans tous les groupes révélant ainsi que ces deux facteurs (HFD et surexpression de Hhip) n'avaient aucune influence sur l'hyperfiltration rénale. Néanmoins, la morphologie rénale a révélé que les souris du groupe HFD présentaient une lésion infraclinique et des signes de vacuolisation tubulaire et des lésions par rapport aux souris ND. Cette pathologie de lésion tubulaire et de vacuolisation était plus prononcée chez les souris transgéniques (Hhip-Tg) que chez les souris non-Tg, ce qui favorisait l'apoptose des cellules tubulaires bénignes et un stress oxydatif accru.

En conclusion, l'obésité provoquée par l'HFD a eu des effets néfastes sur la tolérance au glucose et de légères modifications morphologiques des reins, caractérisées par la présence d'une néphrose osmotique, une augmentation du stress oxydatif rénal et une apoptose pouvant être induites par une augmentation de la FABP4 rénale. Cela a été exacerbé par la surexpression de Hhip dans les tubules rénaux proximaux.

Mots-clés : Diète riche en graisses, expression du gène Hhip, dysfonctionnement des cellules bêta, problèmes chroniques des reins

Abstract

Hedgehog interacting protein (Hhip), a signaling molecule in the Hedgehog Hh pathway, was originally discovered as a putative antagonist of all 3 secreted Hh ligands, i.e., Sonic (Shh), Indian (Ihh), and Desert (Dhh). Hhip regulates cell function via either canonical- or non-canonical Hh pathway. Hhip encodes a protein of 700 amino acids, and is abundantly expressed in vascular endothelial cell-rich tissues, including the pancreas, and kidneys. To date, less is known about Hhip's expression pattern in mature islet cells, and its function under normal and/or disease conditions, such as diet induced-obesity, as well as its role in chronic kidney disease, and kidney dysfunction. Hhip null mice ($Hhip^{-/-}$) display markedly impaired pancreatic islet formation (45% reduction of islet mass with a decrease of beta cell proliferation by 40%), however $Hhip^{-/-}$ mice die shortly after birth mainly due to lung defects.

In our first study, we systemically studied the role of pancreatic Hhip expression by using a whole body knock out in response to 8 weeks high fat diet (HFD) insult, and HFD-mediated beta cell dysfunction *in vivo*, *ex vivo* and *in vitro* using heterozygous ($Hhip^{+/-}$) vs. wild type ($Hhip^{+/+}$) mice. Both HFD-fed $Hhip^{+/+}$ male and female mice developed severe glucose intolerance (IPGTT), which was ameliorated in male and female HFD-$Hhip^{+/-}$ mice. Associated with this glucose intolerance, was hyperinsulinemia, which was observed only in HFD-fed male $Hhip^{+/-}$ mice. HFD-fed $Hhip^{+/-}$ mice had high levels of circulating plasma insulin in both insulin secretion phases compared to HFD fed $Hhip^{+/+}$ mice. In the pancreas, Hhip expression was increased in the islets of HFD-$Hhip^{+/+}$ mice, mainly co-localized in beta cells and none in alpha cells. While maintaining the total islet number, and beta cell mass, male HFD-$Hhip^{+/+}$ mice had a higher number of larger islets, in which insulin content was

reduced; islet architecture was disoriented, with evident invasion of alpha cells into the central core of beta cells; and an evident increase in oxidative stress markers (8-OHdG and NADPH oxidase 2 (Nox 2)). In contrast, male HFD-Hhip$^{+/-}$ mice had a higher number of smaller islets, with increased beta cell proliferation, pronounced glucose stimulated insulin secretion (GSIS), ameliorated oxidative stress and preserved islet integrity. *In vitro*, recombinant Hhip (rHhip) dose-dependently increased oxidative stress (Nox2 and NADPH activity), and decreased the number of insulin-positive beta cells, while siRNA-Hhip enhanced GSIS, and abolished the stimulation of sodium palmitate (PA)-BSA on Nox2 gene expression. We believe our data highlights a novel finding as to how pancreatic Hhip gene inhibits insulin secretion, by altering islet integrity, and promoting Nox2 gene expression in beta cells in response to HFD-mediated beta cell dysfunction.

Diabetes presents high risk factors associated with complications such as chronic kidney disease (CKD) characterized by a gradual loss in kidney function. The increased incidence of diabetic related kidney complications has been recently correlated with increase rate of obesity. We recently established that impaired nephrogenesis in kidneys of offsprings of our murine model of maternal diabetes was associated with upregulation of Hhip gene expression [127]. Subsequently, our recent data also shows that hyperglycemia induced increased renal Hhip gene expression in adult murine kidneys leading to apoptosis of glomerular epithelial cells and endothelial to mesenchymal transition (Endo-MT) - related renal fibrosis [128].

In this current study, we demonstrated how Hhip overexpression in renal proximal tubular cells, contributes to early development of chronic kidney disease after 14 weeks of HFD. Mice in HFD-fed groups showed significantly greater weight gain as compared to mice

in ND fed groups. IPGTT revealed that HFD fed mice also developed glucose intolerance, with no apparent changes in insulin sensitivity. HFD did not impact hypertension, even though we had a modest trend of increase in perirenal fat deposit in the HFD fed subgroups. Renal function as measured by the glomerular filtration rate was normal in all four subgroups, indicating that neither HFD, nor Hhip overexpression promoted renal hyperfiltration. Nonetheless, renal morphology revealed HFD kidneys had subclinical injury, presented signs of tubular vacuolization and damage compared to ND fed mice. This pathology of tubular damage and vacuolization was more pronounced in HFD-fed transgenic (Hhip-Tg) mice compared to non-Tg mice, and this promoted mild tubular cell apoptosis and enhanced oxidative stress. In conclusion, HFD feeding-induced obesity led to detrimental effects on glucose toleranc,e and mild morphological changes in kidneys, characterized by the presence of osmotic nephrosis, increased renal oxidative stress, and apoptosis which might be mediated by an increase in renal FABP4. This was exacerbated by the over-expression of Hhip in the renal proximal tubules.

Key words: High Fat Diet, Hhip Gene Expression, Pancreatic beta Cell Dysfunction, Kidney Dysfuntion

Table of Content

List of Tables

No table of figures entries found.

In your document, select the words to include in the table of contents, and then on the Home tab, under Styles, click a heading style. Repeat for each heading that you want to include, and then insert the table of contents in your document. To manually create a table of contents, on the Document Elements tab, under Table of Contents, point to a style and then click the down arrow button. Click one of the styles under Manual Table of Contents, and then type the entries manually.

List of Figures

List of Abbreviations

α-cell: Alpha cell
β-cell: Beta cell
δ-cell: Delta cell
ε-cell: Epsilon cell
8-OHDG: 8-Oxo-2'-deoxyguanosine
ANOVA: Analysis of variance
AQP1: Aquaporin 1
ATP: Adenosine triphosphate
BSA: Bovine serum albumin
CD4+: Cluster of Differentiation 4
CD8+: Cluster of Differentiation 8
CD36: Cluster of differentiation 36
Cdk4: Cyclin-dependent kinase 4
cDNA: Complementary deoxyribonucleic acid
Ci: Cubitus interruptus
CKD: Chronic kidney disease
CkIα: Casein kinase Iα
Cos2: Costal 2 (Cos2)
DAB: 3, 3 –diaminobenzidine
DAPI: 4′,6-diamidino-2-phenylindole
DHE: Dihydroethidium
Dhh: Desert Hedgehog
DIO: Diet Induced Obesity
DNA: Deoxyribonucleic acid
DM: Diabetes Mellitus
ECL: Enhanced ChemiLuminescence
Endo-MT: Endothelial to mesenchymal transition
ESRD: End Stage Renal Disease
FABP4: Fatty acid binding protein 4
FBS: Fetal Bovine Serum
FFA: Free Fatty Acid
GAD: Glutamate Decarboxylase or Glutamic Acid Decarboxylase
GDM: Gestational Diabetes Mellitus
GLI: Glioma-associated oncogene
Gpcr: G protein-coupled receptor kinase
Gprk2: G protein-coupled receptor kinase 2
Gsk3β: Glycogen Synthase Kinase 3β
GST: Glutathione peroxidase
Glut2: Glucose transporter 2
HBSS: Hanks' Balanced Salt Solution
HES-1: Hairy and enhancer of split-1
HEPES: 4-(2-hydroxyethyl)-1-piperazineethanesulfonic acid
HFD: High Fat Diet

HFHS: High Fat High Sucrose
Hh: Hedgehog
Hhip: Hedgehog interacting protein
Hlxb9: Homeobox HB9
HNF-6: Hepatocyte Nuclear Factor 6
HNF-1α: Hepatocyte Nuclear Factor 1 alpha
HNF-4α: Hepatocyte Nuclear Factor 4 alpha
HNF-1β: Hepatocyte Nuclear Factor 1 beta
HNF-3β: Hepatocyte Nuclear Factor 3 beta
HRP: Horseradish peroxidase
HSC: Hh signalling complex
iNOS: Inducible nitric oxidase
IDDM: Insulin Dependent Diabetes Mellitus
IF: Immunofluorescence
IGT: Impaired Glucose Tolerance
Ihh: Indian Hedgehog
IHC: Immunohistochemistry
IL-1: Interleukin 1
IPF-1: Insulin promoter factor 1
IPGTT: Intraperitoneal glucose tolerance test
IPITT: Intraperitoneal insulin tolerance test
IRS1/2: Insulin receptor substrate ½
KAP: Kidney specific androgen regulated protein promoter
KRBH: Krebs-Ringer bicarbonate-HEPES
mHhip: Mouse Hedgehog interacting protein
MODY: Maturity onset diabetes of the young
mRNA: Messenger ribonucleic acid
NADPH: Nicotinamide adenine dinucleotide phosphate
ND: Normal diet
NEFA: Non esterified fatty acid
NeuroD: Neurogenic differentiation
NDM: Neonatal Diabetes Mellitus
NGN3: Neurogenin-3
NGT: Normal Glucose Tolerance
NIDDM: Non-Insulin Dependent Diabetes Mellitus
Nkx2.2: Homeobox protein Nkx-2.2
NOX: Nicotinamide adenine dinucleotide phosphate oxidase
Nrf2: Nuclear factor (erythroid-derived 2)-like 2
PA: Palmitic acid
Pax4: Paired box protein 4
Pax6: Paired box protein 6
PBS: Phosphate buffered saline
PI3K: Phosphoinositide 3-Kinase
PKA: Protein Kinase A
PKC: Protein kinase C

Ptch: Patched1
qPCR: Quantitative polymerase chain reaction
RBP-J κ: Recombining binding protein suppressor of hairless kappa type J
rHhip: Recombinant Hedgehog interacting protein
RNS: Reactive nitrogen species
RPTC: Renal proximal tubule cell
ROS: Reactive oxygen species
RT-PCR: Real time polymerase reaction
SBP: Systolic blood pressure
Shh: Sonic Hedgehog
siRNA: Small interference ribonucleic acid
Smo: Smoothened
SOD: Superoxide dismutase
STZ: Streptozotocin
SUFU: Suppressor of fused homolog
T1DM: Type 1 Diabetes Mellitus
T2DM: Type 2 Diabetes Mellitus
Tg: Transgenic
WB: Western blot
WHO: World Health Organization

Acknowledgements

This body of work would not have been made possible without the support, and work of a multitude of people both directly and indirectly. I am particularly grateful for my advisor Dr. Shao-Ling Zhang, for offering me this unique opportunity, and also for all the time dedicated to all phases of the research presented within this thesis. It was invaluable and very much appreciated. It is thanks to your supervision that this work came into existence and completion. Thank you for your patience, motivation and enthusiasm. I am also deeply thankful to my co-supervisor, Dr. John Chan, for his insightful comments, encouragement and constructive suggestions.

I would like to thank the members of my dissertation committee: Dr. Ashok Srivastava, Dr. Jennifer Estall, Dr. Jun-Li Liu and Dr. Jolanta Gutkowska for their time, comments and valuable insights.

I would also like to thank past, and present members of the Zhang and Chan Laboratories: Chao-Sheng Lo, Shiao-Ying Chang, Xing-Ping Zhao, Anindya Ghosh, Kana Miyata, Min-Chun Liao and Shuiling Zhao for their contribution in the work presented here, their valuable comments during discussions/meetings, and for creating a friendly work environment. To Mrs Isabelle Chenier, I will always value your day-to-day advice regarding my project(s), and your encouragement during frustrating times was invaluable. Thank you for taking me under your wings, and teaching me how to keep our animals safe, healthy and happy.

I would also like to thank Drs. Marc Prentki, Erik Joly and Marie-Line Peyot for their continued assistance, and expertise in conducting this project.

I am indebted to my many student colleagues for providing a stimulating, and fun environment making the many twists and turns during this PhD journey an enjoyable experience. I am especially thankful to Yves Mugabo, Estelle Simo, Viktoria Youreva, Henry Leung, Ju Jing Tan, Laura Sognibe and Melissa Aubain.

Lastly, I will like to thank my mum, sister, brothers and in-laws for their prayers, words of encouragement and support from far away. Most importantly, I wish to thank my family, my wife Kiria Nchienzia, our Sons- Riley and Roen Nchienzia. I am grateful for your unwavering support, understanding and patience because I know it must have been very

difficult to have as husband/dad a “PhD-to be” husband/dad, to you I dedicate this thesis. I am excited see what our family will be like without me as a student.

A. Introduction

1.0 Diabetes Mellitus

1.1 Brief History of Diabetes Mellitus

Ancient Egyptians were the first to describe diabetes mellitus (DM) approximately 3000 years ago. The Greek physician, Arataeus of Cappodocia, was the first to use the term "diabetes" during the first century A.D., which stems from the Greek word "siphon." Later on, the term mellitus (honey sweet) was subsequently added by Thomas Willis in 1675 after rediscovering the sweetness of patient's urine (first noticed by the ancient Indians). It wasn't until 1776 that Dr. Mathew Dobson, a physician in London, first confirmed that the sweetness of the patients' urine was due to the presence of excess sugar. This method of diagnosing the disease by tasting the patient's urine, was used successfully until the 20th century. During this period, Dr. Dobson also realized that DM in some individuals was fatal as compared to a chronic condition in others. Hence, for the first time, there was a hint of the existence of two types of DM - Type 1 and Type 2 DM.

Paul Langerhans, a German student, while working on his medical doctorate degree in 1869, identified the cells that were later known as the islets of Langherans. Later on, the name *insulin*, which represented the secretions from the islets (Latin, *insula* = islands), responsible for reducing blood glucose levels was first described by de Mayer and Schaefer in 1909 and 1910, respectively. During this period, most of the treatments advanced for DM were very basic and ineffective, included but not limited to milk diets, opium, rice cure, potato therapy, replenishing lost fluids through over feeding. In parallel, Dr Fredrick Allen from the

Rockefeller Institute in New York in 1919, also published a body of work known as the "Total Dietary Regulation in the Treatment of Diabetes" that led to the introduction of a therapy consisting of strict dieting or starvation treatment as another alternative treatment of DM. In 1921, Sir Frederick Grant Banting and Charles Herbert Best, established that insulin deficiency was the main cause of diabetes. They achieved this by using canine insulin extracts, to reverse hyperglycaemia and glycosuria in dogs made diabetic by removing their pancreases, this led to their Nobel Prize win in Physiology and Medicine in 1923. Later, James Collip and John Macleod, further extracted and purified bovine insulin, which was successfully used in the treatment of DM patients. Subsequently in 1936, Sir Harold Percival, further published some research data in which he concisely made the difference between both Type 1 and Type 2 DM [1-5].

Diabetes mellitus (DM), most often referred to as diabetes, is one the oldest disease known to man, and it is currently a global health concern. Irrespective of the pathophysiology involved, chronically elevated levels of serum glucose, known as hyperglycemia, is a common characteristic denominator of diabetes, resulting from either pancreatic β-cell destruction or dysfunction. Diabetes is not only a single disease and considered as a heterogeneous group of metabolic disorders, of carbohydrates, lipids and protein metabolism [6-8].

Numerous pathogenic processes are implicated in the development of diabetes, which involves either the destruction of β-cells of the pancreas, consequently leading to deficiency in insulin production or resistance to insulin's action. The basis in the impairment of carbohydrates, proteins, and lipids always involves defects or deficiency of insulin secretion or its response in target tissues, such as liver, fat and muscles. Diabetes is one of the most highly morbid non-communicable diseases, and has a high prevalence in both developing and

developed countries, reaching epidemic proportions in certain countries [8]. The worldwide prevalence of diabetes is continuously on the rise, and based on data from studies from the International Diabetes Federation in 2013, it was estimated that 8-10% of the world's population suffers from diabetes [9]. This accounts for 451 million people, 9.2% of which are women, and 9.8% are men [9]. Approximately almost half of all these people (49.7%) living with diabetes are undiagnosed [9]. Moreover, there are an estimated 374 million people with impaired glucose intolerance (IGT). With the increasing rate of globalization and industrialization, the prevalence of diabetes is predicted to increase dramatically over the next few decades. At this rate, it is estimated that diabetes and its complications will account for approximately 850 billion USD in terms of the worldwide healthcare expenditure [10-12]. It is also estimated that by the year 2045, the worldwide prevalence of this disease will be approximately 693 million people, hence making diabetes among one of the major health conditions, currently affecting the global population with increasing morbidity and mortality rates [8;10-11;13]. This therefore makes diabetes a major public health challenge in the 21st century, and it is the fourth or fifth leading cause of death in most developed countries [11]. Some of the classical symptoms presented by diabetic patients are polyphagia (increased hunger), polydipsia (increased thirst), polyuria (frequent urination) and sometimes weight loss. Diabetes if undiagnosed, diagnosed late or poorly managed, results in a state of incessant hyperglycemia, that can lead to complications and permanent damage in a wide variety of tissues, such as micro vascular complications, including retinopathy (which can potentially lead to loss of vision), nephropathy (causing renal failure), peripheral neuropathy (with potential risk of foot ulcers and amputations), autonomic neuropathy (leading to gastrointestinal symptoms), and macro vascular complications including coronary artery

disease, stroke, cerebrovascular disease and peripheral arterial disease [14]. As a results of the above complications and irreversible damages, diabetic patients most often experience either a diminished quality of life or a reduced life expectancy.

1.2 Classification of Diabetes Mellitus

Most of the individuals presented with diabetes fall into two major categories, as published by World Health Organization (WHO) in 1980 based on the different causes. The two major classes of diabetes proposed are; insulin-dependent diabetes mellitus (IDDM) and non-insulin-dependent diabetes mellitus (NIDDM), but this was later revised as Type 1 Diabetes Mellitus (T1DM) and Type 2 Diabetes Mellitus (T2DM), respectively. Other types of diabetes, such as gestational diabetes (GDM), permanent neonatal diabetes (NDM), as well as maturity onset diabetes of the young (MODY) have been included in the general classification [15-16]. Even though T2DM is reported to be more prevalent in the general population, T1DM is identified as the chronic form of the disease especially in children. It was not until lately when emerging data now identified increase prevalence of T2DM in children, teenagers and adolescents [8; 17].

1.2.1 Type 1 Diabetes Mellitus (T1DM)

TIDM, also referred to as juvenile diabetes, accounts for approximately 5%–10% of all diabetic cases, and it is considered as the less prevalent form of diabetes. Currently, T1DM mostly affects children and young adults, with adults making approximately 84% of people living with the disease [7; 15]. It is normally characterized by pancreatic β-cells loss, primarily due to an autoimmune process, leading to an absolute deficiency in insulin secretion. Although the aetiology of T1DM is not completely understood, some studies propose the

infiltration of macrophages, CD4+ and CD8+ T-cells as responsible for the autoimmune destruction of pancreatic β-cell islets, which leads to hyperglycaemia. A small percentage of affected individuals, approximately <10%, are classified as type 1B, with no evidence of autoimmunity, and the pathogenesis in these cases is considered idiopathic. Currently, T1DM can also be defined by the presence of one or more autoimmune markers, which include islet cell autoantibodies to GAD (GAD65), insulin, tyrosine phosphatases IA-2 and IA-2β, and ZnT8. There exists quite a variation in the rate of β-cell destruction in T1DM, with rapid destruction in some individuals, mainly infants and children, and slow in others mainly adults. T1DM patient manage their disease by constantly monitoring their blood glucose levels and are also dependent on exogenous insulin to maintain normoglycaemia. The increased hyperglycaemia, resulting from altered insulin secretion causes increased glycogenolysis in the liver, activating gluconeogenetic pathways, and decreases cellular peripheral tissues glucose uptake (muscle and adipose) [7]. The essential symptoms of T1DM include hyperglycemia, polyuria due to osmotic diuresis, thirst because of hyperosmolar state, weight loss due to depletion of fat reserves, negative nitrogen balance, and neurotoxicity as a result of hyperglycemia and ketoacidosis [7; 16].

1.2.2 Type 2 Diabetes Mellitus (T2DM)

T2DM, previously known as adult-onset diabetes, is considered as the most prevalent form of diabetes, accounting for 90–95% of all diabetic cases, and it is thought to be a complex syndrome in nature. T2DM is mostly characterized by two pathological defects: on one hand, impaired insulin secretion as a result of pancreatic β-cell dysfunction, and, on the other, impairment in insulin action via insulin resistance as seen in Figure 1. In other words, individuals with T2DM may not necessarily require insulin treatment for survival, but they

may require insulin for control of hyperglycaemia if this is not achieved with diet alone or with oral hypoglycaemic agents [7-16].

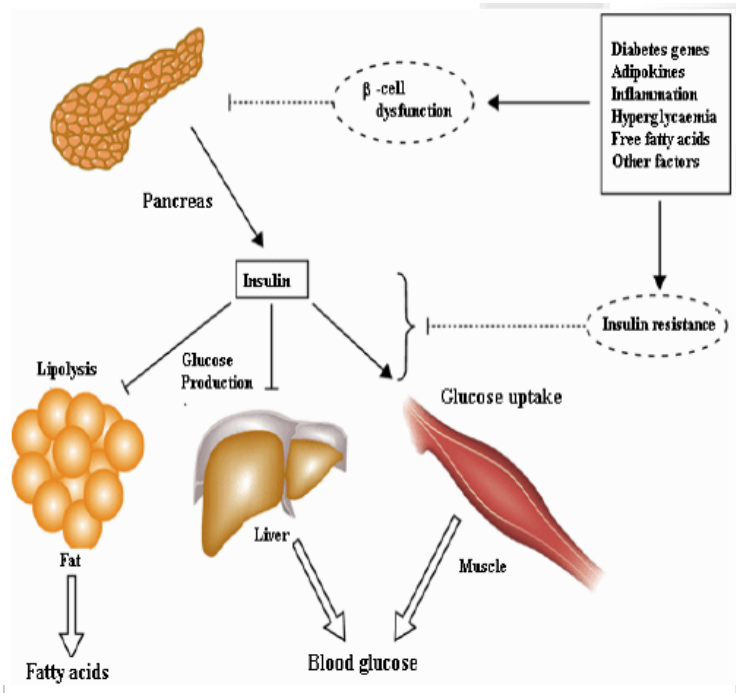

Figure 1: Pathophysiology of hyperglycaemia in T2DM. As a result and combination of impaired insulin secretion and resistance, there is decreased glucose transport into the muscle cells and increased hepatic glucose production, which results to increased hyperglycaemia. Adapted from [16].

Even though the specific aetiologies of T2DM are not fully understood, β-cell autoimmune destruction is not one of its characteristics. T2DM symptoms develop gradually over time, and it is considered to be more of a chronic syndrome, rather than an acute disease. Among the demographics linked with the increase risk of developing T2DM are age, lack of physical activity, race (ethnicity), poor eating habits, socioeconomic status and environmental factors. These all play an important role either in concert or individually in the disease development, and its accompanied complications. One of the major predisposing factors

involved in the development and pathophysiology of T2DM, is overweight or obesity, which eventually results in insulin resistance [18].

1.2.2.1 Obesity as a Predisposing Factor in the Development of T2DM

Obesity has recently gained recognition as a chronic disorder, and a non-communicable disease. Obesity occurs when there is excess fat accumulation (regionally, globally, or both), and it is one of the leading preventable causes of death worldwide [19]. The incidence of obesity is significantly escalating in many nations worldwide. Globally in 2014, 39% of adult aged 18 years and above were overweight, of which 13% were obese, and this number is projected to be doubled by 2025 [20-23]. Obesity, like other chronic diseases, can be linked either to an individual's genetic predisposition to weight gain, environmental influences or a combination of both. One of the main factors also driving obesity is when energy consumptions (i.e. dietary intake), exceeds energy expenditure (i.e. energy loss via metabolic and physical activity). Obesity is currently associated with increased risk of developing several metabolic conditions, of which the most devastating may be T2DM and also insulin resistance [24-25]. With the rise of obesity, pancreatic β-cells insulin production is enhanced, but metabolic response to insulin in organs such as the liver, muscle and adipose tissue is attenuated. This results to an overproduction of insulin by pancreatic β-cells, in order to maintain blood glucose within appropriate levels, ultimately leading to hyperinsulinemia. Therefore, obesity results in both a decrease in insulin sensitivity as well as a modulation of pancreatic β-cell function.

Recently, there is emerging evidence, which shows that there is the pre-existence of insulin resistance in T2DM individuals, prior to the development of hyperglycaemia. In individuals whose insulin resistance predominates, β-cell mass undergoes transformation in

order to increase insulin secretion to compensate for the increase in demand and in the maintenance of glucose homeostasis. Over time, due to long-term compensation mechanisms by the β-cells to meet up with the high insulin demands, the β-cells eventually undergo failure, further damage and apoptosis as seen in Figure 2. T2DM, can often go undiagnosed for many years because the development of hyperglycaemia is gradual, and individuals most often do not present the classical diabetic symptoms. Nevertheless, individuals are still at risk of developing both microvascular and macrovascular complications even when undiagnosed.

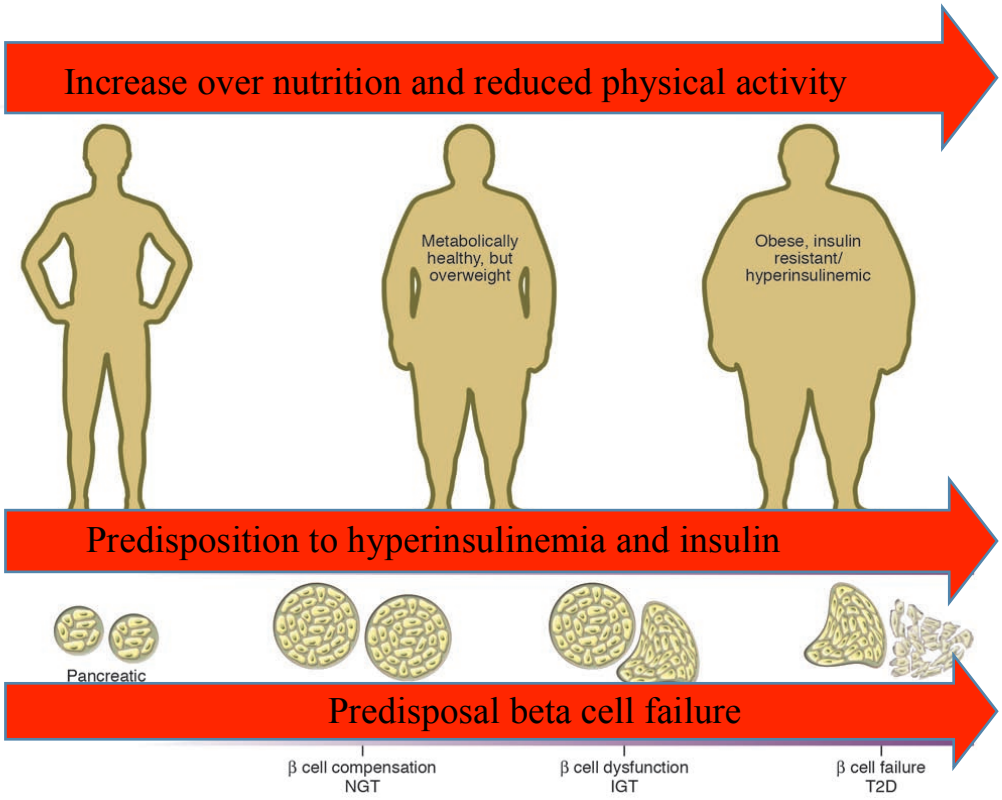

Figure 2: Islet β-cell failure and the natural history of T2DM. T2DM develops in response to over nutrition and lack of physical activity in subjects that have underlying genetic and acquired predispositions to both insulin resistance (and/or hyperinsulinemia) and β-cell dysfunction. Over time, islet β cell compensation for the insulin resistance fails, resulting in a progressive decline in β cell function. As a consequence, subjects progress from normal glucose tolerance (NGT) to impaired glucose tolerance (IGT) and finally to established T2DM. Even after diagnosis of T2DM, β-cell function continues to worsen such that the individuals progress from needing changes in diet/exercise only to requiring oral hypoglycaemic agents and eventually insulin for achievement of adequate glycaemic control. Future therapies will be directed not only to achievement of

euglycemia, but also changing the course of the disease by reversing the processes of β-cell failure. Adapted from [26].

As depicted in Figure 2 above, T2DM is commonly characterized by impaired glucose tolerance, which might be considered as the first check point for the development of T2DM and finally insulin resistance.

1.2.2.2 Characteristics of T2DM

1.2.2.2.1 Impaired Glucose Tolerance (IGT)

IGT, is generally an asymptomatic condition characterized by elevated (though not diabetic) levels of blood glucose after a two hours 75g oral glucose tolerance test. It is now being recognized as a stage in the transition from normality to diabetes. Individuals with IGT, have an increased risk of subsequently developing T2DM as summarized in Figure 6. This presents a critical window where the overt development to T2DM can be prevented through interventions. Even though this is the case, approximately 30% of individuals with IGT might return to normal glucose tolerance over a period of several years. Hence, it is not surprising to note that IGT and T2DM individuals share many characteristics such as insulin resistance and insulin secretory defects [26-27].

1.2.2.2.2 Insulin Resistance (IR)

There exists a fluctuation in insulin sensitivity during the normal life cycle. Systemic insulin resistance is often observed during periods of puberty, pregnancy and also with ageing. Associated with insulin resistance, are changes in lifestyle, such as decrease physical activities and increased carbohydrate consumption. Systemic IR is a condition in which there is a reduction in the responsiveness of the metabolically active organs and tissues in the body such as liver, muscles and adipose tissues to the normal glucose-lowering activity of insulin. This is

a common feature of most, if not all, prediabetic individuals [28-29]. IR plays a major role at the beginning and in the development of whole process of T2DM, and the degree of systemic IR varies from individual to individual.

Development of insulin resistance is dependent on either inherited or acquired factors. The inherited factors are mostly expressed by offsprings from T2DM individuals, who are more prone to be affected by insulin resistance [30]. Moreover, mutations in insulin receptors, glucose transporters and signaling proteins, have all been identified as potential inherited defects. Some of the acquired factors of insulin resistance include, but are not limited to less physical activity, fuel surfeit, ageing, hyperglycemia, hyperlipidemia and high level of plasma free fatty acids (FFA), as well as some medications.

The presence of insulin resistance leads to increase β-cell insulin secretion accompanied with compensatory hyperinsulinemia. Impaired function of β-cell after β-cell compensation, a process where there is expansion of β-cell mass in order to enhance insulin biosynthesis leads to deterioration in glucose homeostasis. As a result, there is the eventual development of T2DM when insulin secretion cannot keep up with the underlying increase in insulin resistance and glucose intolerance [26].

In summary, irrespective of the cause of DM, be it as a result of either genetic, or environmental factors or a combination of both, these all culminates in loss of pancreatic β-cell mass and/or function manifested as hyperglycemia. Upon the establishment of hyperglycemia, individuals attained by all forms of diabetes (T1DM, T2DM, GDM, MODY), are at risk for developing all the complications (microvascular and macrovascular) associated with the disease, although the rates at which it progresses may vary from individual to individual as seen in Figure 3 below.

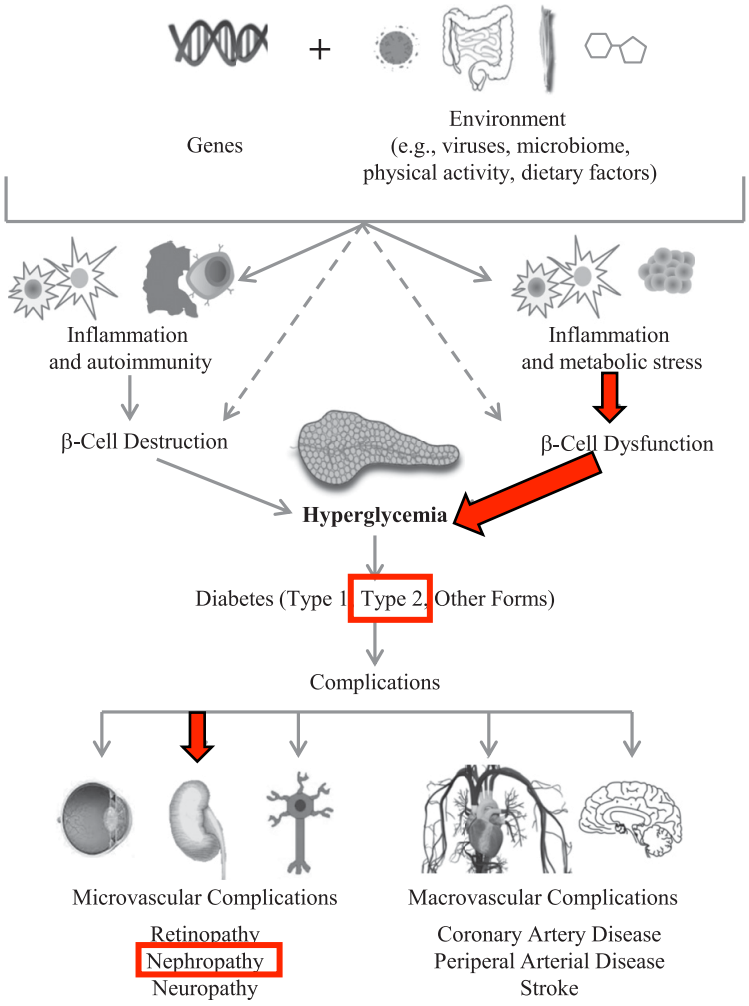

Figure 3: Genetic and environmental risk factors impact inflammation, autoimmunity, and metabolic stress. These states affect β-cell mass and/or function such that insulin levels are eventually unable to respond sufficiently to insulin demands, leading to hyperglycemia levels sufficient to diagnose diabetes. Adapted from [17].

1.3 Glucose Metabolism

1.3.1 Normal Physiology

Upon ingestion of food, carbohydrates are digested in the gut to glucose, which are absorbed directly into the blood streams. The absorbed glucose leads to an elevation of blood

glucose levels, which stimulates insulin release from the pancreatic β-cells. Insulin in turn binds to specific receptors and increases the rate at which glucose is taken up by peripheral tissues. When the physiological concentration of glucose is high, liver and muscles through the process of glycogenesis, can store glucose in the form of glycogen [31]. Conversely, in fasted states or low glucose concentrations, the liver can either release glucose from glycogen, a process referred to as glycogenolysis, or synthesize glucose from other substrates such as lactate, glycerol, and glucogenic amino acids via gluconeogenesis [31-32]. All of the above are regulated by circulating insulin levels.

Under diabetic conditions, blood glucose regulation by insulin is either altered or compromised. This is normally due to the loss of insulin-producing β-cells of the pancreas, resulting in decrease insulin secretion. This can be as a result of either an increase glucose concentration, or chronic hyperglycaemia referred to as glucotoxicity, or persistent exposure to free fatty acid levels, known as lipotoxicity, or because of both termed glucolipotoxicity.

1.3.2 Glucotoxicity

This refers to the deleterious effects on pancreatic β-cell phenotype (especially glucose-stimulated insulin secretion) to high concentration of glucose. Evidence points to the fact that, hyperglycemia results to depletion of insulin stores as well as a decrease in insulin gene expression and pancreatic β-cells such as MafA, Pdx1, or Nkx6.1. Studies have identified multiple biochemical pathways and mechanism involved glucotoxicity damage to pancreatic β-cells. This includes but not limited to oxidative stress, increased ER stress, glucose autooxidation, non-enzymatic glycation, protein kinase C (PKC) activation which culminates in pancreatic β-cell de-differentiation and cell death by apoptosis [33;34].

1.3.3 Lipotoxicity

Chronic exposure of pancreatic β-cell to high levels of free fatty acid (FFA) levels, exerts negative effects on β-cell function, especially in the area of glucose stimulated insulin secretion. There are studies which highlight the degree of FFA toxicity on pancreatic β-cell, and this is dependent on different parameters, such as the concentration of the unbound FFA, its level of saturation or even the chain length. However, the detrimental effects of FFA on pancreatic β-cell, is more evidenced in the presence of hyperglycemia when FFA oxidation in the mitochondria is compromised leading to a decrease in insulin gene expression [33; 34].

1.3.4 Glucolipotoxicity

This phenomenon explains the toxic effects of FFA on pancreatic β-cells in the presence of hyperglycemia. Hyperglycemia in this context results in a decrease of FFA oxidation. Even though, increase glucose or FFA acid concentration alone has been shown to be detrimental to pancreatic β-cells phenotype, a combination of both has been shown to be synergistic, since they have some overlapping mechanisms of action [35]. The harmful effects of glucolipotoxity leads to the inhibition of both insulin gene expression and insulin secretion. This eventually terminate in β-cell death by apoptosis, promoted by oxidative stress, inflammation and ceramide formation [34 - 36].

In summary, exposure of pancreatic β-cells to high concentrations of glucose, and lipid, leads to altered pancreatic β-cell gene expression and function. This may contribute to the observed deterioration of the functional β-cell mass especially in T2DM. These glucolipotoxic effects may occur as a result of various types of stress, such as oxidative stress, ER stress and cytokine-induced apoptosis.

1.3.5 Oxidative Stress and Reactive Oxygen Species (ROS)

Oxidative stress and ROS, are known to be involved in the pathophysiology of many disease conditions, such as DM and its complications. In physiological systems, metabolic pathways such as tricarboxylic acid (TC) cycle, and the respiratory chain generate reactive oxygen species (ROS), such as hydroxyl radical ($OH^{\cdot}$), hydrogen peroxide (H_2O_2) and superoxide anion ($O_2^{\cdot-}$) as summarized in Figure 6. Tissue and cellular oxidative stress, is as a result of the disproportion between the pro-oxidants and anti-oxidants. This can be enhanced by either an overproduction of ROS or due to low expression of anti-oxidant enzyme activities. Excessive ROS production, results in cellular dysfunction due to modifications of both the structure, and function of lipids and proteins. In the pathology of DM, oxidative stress can be initiated by increase in cytokine exposure (T1DM), or nutritional stress (glucose and lipids- T2DM), or a combination of both [37-38].

1.3.5.1 Pancreatic β-Cell Oxidative Stress

Pancreatic β cell loss and dysfunction are central to the development of DM. Oxidative stress as a result of either hyperglycaemia, or hyperlipidaemia, in β-cells is recognized as one of the leading contributing factors to pancreatic β-cell loss, and dysfunction in both human and rodent diabetic islets [39]. This results in the reduction of insulin expression in β-cells, hence, impairing glucose stimulated insulin secretion (GSIS) and promotes β-cell apoptosis. This is achieved by increasing DNA and protein oxidation levels, lipid peroxidation and cellular stress-sensitive pathway activation through a variety of mechanisms [41-42].

Oxidative stress results from an imbalance between proantioxidants and antioxidants, with an increase in the former leading to a loss of redox signalling. Compared to other tissues,

pancreatic β cells have been shown to be vulnerable to oxidative stress. This is because they express low levels of endogenous free-radical detoxifying enzymes such as, glutathione peroxidase (GST), superoxide dismutase (SOD), catalase and nuclear factor (erythroid-derived 2)-like 2 (Nrf2) [43-44]. Hence under conditions of oxidative stress, pancreatic β-cells are overwhelmed resulting in organ dysfunction. Mitochondrial oxidation, has been reported to be one of the major source of reactive oxygen species (ROS) production in pancreatic β-cells, especially during metabolic overloads, such as high exposure to glucose (glucotoxicity), free fatty acids (lipotoxicity) or a combination of both (glucolipotoxicity) [40].

Recent emerging evidence now highlights inducible nitric oxidase (iNOS), protein kinase C (PKC), and the NOX family of NADPH oxidases comprising the prototypical phagocyte NADPH oxidase NOX2, as a major source of pancreatic ROS generation. Increase Ca^{2+} stimulation has been positively correlated with increase ROS concentrations in β-cells. This increase in intracellular Ca^{2+}, through PKC activation, may activate NOX-dependent generation of ROS, and thus induce oxidative stress and/or apoptosis. The implication of NOX in β-cell dysfunction, is supported by observations that several NOX isoforms are expressed in pancreatic β-cells, including NOX-1, NOX-2, NOX-4, NOXO1, and NOXA1, where under conditions of stress they functionally regulate insulin secretion and cellular integrity. NOX enzymes generate ROS, by transferring one electron from NADPH to oxygen generating $O_2^{\cdot -}$ as illustrated in Figure 6 [45]. Furthermore, exposure of isolated islets from T2DM to high glucose, induces increases in intracellular peroxide levels, and subsequent antioxidant treatment partially protects these T2DM animal models against the development of hyperglycaemia. Also, recent *in vivo* data, suggest that oxidative stress increased in pancreatic β-cells of animal models and patients with Type 2 diabetes [46-48]. Additionally, an increased

expression of NOX2 (which is the most predominant isoform of the NOX family in the islets) is observed in islets, which may exacerbate disease aggravation over time, by damaging insulin-producing β-cells [49-50].

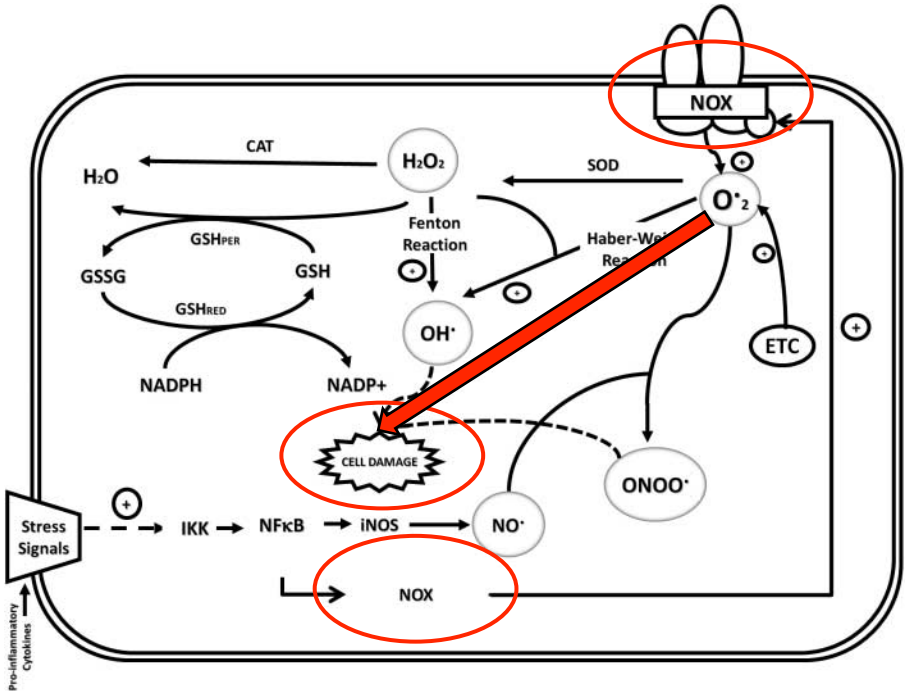

Figure 4: ROS/RNS species formation and antioxidant defense. ROS and NO may be generated by appropriate/inappropriate stimuli. These molecules may become toxic unless rapidly removed by the pathways described. GSSG, glutathione disulfide; GSH, glutathione; GSHRED, glutathione reductase; GSHPER, glutathione peroxidase; CAT, catalase; SOD, superoxide dismutase; ETC, electron transport chain; NOX, NADPH oxidase; IKK, I κ B kinase; NFκB, nuclear factor κB; iNOS, inducible nitric oxide synthase. Adapted from [39].

Pancreatic β-cell death as a result of apoptosis, via increased ROS affect numerous genes involved in β-cell development, as well as in insulin secretion and synthesis.

1.3.6 Genes Involved in Pancreatic β-cells

By using knockout mice as an experimental model, together with human data from maturity onset diabetes of the young (MODY), developmental biologist have identified

potential biological candidate genes involved in β-cell development, differentiation, regeneration, regulation of insulin gene transcription and as well as in the glucose sensing–insulin secretion coupling machinery as seen Figure 7. During pancreas organogenesis, the genes involved have been classified into 3 categories, which include top, intermediate and lower levels [51]. Top-level genes are implicated in anlage, and whole pancreatic morphogenesis, such as members of the notch-signaling pathway, delta-like gene-1, RBP-J κ and Hes-1. In addition, it is extended to homeodomain transcription factors: Hlxb9, IL-1 and IPF-1, control exocrine and endocrine development of the pancreas. The genes of the intermediate level, are involved in the regulation of endocrine differentiation and islet morphogenesis, including HNF-6, Pax6, Pax 4, Nkx2.2, NGN3, NeuroD, as well as a cyclin-dependent kinase Cdk4, that regulates endocrine differentiation and morphogenesis. The lower level consist of important genes that are associated with the transcription of insulin, and glucose genes of the differentiated β-cells, like IPF-1, HNF-1α, HNF-4α, HNF-3β and HNF-1β [51].

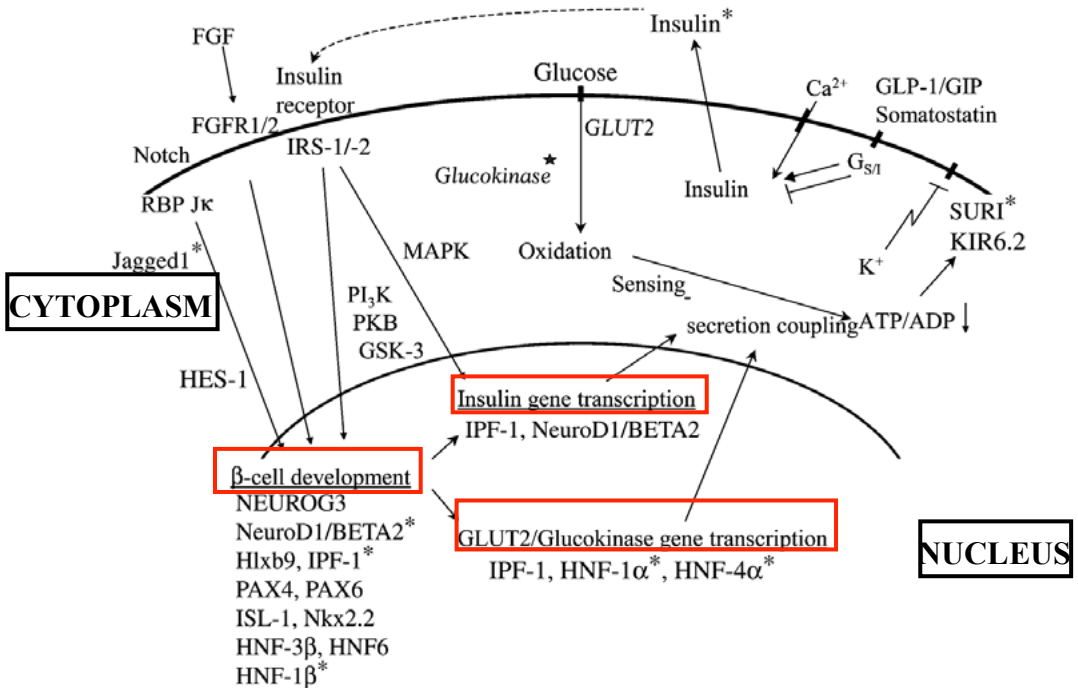

Figure 5: Genes involved in pancreatic ß-cell development, insulin gene transcription and insulin secretion in the cytoplasmic and nuclear compartments. Left: pathways transmitting signals generated at the plasma membrane through the cytoplasm and resulting in the nuclear activation of specific transcription factors regulating ß-cell development, differentiation, insulin gene transcription, GLUT2 gene transcription and glucokinase gene transcription. Right: glucose and ligand regulated insulin secretion machinery. Top: insulin is suggested to act directly on β-cells via an autocrine feedback loop. '*' means the β-cell genes that have been identified to be directly involved in human insulin secretory disorder and diabetes mellitus. Adapted from [51].

1.4 Current Models for Studying Diabetes Mellitus

In view of the fact that there is an increasing prevalence in the rate of DM, together with its associated pathologies, and complications, it is of utmost importance to study and understand the complex mechanisms/pathways involved in this disease, as well as the pathophysiology of T1DM, T2DM, GDM, NDM and MODY. Animal models have been used

to gain more insights in the last few decades in the study of all forms of diabetes, and in the understanding of disease diagnosis, progression, therapeutic responses, as well as the specific aspect of the disease under investigation. [52-54]. Therefore, it is very important to choose a reliable, and good animal model to elucidate the disease mechanisms, and evaluate new experimental therapies. The most common strategy applied, when using animal models, is the use of a model in which the disease process closely resembles the human condition. Alternatively, genetic manipulations, can also be used to assess the importance of genes, and proteins in the development and pathogenesis of the disease, but both strategies are most often used together. Animal models are indispensable, because they present us with a way to study the disease in an *in vivo* system, and to mimic the human disease condition more closely. The most common animal model employed to study disease mechanisms, or in the development of new therapies, especially diabetes, are rodents (mice and rats). Rodents are predominantly used because they present many advantages, such as their small sizes, ease of availability, fast breeding rates, short life span, their economic value, and the feasibility of conducting longitudinal studies with larger numbers of animals [52; 54]. Figure 6 is a schematic representation of the animal models for the diabetes studies.

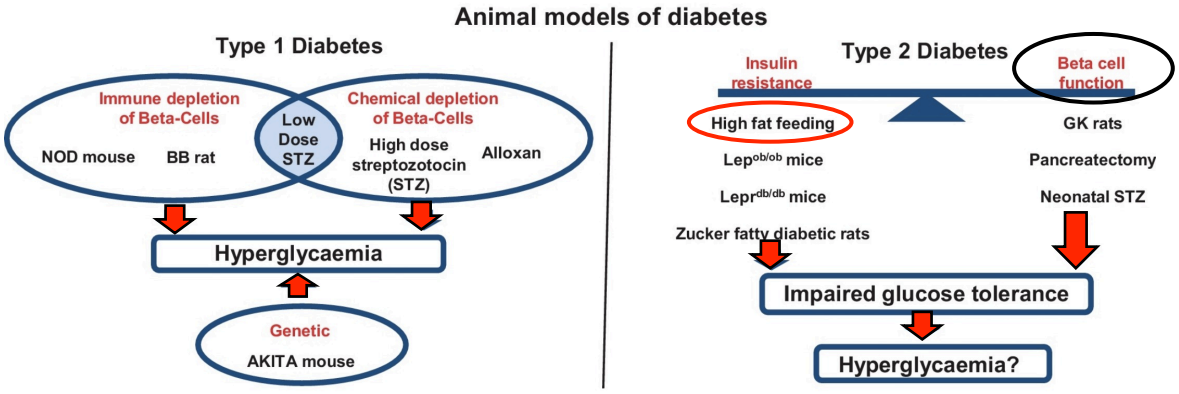

Figure 6: Schematic summary of animal models in the study of Diabetes Mellitus. Adapted from [52].

1.4.1 Animal Models for Type 2 Diabetes Mellitus

T2DM is a complex disease, whose pathogenesis involves several genetic and environmental factors. It is mainly caused by inadequate β-cell compensation in response to insulin resistance, which ultimately culminates in hyperglycemia because of insulin deficiency. T2DM, has been shown to be closely associated to obesity, which is involved in the pathology of insulin resistance. Hence, in understanding the pathophysiology of T2DM, it is crucial importance to develop an animal model that closely and accurately replicates the pathogenesis of human T2DM, which will enable the identification of preventative, and therapeutic strategies, targeting both the disease and its associated pathologies. The choice of the animal model will therefore depend of the question to be addressed, its relation to the pathogenesis of the disease, or to the treatment of a specific aspect of the disease.

1.4.2 Diet-Induced Obesity (DIO) Models

Obesity in rodents, can be either induced by high fat, or high-energy diet. This model is relevant given that, it is a close reflection of the mechanism of obesity-induced diabetes in humans, with similar disease pathogenesis. Models of DIO involves typically switching the

animals from a relatively low energy-density diet, which is low in fat, and rich in carbohydrates, and fibre, to one that is rich in fat, and sugar, and a higher energy density. These models feature relatively subtle obesity phenotypes, in which accumulation of body fat occurs over a relatively long period of time. Although the detrimental metabolic consequences of the diet are apparent within a few days after introducing the diet, longer periods of feeding are advised in order to achieve a significant weight gain, usually 8 weeks or more. In this model, characteristically energy intake far more exceeds energy expenditure. The corresponding weight gain correlates with insulin resistance, and abnormal glucose metabolism, even though the animal might not necessarily develop overt T2DM. It is important to take into consideration the strain of the mouse, since it has been reported that it affects the susceptibility to obesity [55-57].

1.4.2.1 High Fat High Sucrose (HFHS) Diet Model

Abnormal blood glucose homeostasis in rodents can be achieved by feeding them HFHS diet [56]. It should be noted that, although the overall caloric intake is increased in this diet, there is an overall reduction in the food consumption as a result of the high calorific value of the diet. Combining high-fat, and high-sugar diet, is thought to closely resemble the diet that dramatically increased obesity levels in humans over the past few decades. HFHS diet results in metabolic disorders, including obesity, hyperinsulinemia, insulin resistance, glucose intolerance, hepatic steatosis and inflammation [59; 60].

1.4.2.2 High Fat Diet (HFD) Model

Obesity can also be induced in rodents with high-fat diet. This diet consist of increasing the dietary fat content of their chow from approximately 11% to 58%. Feeding

C57BL/6J mice with HFD was first described in 1988 in Japan, and since then it has been used in numerous studies and commercially available. As earlier mentioned, even though increased weight gain can be detected within a week of starting the diet, HFD is typically administered over a longer time period (8–12 weeks). This model is usually characterized by significant obesity, hyperinsulinemia, insulin resistance and pronounced glucose intolerance. In addition, they exhibit marked fasting, as well as basal hyperglycaemia, in contrast to normal basal glucose level seen in C57BL/6J ($Lep^{ob/ob}$) mice. Even when overt DM is absent, insulin resistance leading to glucose intolerance is still a characteristic of this model, so these mice can also model an obesity-induced pre-diabetic state. The above-mentioned advantages make this model a very popular strain to use in the study of T2DM [52; 61-63].

1.4.2.2.1 Advantages of the HFD Model

- They effectively model the pre-diabetic states, and mimic the symptoms, as well as to study the progression of the disease.
- This model permits the study of factors that can be controlled at earlier stages of the disease, and study behavioral patterns.
- Provide insights on the influence of HFD in the studying of factors, such as food intake, energy expenditure, glucose tolerance, and insulin resistance.
- Useful in evaluation of anti-obesity compounds, and therapeutic agents, because they closely mimic human obesity.

- Models many of the complications of obesity, and metabolic syndrome, such as islet cell changes, leptin, corticosterone, adiponectin, adipose depots, nephropathy, retinopathy and neuropathy.

2.0 The Pancreas

2.1 Structure

The pancreas is long and slender in shape, measuring approximately 16 to 26cm, and located behind the stomach in the upper left abdomen. It is surrounded by other organs such as the spleen, liver, and duodenum. The pancreas originates from two epithelial buds during embryonesis: the ventral bud, which gives rise to the posterior part of the pancreatic head, and the dorsal bud, which gives rise to the anterior part of the head, the body, and the pancreatic tail [1; 64]. The pancreas is highly vascularized by several major blood vessels, such as the superior mesenteric vein, the portal vein and the celiac axis as summarized in Figure 7.

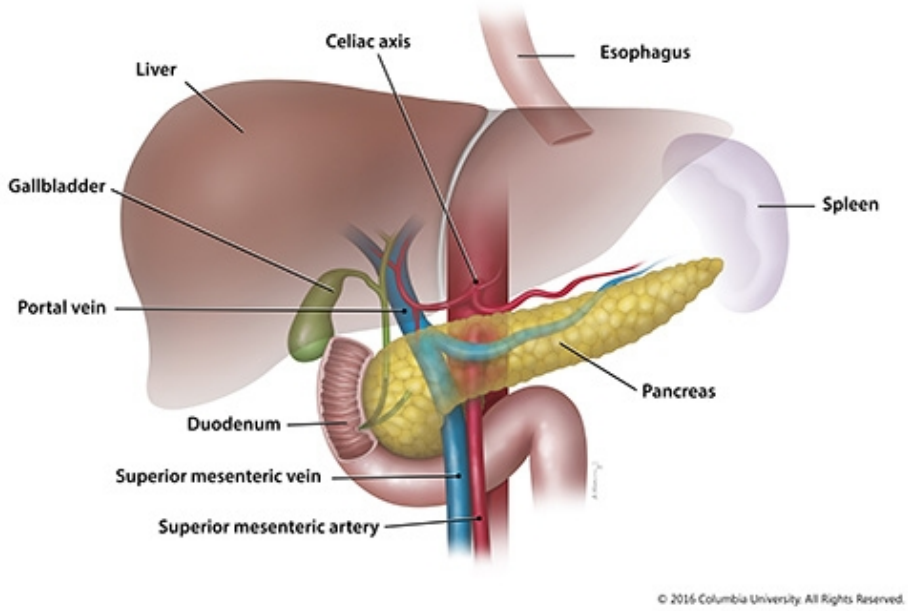

Figure 7: The pancreas with surrounding organs and vessels. Adapted from [65].

2.2 Function

Approximately 95% of the pancreas consist of exocrine tissues, which is responsible for the production of digestive enzymes (trypsin and chymotrypsin to digest proteins; amylase for carbohydrate digestion; and lipase for fat break down) and sodium bicarbonate, while the 5% of the remaining tissue consist of endocrine cells, known as the islets of Langerhans, whose role is to produce hormones involved in glycemic control [66; 67]. The pancreatic islets consist of five main groups of cells scattered throughout the pancreas as such as, the alpha (α), beta (β), delta (δ), polypeptide positive (PP), and epsilon (ε) cells, as summarized in Figure 8.

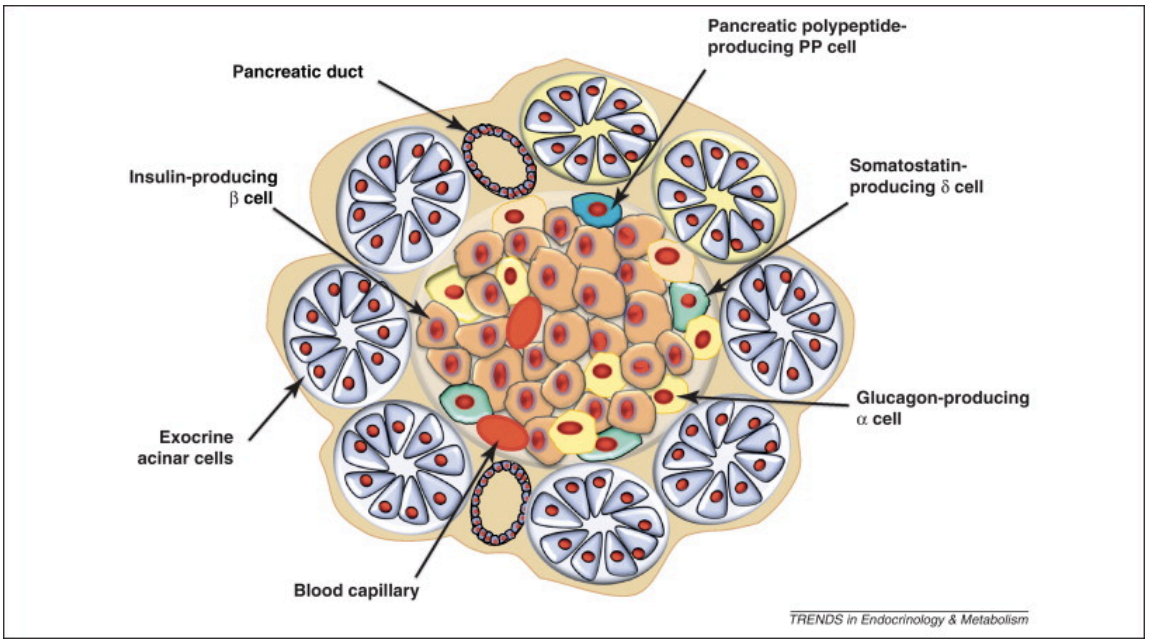

Figure 8: The endocrine pancreas with the different types of cells which make up the islets of Langerhans. Adapted from http://quasargroupconsulting.com/anatomy/pancreas.php.

2.2.1 Alpha (α) Cells

Alpha (α) cells, make up approximately 20% of the islets of Langerhans, and secrete the hormone glucagon. Glucagon principally raises blood sugar levels, and plays an important role in glucose homeostasis, hence counteracting the activity of insulin. It is typically secreted in the fasted state. It stimulates the process of glycogenolysis (conversion of glycogen to glucose), and gluconeogenesis (glucose generation from non-carbohydrate carbon substrates, such as amino acids). The counteraction of glucagon is important in preventing hypoglycaemia, which has been shown to be a response that is blunted in diabetes mellitus [1; 66; 67].

2.2.2 Beta (β) Cells

Beta (β) cells, are responsible for the production of the hormone insulin, and accounts for close to 75% of the islets of Langerhans. They are the most studied cell type of all the cells in the islets. Insulin is primarily responsible for lowering of blood sugar levels and is also very important in maintaining glucose homeostasis. The most important function of insulin is to regulate and facilitate glucose uptake in peripheral tissues like the adipose, and skeletal tissues, while suppressing hepatic glucose production. As blood glucose levels rises, there is an increase in insulin secretion, which leads to the activation of tyrosine kinases, and triggers the phosphorylation of cellular substrates, including insulin receptor substrate. This results in the intracellular movement of vesicles containing glucose transporter to the cell membrane, resulting in the facilitated transport of glucose into the cells [1; 66; 67].

2.2.3 Delta (δ) Cells

Delta (δ) cells, make up 4% of the islet population, and secrete the hormone somatostatin. Other organs, such as the hypothalamus, the gastrointestinal tract, and the central nervous system, can also secrete this hormone. Somatostatin has also been shown to negatively regulate both insulin, and glucagon release in a paracrine fashion [1; 66-68].

2.2.4 Polypeptide Positive (PP) Cells

The polypeptide positive (PP) cells, account for approximately 1% of the total cells found in islets and secrete the hormone polypeptide. The major role of polypeptide has been associated with satiety, though it has been reported to also negatively regulate both pancreatic endocrine, and exocrine secreting activities [66; 67].

2.2.5 Epsilon (ε) Cells

They are responsible for secreting ghrelin, which are thought to be important in growth hormone release, metabolic regulation, and energy balance. They make up around 1% of the islet cellular population [66: 67].

Even though the cells that make up the islet of Langerhans have different regulatory function, they all act in concert in the regulation glucose homeostasis, which is critical for many physiological processes.

The pancreatic β-cells, as aforementioned are the most studied of all the pancreatic cell types and play a central role in the etiologies of both T1DM and T2DM. To further understand and treat or prevent this condition, increased knowledge of the mechanisms (cellular and molecular) responsible for β-cell failure is warranted. In vitro studies, employing the use of pancreatic β-cell lines have proven to be invaluable in understanding the molecular mechanisms, associated with both disease conditions especially in the area of translational research.

2.3 Pancreatic β-Cell Lines

The use of functional pancreatic beta cell lines in diabetes research has proven to be useful and effective, especially in the areas of glucose stimulated insulin secretion (GSIS) and, in the understanding of the underlying mechanisms [69-71]. Recently, there has been great improvements, and breakthrough in establishing pancreatic beta cell lines, that still maintain the original insulin secretion regulation capacity as *in vivo* [72]. MIN6, and INS1 cell lines produced from transgenic animals that specifically express the SV40 antigen, are often the most used pancreatic beta cell lines. This is because they have the best physiological response to glucose [71].

2.3.1 MIN6 Cells

MIN6 cell line, derived from a transgenic C57BL/6 mouse insulinoma have been shown to form islet like structures in culture. These cells express both Glut2, and glucokinases and their response to glucose within physiological ranges is dependent on the presence of nicotinamide. In culture, they tend to lose their insulin secretory capacity to glucose, perhaps because they sometime, lose or express low levels of genes responsible for glucose responsiveness [71; 72].

2.3.2 INS-1 Cells

The INS-1 cell line derived from rat after induction by x-ray radiation, is a well-established cell line that has been used in numerous *in vitro* studies. They have been used to elucidate pancreatic islet β-cell function, since they possess many characteristics inherent to primary β-cells. INS-1 832/13, is a sub clone of INS-1 obtained after a stable transfection with a CMV promoter-human insulin expression plasmid, carrying a geneticin (G418)-resistance marker used for selection [73-74]. This cell line has many important characteristics such as, an enhanced response to glucose within physiological ranges (approximately 10 to 15-fold elevation in insulin secretion when the glucose level in the medium is raised from 3 to 15 mmol/l), which favorably compares with the responses obtained from fresh isolated rat islets (due to Glut 2 and glucokinase expression), possess relatively high insulin content, and synthesize both proinsulin I and II [73-79]. This cell line also has the added advantage of maintaining their insulin secretory response to glucose over an extended period in culture, while still maintaining their ability to proliferate in culture [76]. A major disadvantage associated with this cell line is the requirement of mercaptoethanol (toxic substance which can cause irritation and protein denaturation) in the culture media, which has been shown to be

important in preserving most of the important functional characteristics, while also maintaining their propagative properties [73]. The above-mentioned characteristics of INS-1 832/13 cells make them an invaluable system, especially in investigating the molecular mechanisms involved in the synthesis, storage, and secretion of insulin.

2.4 GSIS (Glucose Stimulated Insulin Secretion)

Pancreatic β-cells are principally responsible for insulin synthesis, and release in order maintains appropriate blood glucose levels. The release of insulin from pancreatic β-cells is tightly regulated and has been shown to be impacted by an array of metabolites (glucose, proteins, amino acids and FFA etc.), neurohormonal amplifiers (glucagon-like peptide-1 (GLP-1)), and pharmacological agents (sulfonylureas) [80]. Although insulin secretion can be triggered by several factors as listed above, glucose-stimulated insulin secretion (GSIS), is considered the primary and major pathway involved in insulin secretion. Impaired GSIS has been shown to be a major factor in hyperglycemia, which is a major characteristic of T2D, and involved the pathogenesis of the disease. GSIS is achieved by the generation of different signals within the pancreatic β-cells. This is a well characterized process *in vivo,* and involves the following sequence of events especially in the case of increase circulating glucose (hyperglycemia) [80-81];

- Increase glucose levels results in increase glucose uptake by pancreatic β-cells, through passive diffusion via glucose transporter Glut2. Once in the pancreatic β-cells, glucose is metabolised by oxidative glycolysis to pyruvate and mitochondrial oxidation.

- This leads to increase ATP production, resulting in an increase in the ATP/ADP ratio. The rise in ATP/ADP ratio further leads to the closure of the ATP-sensitive potassium (K^+-ATP) channels, and subsequently membrane depolarization.
- Membrane depolarization opens the voltage-dependent calcium channels, mediating a rise in the cytoplasmic Ca^{2+} concentration, and increase cytosolic calcium facilitates the exocytosis of insulin-containing granules.

The molecular and cellular steps showing how an increment in extracellular metabolites (glucose, FFA), and hormones (GLP-1) leads to increase insulin secretion.

3.0 Hedgehog Interacting Protein (Hhip)

3.1 Hedgehog (Hh) Signaling

The Hh pathway, was first discovered during embryonic genetic screening, aimed at understanding body segmentation in *Drosophilia melanogaster*. This screening revealed that mutant embryos for Hh developed as prickly little balls, similar to a hedgehog, hence, the name of the protein and pathway [82]. Even though the core components of the Hh pathway were initially discovered and identified in *Drosophilia*, it has been shown that they can be conserved in other species, such as invertebrates, and vertebrates, with the same mechanism of action. Activation of the Hh pathway during embryogenesis ensures proper embryonic cell differentiation, and organ development, including the lungs, brain, and pancreas, whereas deregulation of the pathway results in developmental defects. In adult tissues, the Hh pathway remains relatively quiescent [83-85]. The signaling molecules of the Hh pathway are known as Hedgehog (Hh) proteins.

Three mammalian hedgehog genes have been identified: Sonic hedgehog (Shh) protein, Indian hedgehog (Ihh) protein, and desert hedgehog (Dhh) protein. These proteins are expressed in different tissues, at different stages of development, and have different biological activities. Shh, is the most studied, and has the broadest expression pattern of all the Hh ligands. It is involved in the development of various organs during embryogenesis. It has been shown to regulate the patterning of limbs, and cell type specification in the central nervous system. Shh signalling can be autocrine (where it binds to the same cell from which it is excreted), or paracrine (where it binds to the nearby cells or induces changes in cells at longer distances). Ihh signaling regulates proliferation, and differentiation of chondrocytes in skeletal

morphogenesis. It is actively involved in the development of mammary glands, gastrointestinal tract, and the pancreas, where it plays a key role in the differentiation of germ cells. Dhh signaling is implicated in the development of sperm cells, and also necessary for the development of the glia cells that insulate the peripheral nerves. In general, Shh activity is more pronounced at early stages of development to regulate patterning and growth, while Ihh activity is seen later in the process of endochondral bone formation in limb development. The Hh proteins are distributed in tissues in a gradient manner, and cells respond to different thresholds of Hh with distinct responses [88; 89 - 91; 99]. Hh signal transduction typically occurs in the cells adjacent to ligand producing cells (autocrine effect), but also at a significant distance from their site of production (paracrine effect) [87].

The importance of Hh signaling pathway in the regulation of development was delineated in vertebrates, where defective Hh pathway signaling led to offspring with brain, facial and other midline defects, such as holoprosencephaly (failure of forebrain development), or microencephaly, cyclopia, and absence of nose or cleft palate [92; 93]. Recently, evidence points to the fact that Hh signaling extends beyond the developmental stages, with vestigial activities during adult life. In mature tissues, Hh signaling has been shown to be involved mainly in tissue maintenance, and repair, such as the maintenance of brain stem cell niches, renewal of gut epithelium, and hematopoietic cell differentiation, or when inappropriately reactivated like in several cancers making the Hh pathway an important therapeutic target [94].

Hh ligands are synthesized as precursor proteins comprised an N-terminal known as the ‘Hedge’ domain, and a C-terminal referred to as the ‘Hog’ domain. The Hedge domain is primarily responsible for the protein’s signaling activity [95; 96]. The Hog domain can be

further subdivided into an N-terminal Hint domain, and a C-terminal sterol-recognition region (SRR), that binds cholesterol responsible for trafficking and movement [97 - 99]. The Hint domain promotes the autocatalytic cleavage of full-length Hh ligand (45 kD), in the endoplasmic reticulum, which leads to the covalent coupling of a cholesterol moiety to its C-terminus (19kD). Subsequently, the N-terminus of cleaved Hh protein becomes palmitoylated, a modification essential for Hh activity, and signaling as illustrated in Figure 9 [85; 96; 99]. This dual lipidation renders Hh proteins highly hydrophobic, a property that causes their retention in the plasma membrane. While hydrophobic in nature, Hh can be transported in lipoprotein particles [100 - 102] and via heparin sulphate proteoglycans, hence its paracrine effect [103; 104].

Hh signaling pathway activation is mediated by two membrane-bound proteins: the receptor Patched1 (Ptch, transmembrane protein receptor), and activator Smoothened (Smo, a seven-transmembrane protein). In the absence of an Hh ligand, Ptch represses the activity of Smo, by inhibiting its translocation into the cell. Hence, the zinc finger transcriptional factor, Gli, a downstream component of Hh signaling, is prevented from entering the nucleus through interactions with cytoplasmic protein, including fused and suppressor of fused (Sufu). This collectively results in the repression of the transcriptional activation of Hh target genes. Conversely, activation of the Hh pathway is initiated through binding of any of the three mammalian ligands, Shh, Dhh, or Ihh (all represented as Shh in Figure 10) to Ptch1 resulting in the lysosomal degradation of the complex, relieving the repression of Smo. The binding of Hh ligand results in de-repression of Smo, thereby activating a cascade of reactions that leads to the translocation of the active form of Gli to the nucleus to regulate transcription of Hh

target genes. Hence, inactivation of Ptch1, results in a cell autonomous activation of the Hh response pathway as depicted in Figure 9 [77; 100].

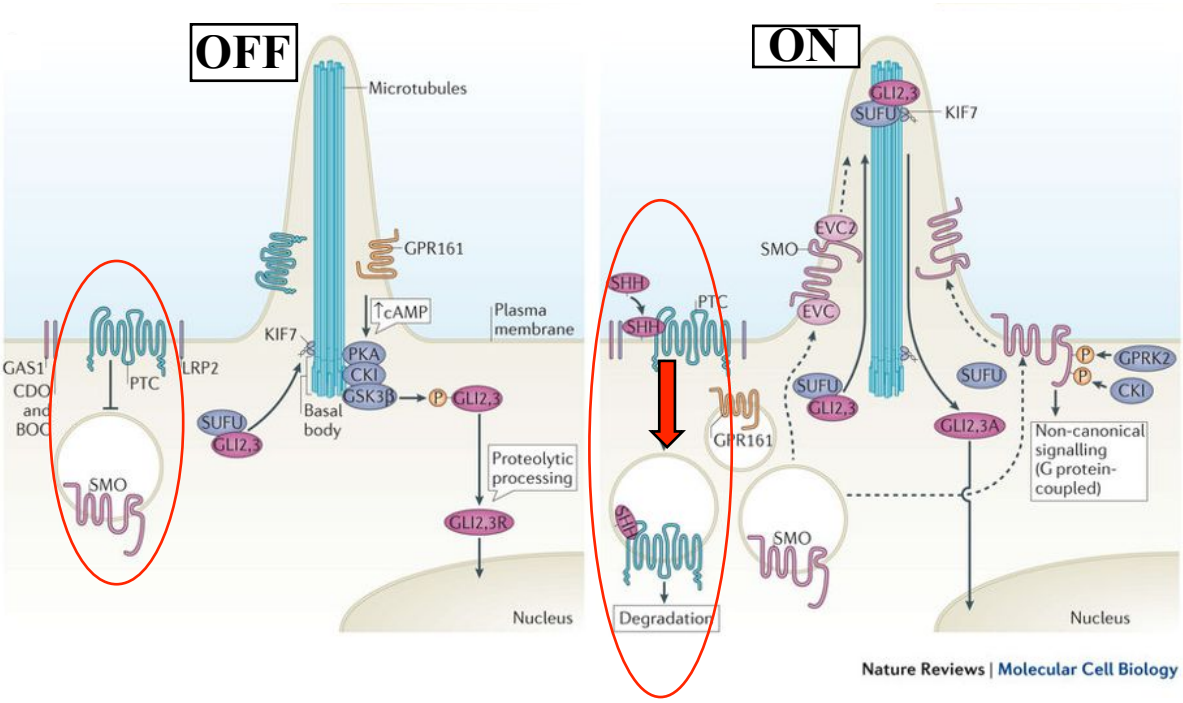

Figure 9: Reception of Hedgehog and initiation of signal transduction. In *Drosophila melanogaster*, the transmembrane proteins Interference Hedgehog (Ihog) and Brother of Ihog (Boi) promote Hedgehog (Hh)-Patched 1 (Ptc) binding. Hh also interacts with glypicans. Ligand-free Ptc represses Smo by triggering its rapid degradation and/or its confinement to an intracellular compartment (left panel, 'off'). Furthermore, in the absence of Hh, the Hh signalling complex (HSC), which includes Costal 2 (Cos2), Fused (Fu), Suppressor of Fu (SuFu) and Cubitus interruptus (Ci), is associated with microtubules. This complex promotes, through the activity of protein kinase A (Pka), casein kinase Iα (CkIα) and glycogen synthase kinase 3β (Gsk3β), the formation of the Ci repressor form (CiR). Binding of Hh to Ptc relieves Smo repression. Smo translocates to the membrane and is activated by phosphorylation on its carboxy terminal tail, by PKA, CkIα and G protein-coupled receptor (Gpcr) kinase 2 (Gprk2), which induces a conformational change. This promotes its association with the HSC and the sequential activation of Fu and Cos2, which releases uncleaved Ci from the HSC, activating Ci (CiA). Adapted from [99].

3.1.2 Hedgehog Pathway in the Developing Pancreas

Hedgehog signalling influences and plays multiple roles during the development of both endocrine and exocrine pancreas. During murine embryogenesis, the pancreatic epithelium forms from the embryonic foregut endoderm before embryonic day 8.0. The first morphological signs of pancreas formation are seen with the invagination of the dorsal pancreatic buds from the endodermal epithelium. Ultimately, a unified pancreas is formed with a ventral domain nestled in the duodenal loop, and the dorsal portion right beside the stomach, and spleen. Hh signalling, and pathway appears to be greatly involved in multiple roles during mouse embryonic pancreas development. During the early stages of gut formation, the expression of Shh, and Ihh is found throughout the endoderm epithelium, although both genes are later absent from the early endodermal area specified to become the pancreas. Similarly, Ptch expression was also found in the mesenchyme by *in situ* hybrization studies carried out on embryonic day 9.5. By embryonic day 13.5, several components of the Hh pathway, such as Ihh, Dhh, Hhip and Ptch1, can be seen within the developing pancreas as shown in Figure 10.

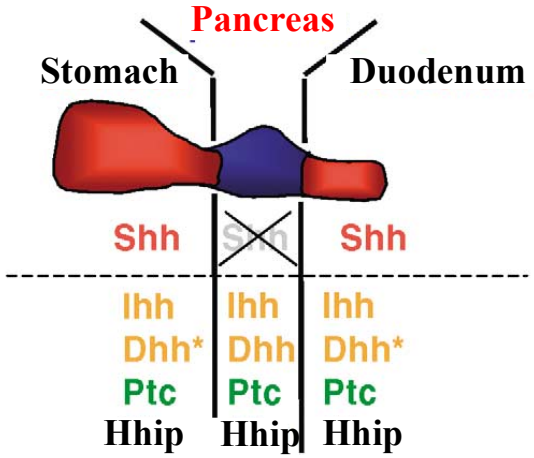

Figure 10: Expression of hedgehog signaling members in the fore-midgut area. Shh is excluded from pancreatic tissue during embryogenesis and expression patterns of other hedgehog signaling components in the pancreatic region. Orange, ligands; green, receptors; *, not tested. [105].

Moreover, with the mature pancreas, the expression of Ihh, Dhh, Hhip, Ptch1, and Smo has been identified in both the islets, and the ductal cells as seen in Figure 11 [93]. The expression of some Hh ligand within the pancreatic tissue, (Ihh), or in adjacent tissues, (Shh), suggests pancreas development is regulated by a graded response to Hh signalling. During the early stages of organogenesis, Hh signalling response is low to ensure the proper establishment of organ boundaries, and tissue architecture, and it is subsequently upregulated during late developmental stages, promoting tissue proliferation, and maturation. Gain of function studies revealed that, Hh pathway deregulation leads to severe changes in pancreas morphogenesis, and function [106; 107]. Furthermore, when Hh signaling in mouse embryos was increased by deletion of Ptch1 in mesenchymal cells, the resulting embryos displayed disrupted islet morphology, and cellular composition alongside hyperplasia of the mesenchyme, accompanied by the acquisition of smooth muscle like phenotype [86]. In parallel Nielsen et al, confirmed the suggested concept of graded Hh signaling in human pancreas organogenesis. In human pancreas, Ihh, Ptc, and Smo are localized in the islet cells in a similar pattern as in murine pancreas. It has been observed that early on in human pancreatic development (approximately 7.5 weeks of gestation), the expression of Gli3 (part of the Gli family of transcription factors, which are downstream of Hh signaling), was found in the developing pancreatic ducts, while Smo, and Gli2 were absent. Conversely, between gestational weeks 14 to 18, Smo, and Gli2 were highly expressed, whereas Gli3's expression was greatly reduced.

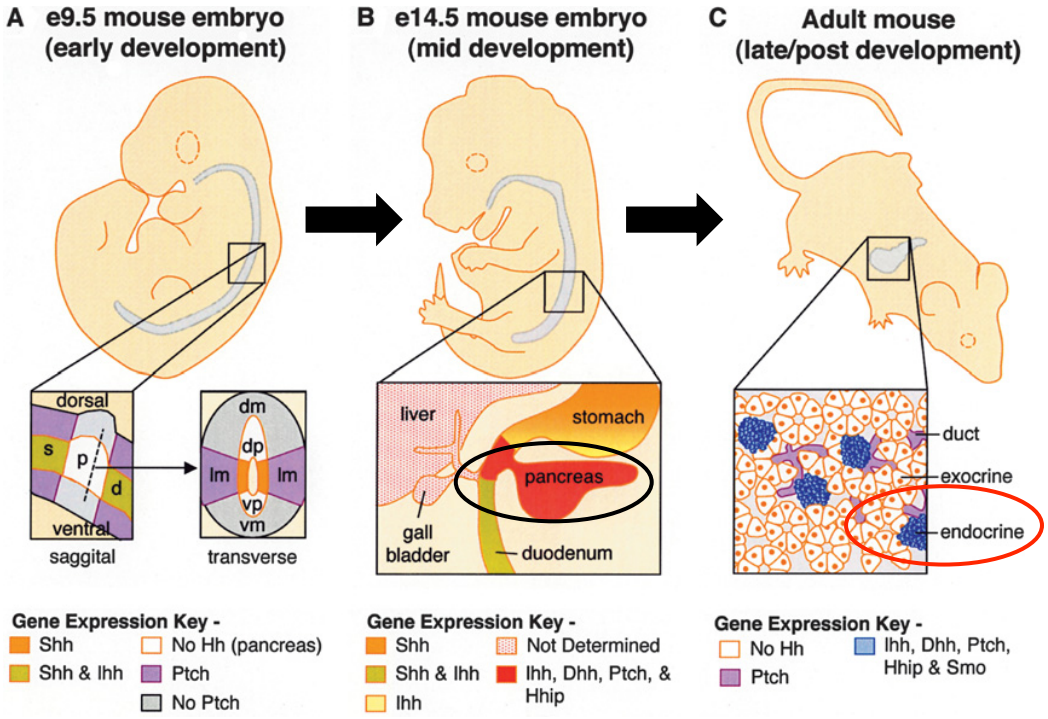

Figure 11: Hedgehog signalling during mouse pancreas development. (A) E9.5 mouse embryo (early development). In the sagittal section, Shh is expressed in the specified stomach (s) endoderm, anterior to the specified pancreatic (p) endoderm. Shh and Ihh are expressed in the specified duodenal (d) endoderm, posterior to the pancreatic endoderm. Ptch expression surrounds Hh expressing areas. In the corresponding transverse section through the pancreas, Shh is expressed along the lateral epithelium, and Ptch is found within the reciprocal lateral mesenchyme (lm). There is no expression of Shh in the dorsal (dp) or ventral (vp) pancreatic epithelium, and there is no Ptch expression in the neighbouring dorsal (dm) and ventral (vm) pancreatic mesenchyme. (B) E14.5 mouse embryo (mid development). In the stomach, Shh is expressed along a gradient with highest expression in the anterior stomach. Conversely, Ihh is expressed along a gradient with highest expression in the posterior compartment. Both Shh and Ihh are expressed in the duodenum, and Ihh, Dhh, Ptch and Hhip are detected in the pancreas. Expression of Hh signalling components has not been determined in developing liver or gall bladder at e14.5. (C) Adult mouse (late/post development). Ihh, Dhh, Ptch, Hhip and Smo are expressed in islet endocrine cells. Ptch expression has been detected in pancreatic ducts. Hh signalling components are not normally expressed in exocrine cells. Adapted from [90].

3.1.2 Hedgehog Pathway in the Adult Pancreas

Traditionally, Hh signalling was thought to be quiescent in adult tissues, but increasing and interesting data now support the hypothesis that there is active Hh signalling in the mature pancreas, implicated both in tissue maintenance and function. The expression of Hh ligands in the mature pancreas seems to be restricted to the pancreatic ducts, and islets. In contrast to Shh, both Ihh, Ptc1 and Smo have been typically shown to be expressed in the β-cells of islets, and colocalized with insulin as seen in Figure 12 [88; 117-119].

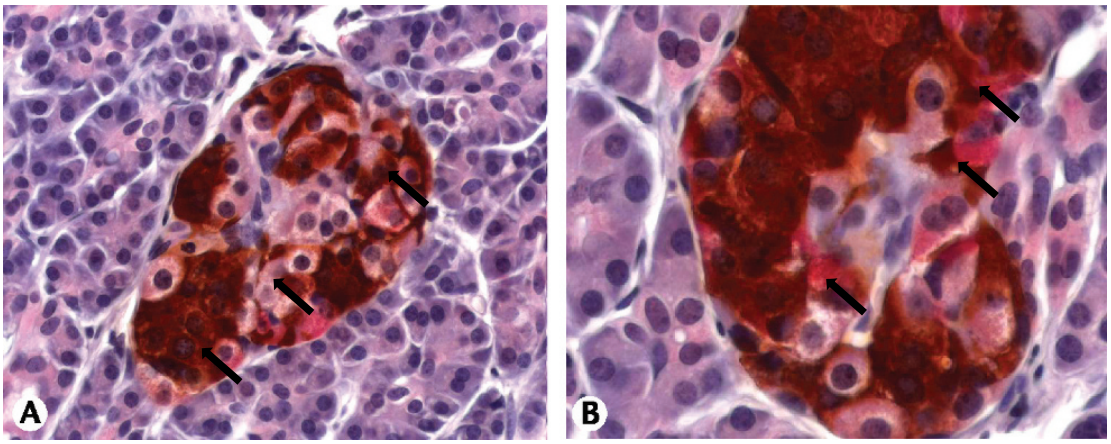

Figure 12: Co-expression of Ihh and insulin in normal pancreatic islets. Double staining immunohistochemistry was performed in normal pancreatic tissue samples using anti-Ihh (red) polyclonal and anti-insulin (brown) monoclonal antibodies. Note that some islet cells express only Ihh, some express only insulin, and some do not express either molecule. Adapted from [117].

Majority of the most convincing and compelling data supporting the implication of Hh pathway in mature endocrine cells is from *in vitro* studies. Ectopic expression of Shh in rat insulinoma cell line INS-1, resulted in increase of both insulin production, and secretion at the transcriptional levels [118]. Another parallel study from Thomas et al, showed that rat insulin 1 promoter contains a Hh responsive regions, that comprise the glucose response elements Far (E2) and Flat (A2/A3). Activation of Hh signaling in INS-I cells by ectopic Hh expression,

resulted in an increase in the transcriptional activation of the multimerized FarFlat reporter construct. Furthermore, western blot analysis showed ectopic Hh expression resulted in an increase in nuclear IDX-1 (Islet Duodenum Homeobox-1) protein levels, thereby, providing a mechanistic explanation for Hh-mediated regulation of the insulin promoter. In transient transfection studies with a 24.5-kb mouse IDX-1 promoter-reporter construct, ectopic Hh expression also increased transcriptional activation of the IDX-1 promoter in a dose-dependent manner. These results support the notion that IDX-1 gene at least in part is a direct regulatory target of Hh signaling in insulin producing pancreatic β-cells.

The Hh pathway has been shown to be negatively regulated by a cell surface protein, Hedgehog Interacting Protein (Hhip). Hhip is a naturally occurring negative regulator of the Hh signalling pathway. Hhip, a transmembrane glycoprotein, acts as a biological antagonist of the Hh pathway, and it is upregulated in response to Hh signaling. Hhip was discovered by screening mouse cDNA expression library for proteins that can bind to all the Hh pathway ligands [85]. Human and mouse Hhip gene shares approximately 94% homology, and its expression has been identified in most human foetal and adult tissues [85; 110].

During development, Hhip expression has been demonstrated in adjacent tissues to the pancreas, such as the duodenum, and the stomach. Biochemical studies have shown that Hhip binds to all three mammalian hedgehog proteins (SHH protein, IHH protein and desert DHH protein), with equal affinity to inhibit their biological activities with the same affinity as Ptch [86]. By competing with Ptch for binding of hedgehog ligands, Hhip negatively regulates the Hh pathway. Evidence points to the fact that, ectopic expression of Hhip inhibits Hh signaling in bone, and pituitary glands, while loss of Hhip function results in increase of Hh signaling, highlighting the inhibitory role of Hhip [85; 112]. Interestingly, increased Hhip expression is

observed predominantly in vascular endothelial cells, but down regulated in Human umbilical vein endothelial cell (HUVEC), during angiogenesis. Alternatively, Hhip mRNA levels were significantly decreased in several human tumours, as well as in vascularized human tumours grown in nude mice. These data together lend support to Hhip's role as a naturally occurring Hh signalling pathway regulator [85].

3.2 Hhip and the Pancreas

The activities of the Hh signaling pathway, and its associated ligands are controlled by ligand binding proteins, such as Ptch, or negative regulators like Hhip. Hhip, being a transcriptional target of Hh signaling pathway was shown to be colocalized with Ptch, in adjacent tissues to the pancreas, that have an active Hh ligand expression, and activity [88; 106]. Since there is the expression of some of the Hh ligands during pancreas organogenesis, to further establish the expression, and role of Hhip in the developing pancreas, a heterozygous Hhip-LacZ knock-in animals that express lacZ under the control of the endogenous Hhip promoter was used to determine Hhip's expression pattern in the fore-mid gut area by staining for β -galactosidase activity [88]. Interestingly, the expression of Ptch, and Hhip was found in tissues adjacent to the pancreas, such as stomach, and duodenum; nonetheless, macroscopic analysis did not reveal any β-galactosidase activity in either the embryonic or adult pancreatic tissue [88]. Upon analysis of adult tissue, there was the revelation of very low levels of β-galactosidase activity within pancreatic islets. A more sensitive RT-PCR analysis further revealed low levels of Hhip expression throughout pancreas development and in mature tissue.

Likewise, low levels of Hhip expression was also confirmed in studies by Kayed et al, comparing Hhip levels in normal human pancreas as oppose to cancerous human pancreatic

tissues (chronic pancreatitis (CP) and (pancreatic ductal adenocarcinoma (PDAC)), which had a fourteen- and fifteen-fold increase respectively as seen in Figure 13 [110].

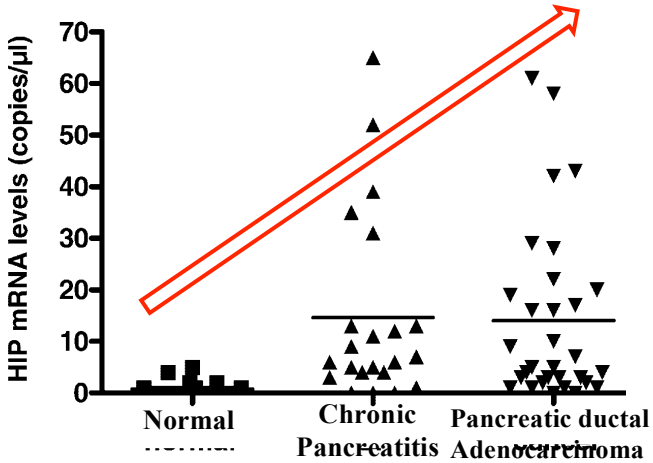

Figure 13: Real-time quantitative RT-PCR: mRNA was extracted from pancreatic tissues as described in the Methods section. (A) analysis of Hip mRNA levels in pancreatic tissues, normal (n 1⁄4 20) (black squares), CP (n 1⁄4 22) (upright triangles) and PDAC tissue samples (n 1⁄4 31) (inverted triangles). Adapted from [110].

Hhip homozygous ($Hhip^{-/-}$), and heterozygous ($Hhip^{+/}$) mutant mice were further used to delineate Hhip's function in regulating Hh signaling during pancreas organogenesis, and to analyze for β-galactosidase activity. Significant increases of β-galactosidase activity in homozygous ($Hhip^{-/-}$) embryos compared to heterozygous ($Hhip^{+/-}$) mutants suggested an increase in Hh signaling with loss of Hhip. Furthermore, RT- PCR data of Gli mRNA levels (a downstream target transcription factor and target gene of Hh signaling), showed a significant increase in homozygous ($Hhip^{-/-}$), compared to heterozygous ($Hhip^{+/-}$) embryos, illustrating loss of Hhip potentiates Hh signaling during pancreatic organogenesis. This also highlights the role of Hhip as a negative regulator of Hh signaling, and the importance of regulating Hh pathway signaling during development, and in disease conditions.

Organ formation analysis in the fore-midgut area (where the pancreas buds during organogenesis), indicates that pancreatic morphogenesis is disrupted as a result of a loss in Hhip. In the most severe cases, there was fusion of both dorsal, and ventral parts of the pancreas, forming a compact mass of tissue that is reduced in size. During normal pancreas organogenesis, the ventral pancreas tissue is attached to the dorsal duodenal region, extending ventrally to the mediolateral duodenal area. In Hhip mutant mice, there was the formation of ectopic pancreas, but the pancreatic tissue was shown to be incorporated into the duodenum, and the spleen which normally buds off from the stomach mesenchyme posterior region, was also shown to be deformed and reduced in mass. All the above observations highlight the importance of Hhip's function in proper organ (pancreas and spleen) formation. Unfortunately, the potential effect of Hhip in the functioning of the adult pancreas could not be evaluated as Hhip homozygous null mutants die at birth due to lung malformation.

Identification of Hh signaling components in pancreatic endocrine cells shows their activity is required for some aspects of cell differentiation, as well as for proper organ functioning. Pancreatic islets formation normally starts at the end of gestation, when the four major different endocrine cell types (α,β, δ and γ cells) aggregate as clusters of cells. Compared to Hhip ($Hhip^{-/-}$) mutant mice, pancreatic sections from Hhip ($Hhip^{+/+}$) wild type mice shows that the islets do form distinct, and discrete clusters of cells characterized by a central core of insulin-producing β-cells, surrounded by glucagon positive α-cells, while the latter shows that the pancreatic endocrine cells were still clustered into distinct islet-like structures, but with a significant reduction in the size of the resulting aggregates. In contrast to Hhip ($Hhip^{+/+}$), Hhip ($Hhip^{-/-}$) mutant had an approximated 45% reduction in islet area after adjustments for changes in body mass. The loss in larger islets (>4000 μm^2) in Hhip ($Hhip^{-/-}$)

mutant was identified as the main contributing factor to the decrease in total islet area, while preserving their ratio of smaller islets (<4000μm^2). Double immunofluorescence staining of insulin/Ki-67 (a marker for proliferation), confirmed the loss of pancreatic β-cell was as a result of a significant decrease in proliferation in the Hhip (Hhip$^{-/-}$) mutant compared to Hhip (Hhip$^{+/+}$) wild type mice. Analysis of mature β-cell markers such as Pdx1, and Glut2 (glucose transporter 2) were also analyzed in these mice to further delineate the effect of increased Hh signaling, and the influence on pancreatic β-cell differentiation. Interestingly, the expression levels of the markers were unchanged in both genotypes, illustrating that elevated Hh signaling primarily impairs pancreatic β-cell proliferation, and not differentiation as shown in Figure 14.

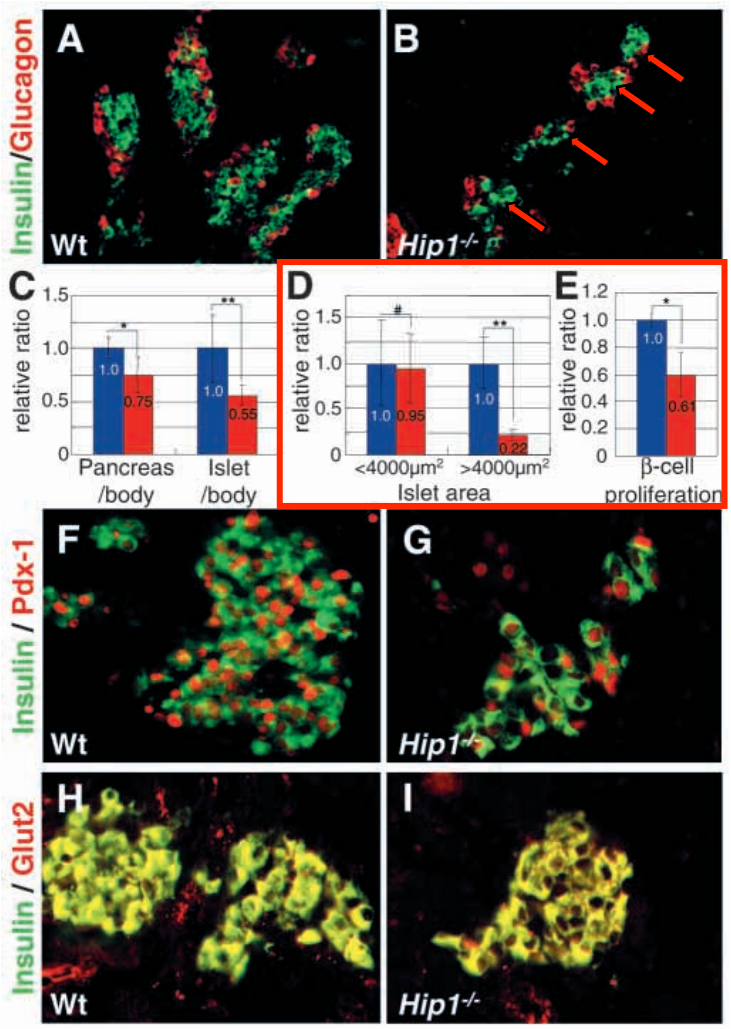

Figure 14: Islet mass and β-cell proliferation is decreased in *Hhip*$^{-/-}$ embryos. Islets were stained with antibodies directed against centrally located insulin (green) and marginally located glucagon producing cells (red). Hhip function is required for normal islet morphogenesis (A, B). Clusters of insulin- and glucagon-positive cells form but are significantly smaller than the ones in control embryos (wild-type or heterozygotes, compare B with A). To adjust for differences in body mass, pancreas weight and islet area were divided by body weight. Quantification of islet areas revealed a 45% reduction that is more pronounced than the general loss of pancreatic tissue (C, blue, control; red, *Hhip*$^{-/-}$). The reduction in islet mass is due to the loss of larger islets (>4000 µm^2, while the number of smaller islets (>4000 µm^2) is maintained in Hhip mutants (D, blue, control; red, *Hhip*$^{-/-}$). Staining for the nuclear marker Ki-67 showed that proliferation of β-cells at E18.5 is reduced by 39% (E, blue, control; red, *Hhip*$^{-/-}$). Changes in islet morphogenesis and β-cell proliferation are not due to incomplete cell differentiation (F-I). β-cells express mature markers, including Pdx1 (F, G; insulin, green; Pdx1, red) and glucose transporter 2 (H, I; insulin, green; Glut2, red). Adapted from [88].

Interestingly, besides its involvement in embryogenesis, Hh and Hhip signaling can also be involved in various stages of carcinogenesis in different tumors, such as in pancreatic, and esophageal cancer, where Hh signaling pathway activation is found in both the early stages, as well as in metastatic forms of the tumors. In other tumors, for example gastric cancer, and prostate cancer, Hh signaling pathway activation is associated with tissue invasion, and increased metastatic potential [106; 120-121]. Hh signaling was also shown to rescue pancreatic β-cells from cytokine-induced apoptosis, by suppressing nuclear factor- κ B promoter activity, resulting in attenuation of inducible nitric oxide synthase (iNOS) 2 expression, and nitric oxide (NOX) production [122].

3.3 Hhip and Diabetes Mellitus

Even though the Hh signaling pathway is quiescent in adult tissues, low level of Hhip gene expression has been detected in normal mature pancreas, precisely in peripheral cells of the islets, and in the smooth muscle cells of blood vessels, but conspicuously absent in the pancreatic acini, with an upregulation in pancreatitis. Genome-wide diabetes profiling database revealed that as compared to lean animals, there seems to be a significant up-regulation of Hhip mRNA levels in the islets of both 4, and 10, weeks old diabetic ob/ob mice (these mice carry a single autosomal recessive mutation on the gene encoding leptin leading to a disruption in the satiety pathway) both on the C57/BL6, and BTBR backgrounds [123]. Analysis of other tissues such as the liver, adipose, soleus, gastrocnemius and hypothalamus from the same mice did not reveal any changes in Hhip levels, emphasizing the importance of Hhip to the islets and in DM especially T2DM as summarized in Figure 15.

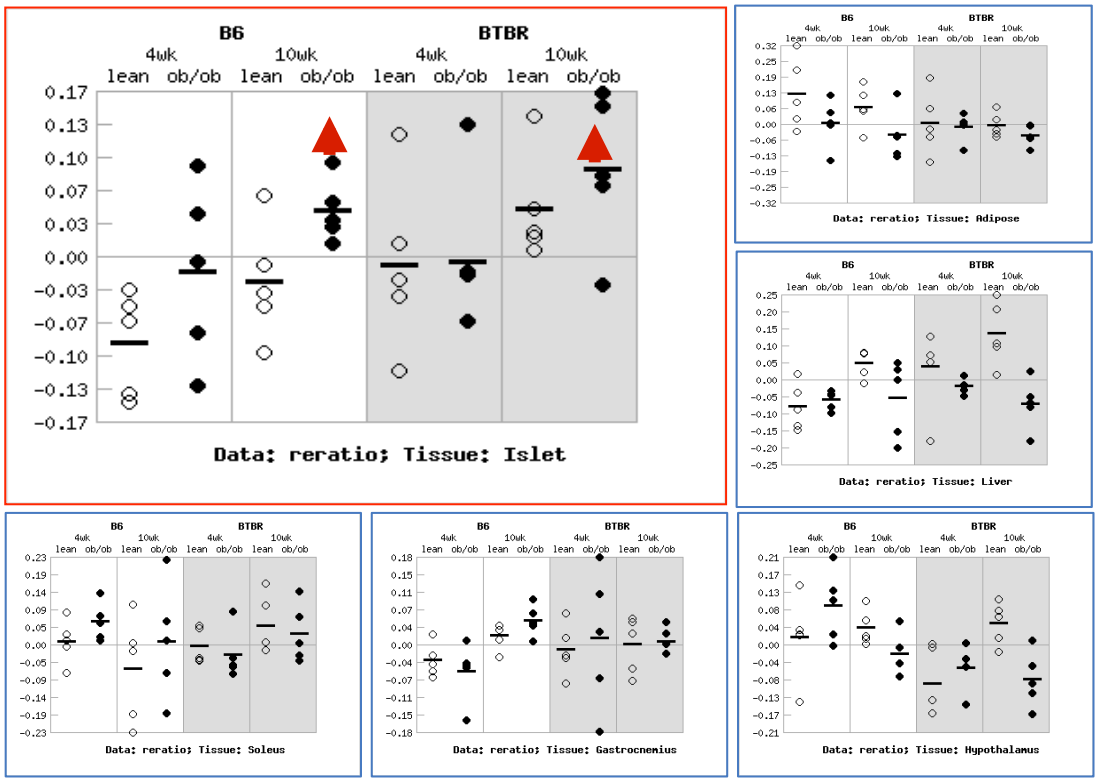

Figure 15: Hhip mRNA expression in Ob/Ob mice. Genome-wide diabetes profiling revealed increase Hhip mRNA levels in islets of both 4 and 10 weeks old diabetic ob/ob mice compared to lean controls. Adapted from [123].

B: Published Article 1

Hedgehog Interacting Protein (Hhip) Regulates Insulin Secretion in Mice Fed High Fat Diets

Henry Nchienzia[1], Min-Chun Liao[1], Xin-Ping Zhao[1], Shiao-Ying Chang[1], Chao-Sheng Lo[1], Isabelle Chenier [1], Julie R. Ingelfinger [2], John S.D. Chan[1] and Shao-Ling Zhang [1§]

[1]Université de Montréal
Centre de recherche du Centre hospitalier de l'Université de Montréal (CRCHUM)
Tour Viger, 900 rue Saint-Denis, Montréal, QC, Canada H2X 0A9

[2] Harvard Medical School
Pediatric Nephrology Unit
Massachusetts General Hospital
55 Fruit Street, Boston, MA 02114-3117, USA

[§] To whom correspondence should be addressed: Shao-Ling Zhang, Ph.D.
Tel: (514) 890-8000 ext. 15633
Fax: (514) 412-7204
Email: shao.ling.zhang@umontreal.ca

Short Title: Hedgehog interacting protein (Hhip) gene and pancreatic beta cell dysfunction

Key words: High Fat Diet, Hhip Gene Expression, Pancreatic beta Cell Dysfunction

Author Contribution

SLZ is the guarantor of this work, had full access to all study data, and takes responsibility for data integrity and the accuracy of data analysis. JSDC and SLZ were principal investigators and were responsible for the study conception and design. HN wrote the first draft of the manuscript, and SLZ drafted/reviewed/edited the manuscript. HN (Figures 16, 17, 18, 19, 21, 22, 23, and 24), MCL (Figures 25b, 26a and 28a), XPZ (Figures 20, 26b, 27 and 28a and b), SYC (Figure 25a), CSL (design and discussion), IC (Figures 16a, 18a, 19a, design and discussion) and SLZ contributed to the experiments and collection of data. JRI contributed to data discussion and reviewed/edited the manuscript. All authors were involved in the analysis, interpretation of data and contributed to the critical revision of the manuscript. All authors provided final approval of the version to be published.

ABSTRACT

Hedgehog interacting protein (Hhip), is essential for islet formation, and beta-cell proliferation during pancreatic development; abnormally elevated Hhip expression has been linked to human pancreatitis. Here, we investigate the role of Hhip in modulating insulin secretion in adult Hhip mice ($Hhip^{+/-}$ vs. $Hhip^{+/+}$) fed high fat diet (HFD). Both sexes of HFD-$Hhip^{+/+}$ mice developed impaired glucose intolerance, that was only ameliorated in male HFD-$Hhip^{+/-}$ mice that had high levels of circulating plasma insulin, but not in female HFD-$Hhip^{+/-}$ mice. HFD stimulated Hhip gene expression, mainly in beta cells. Male HFD-$Hhip^{+/+}$ mice had more large islets in which insulin content was reduced; islet architecture was disordered; and markers of oxidative stress (8-OHdG and Nox 2) were increased. In contrast, male HFD-$Hhip^{+/-}$ mice had more small islets with increased beta cell proliferation, enhanced GSIS, less oxidative stress and preserved islet integrity. In vitro, recombinant Hhip increased Nox2 and NADPH activity and decreased insulin-positive beta cells. siRNA-Hhip increased GSIS and abolished the stimulation of sodium palmitate (PA)-BSA on Nox2 gene expression. We conclude that pancreatic Hhip gene inhibits insulin secretion by altering islet integrity and promoting Nox2 gene expression in beta cells in response to HDF-mediated beta cell dysfunction, a novel finding.

1.0 Rationale and Background Knowledge

The role of Hh signaling in adult tissue is much reduced compared to that in the embryo, or neonate, and may be limited but important to a few sites, such as a hair growth, spermatogenesis, the proliferation of stem cells in the hemopoietic system, mammary glands, and areas of tissue damage, where it is primarily involved in tissue repair [87; 111; 124]. The ability of Hh signaling pathway ligands to induce proliferation, especially in embryogenesis, and tissue maintenance, is very important. Recently, it has been recognized that the aberrant activation of the Hh signaling pathway is also involved in many disease conditions, such as cancers (including basal cell carcinomas (BCCs-human skin cancer), medullablastomas (childhood brain cancer), gliomas, digestive tract, pancreatic and small-cell lung tumours), and diabetes mellitus (in islets and kidneys of Ob/Ob, Akita and db/db mice) respectively. Under pathological conditions, they actively initiate proliferation, differentiation, and the acceleration of tumor growth in a variety of tissues. This highlights the importance of regulating the Hh signaling pathway and presents a potential therapeutic target [87; 93;124-126]. Pharmacological regulation of the Hh signalling pathway has been achieved with cyclopamine, a naturally occurring alkaloid, which was the first SMO antagonist. Besides pharmacological inhibitors, Hhip, is the only naturally occurring negative regulator of the Hh signalling reported in the literature that competes with Ptch1 for Hh ligand binding [85; 110].

Hhip is necessary for proper pancreas organogenesis, since Hhip null mice ($Hhip^{-/-}$) display markedly impaired pancreatic islet formation (45% reduction of islet mass with a decrease of β-cell proliferation by 40%). This underscores the importance of Hhip gene expression to the pancreas. However, $Hhip^{-/-}$ mice die shortly after birth mainly due to lung defects [88].

We recently showed that impaired nephrogenesis in kidneys of offsprings of our murine model of maternal diabetes was associated with up-regulation of Hhip gene expression [128]. We subsequently established with our recent data that hyperglycemia induced renal Hhip gene expression in adult murine kidneys of both T1DM (Akita) and T2DM (db/db), leading to apoptosis of glomerular epithelial cells, and was responsible for endothelial to mesenchymal transition (Endo-MT)- related renal fibrosis [127]. The contribution of Hhip gene and protein expression, and its implication in the functioning of adult murine pancreas under normal and disease conditions, especially in a model of T2DM, has not yet been elucidated or established.

2.0 Research Questions/ Hypothesis/Aims/Objectives

2.1 Research Question

For this dissertation we asked the following questions:

- Question 1: What is the distribution pattern of Hhip/which cells are most targeted within the endocrine pancreas under High Fat Diet feeding?
- Question 2: What are the pathophysiological effects associated with/impacts of pancreatic Hhip gene expression under High Fat Diet feeding?
- Question 3: What are the potential mechanisms of High Fat Diet induced pancreatic Hhip gene expression *in vivo and in vitro*?

2.2 Ph.D. Thesis Hypothesis

The long-term goal of our research and of this chapter is to understand the pathophysiological function of pancreatic Hhip. We hypothesized that in a model of high fat diet-induced obesity, increase Hhip gene expression as a result of high fat diet feeding promotes β-cell dysfunction, hence compromising glucose stimulated insulin secretion (GSIS). Because Hhip null mice ($Hhip^{-/-}$) mice die shortly after birth due to lung malformation, in this study, we employ the use of Hhip ($Hhip^{+/-}$) heterozygous mice to investigate the role of Hhip beyond the embryonic endocrine pancreas development. Although it has been shown that Hhip is vital in murine endocrine development, no data has been published specifically demonstrating the pathophysiological role of Hhip in adult murine pancreas.

2.3 Aims/Objectives

Therefore, the objective of this dissertation was to investigate the pathophysiological role of Hhip, and the effect of increasing Hhip in pancreatic β-cells, its function under diabetic conditions in a model of diet induced-obesity, and further elucidate the underlying mechanisms of action *in vivo, ex vivo* and *in vitro.*

3.0 Materials and Methods

3.1 The *in vivo* and *in vitro* Models

3.1.1 *In vivo* Models

Both wild type ($Hhip^{+/+}$), and heterozygous Hhip ($Hhip^{+/-}$) male and female mice were used for this current study (Jackson Laboratories, $Hhip^{tm1Amc}$/J; mixed background), since $Hhip^{-/-}$ die after birth due to lung malformation. Adult $Hhip^{+/-}$ are indistinguishable from control littermates $Hhip^{+/+}$. Mice were housed under standard humidity and lighting conditions (12 h light–dark cycles), with free access to standard normal chow, high fat diet, and water ad libitum. 6 weeks old male and female ($Hhip^{+/-}$ and $Hhip^{+/-}$) mice were either fed normal chow (ND) (18% protein with 6.2% fat, 24% calories from protein, 18% fat and 58% carbohydrate) (Harland, Teklad, Montreal, Canada), or high fat (HFD) (20.5% protein with 36% fat, 14% calories from protein, 60% fat and 26% carbohydrate) (Bio-serv, Flemington, NJ) up to 14 weeks of age as previously reported [129]. After euthanasia at 14 weeks, pancreata were rapidly harvested, cleaned of all fat, weighed, immediately immersed in 4% paraformaldehyde and stored at 4°C for fixing. Tissues were subsequently embedded in paraffin after successful dehydration in ethanol for either immunohistochemistry (IHC), and/or immunofluorescence (IF). Animal care and procedures were approved by the Institutional committee for the protection of animals of the of the Centre de Recherche du Centre Hospitalier de l'Université de Montréal (CIPA-CRCHUM).

3.1.2 *In vitro* Model

To elucidate the mechanism of action of pancreatic Hhip *in vitro*, we employed the use of rat pancreatic β-cell line INS 832/13 (which has been shown to respond to glucose concentrations (2.8-16.8mM) within physiological ranges), kindly provided by Dr. Marc Prentki (CRCHUM, Montreal, QC. Canada. These cells (passage 51-53) were cultured in complete medium composed of RPMI 1640 medium supplemented with 10% fetal bovine serum, 50 μM β- mercaptoethanol, 10 mM HEPES, 2 mM L-glutamine, 1 mM sodium pyruvate, and 50 mM beta-mercaptoethanol. Cells were grown in a 37^{o}C incubator under a humidified atmosphere containing 5% CO_2 and 95% air.

3.2 Biological, Metabolic Parameters and Physiological Measurements

3.2.1 Biological and Metabolic Parameters

Body weight (BW, g- measured in the morning), and energy intake (kCal/week- calculated from food comsumption after weighing the food in the morning) were monitored weekly throughout the course of the experimental study. Mice body composition (fat and lean mass as a percentage of body weight) was assessed before, and after the study using an EchoMRI-700 at the Rodent Cardiovascular Phenotyping Core Facility (CRCHUM).

Intraperitoneal glucose tolerance test (IPGTT), and intraperintoneal insulin tolerance test (IPITT) were performed according to a standard protocol with 6- and 4-hours fasting period at the age of 14 weeks respectively, as reported elsewhere [129]. In brief, for IPGTT, 3μl of tail blood was used to measure fasting blood glucose with a portable glucometer and glucose test strips using an Accu-Chek Performa glucose meter (Roche Diagnostics, Laval,

Canada). Subsequently, animals received 2g/kg body weight sterilized and filtered glucose intraperitoneal (ip) injection and blood glucose was measured at 15, 30, 60, 90 and 120 mins from tail blood post injection. 15µl of blood was collected using heparinized capillary tubes at each time point, and plasma obtained after centrifugation of blood samples was stored at −20°C until assayed for insulin. Circulating plasma insulin was measured by mouse ultrasensitive ELISA jumbo kit (Alpco Diagnostics, Salem NH).

For IPITT, fasting blood glucose was measured as above. Animals also received an ip injection of 1 Units/kg filtered-sterilized insulin (Eli Lilly Canada, Toronto, Canada) and blood glucose was measured as described above for 15, 30, 60 and 90 mins respectively, post injection.

Systolic blood pressure (SBP), was monitored using the tail-cuff method with a BP-2000 Blood Pressure Analysis System (Visitech System Inc., Apex, NC) as reported [129]. Acclimatization of animals to SBP measurement was done starting at 13 weeks of age, which served as a 1week pre-training period (SBP measured thrice weekly), followed by actual SBP measurements three times a week at 14 weeks of age.

3.2.2 Islet Isolation, Culture and Glucose Stimulated Insulin Secretion (GSIS)

The islet protocol as used by [139] was followed. In brief, islets from both ND and HFD fed mice were isolated by injecting 3ml of collagenase P (0.65mg/ml in HBSS/HEPES) into the pancreas after cannulation of the bile duct, performed under a dissecting microscope. Pancreas were subsequently incubated for 12 mins at 37^{o}C water bath, and vigorously washed with 5% BSA-HBSS to remove collagenase. Tubes were further centrifuged at 333 g for 3 mins at 4^{o}C, and the supernatant gently discarded. 5%-BSA-HBSS was gently added to

redissolve pellet. The resulting mixture was filtered through a mesh fabric into new corresponding tubes, and again centrifuged at 333 g for 3 mins at 4°C. The pellet was further resuspended in Histopaque 1191 and 1077 (Sigma), and topped off with 5% BSA-HBSS, respectively. The mixture was centrifuged at 2700g for 25 mins; the individual pancreatic islets were collected under a dissecting microscope. Part of the islets were used directly for Western Blot (WB), and qPCR analysis, while islets for GSIS were kept in culture at 37°C in 2.8mM glucose RPMI complete medium, supplemented with 10% fetal bovine serum (FBS) for overnight recovery.

After recovery, batches of 10 islets in triplicates were distributed in 6 well plates, and pre-incubated for 45 minutes at 37°C, 5% CO_2 in Krebs-Ringer bicarbonate buffer containing 10mM HEPES (pH 7.4, KRBH), 0.5% defatted BSA (d-BSA), and 2.8mM glucose. Media was changed, and replaced with fresh in KREBH/0.5% d-BSA at 2.8 glucose for 1 hour at 37°C, 5% CO_2. They were subsequently incubated for 1hour in KRBH/0.5% d-BSA at 2.8, and 16.9mM glucose respectively at 37°C, 5% CO_2 to determine glucose stimulated insulin secretion. Media was collected after incubation, spun at 5000rpm at 4°C for 5 mins and kept at -20°C for insulin measurements. Total islet insulin content was measured by acid-ethanol (0.2 mM/l HCL in 75% ethanol) extraction after overnight incubation of islets in 1ml at 4°C, sonicated for 30secs, and centrifuged at 13000g for 10 mins at 4°C. The supernatant was collected and stored -20°C for further analysis. Insulin in both supernatant and islet extracts were measured at the Cellular Physiology Core Facility (CRCHUM).

3.2.3 β-Cell Mass, Islets Number and Size Measurements

Several pancreatic and islet parameters were analyzed at the Cellular Physiological Core Facility (CRCHUM). Longitudinal 5μm paraffin ribbon like sections of embedded

pancreas was mounted on adhesive positively charged slides to facilitate analysis. At 30μm interval, 3 sections/animal from 4-6 slides were deparaffinised in xylene, and subsequently hydrated in ethanol, and PBS solutions respectively. The hydrated slides were stained by Hematoxylin-Eosin staining and mounted in Permout (Fisher Scientific) according to a standard protocol. Slides were scanned at 20X magnification (scan bright field scope system) by using an Aperio ScanScope model CS slide scanner (Leica Biosystems Inc., Concord, ON, Canada), to assess islets/β-cell area, and whole pancreas area via the Apero Pixel count algorithm v9 (ImageScope v12.3.2.5030, Leica Biosystems Inc.) This was followed by β-cell area to whole pancreas calculations. β-cell mass, was subsequently calculated by multiplying the ratio of beta cell area to whole pancreas area whole pancreas area, by using the whole pancreatic masses (mg) measured before pancreata fixation. Morphometric measurements were performed by manually identifying regions of interest around islets. The surface of all islets from atleast 4 sections (>400 islets), were calculated for each region of interest (ImageScope) and used to generate the size frequency distribution profile.

3.2.4 Histology

Slides were deparaffinised in xylene, and subsequently hydrated in ethanol, and PBS solutions respectively. To analyze β-cell proliferation, antigen retrieval was achieved by microwaving deparaffinised slides for 10mins in 10mM sodium citrate buffer pH 6.0. Hydrated slides for IF, and IHC were subsequently washed in PBS, and sections circled with a PAP pen, and treated with trypsin for 12mins at 37°C. Slides were rinsed again in PBS pH 7.4, and blocked in 10% normal donkey serum for 1 hour, and further incubated in a wet chamber overnight with the respective primary antibody at 4°C.

For IF, slides were subsequently incubated with a mix of conjugated secondary antibodies fluorophore, for 2h at room temperature protected from light. Nuclei staining was achieved by using 1 μg/ml 4', 6'diamidino-2-phenylindole (DAPI) staining, following incubation of secondary antibodies, and mounted in movial mounting media.

For IHC, slides were further analyzed using the ab64261-Rabbit specific HRP/DAB (ABC) detection kit according to the manufacturer's instructions (Abcam, Cambridge, MA, USA).

3.2.5 Oxidative Stress and Real-time Quantitative PCR (qPCR)

Oxidative stress was determined by 8-hydroxy-2-deoxyguanosine (8-OHdG) staining (a biomarker for oxidative stress), or dihydroethidium (DHE) staining (a cell permeable fluorescent dye, redox indicator) marker for reactive oxygen species (ROS) damage, and also NADPH oxidases (Nox 1, 2 and 4), gene expression and NADPH activity. qPCR (Fast SYBR green mastermix kit, and the 7500 Fast real-time PCR system; Applied Biosystems, Foster City, CA, USA). qPCR primer sequences are listed in Table 1.

Table 1 - Primers sequences

Gene	Primer sequences	Reference Sequence
18S ribosomal RNA	S: AGTCCCTGCCCTTTGTACACA AS: CGATCCGAGGGCCTCACTA	NR_003278.3
β-actin (Rat)	S: ATCGGCAATGAGCGGTTCC AS: AGCACTGTGTTGGCATAGAGG	NM_031144.3
Glut2	S: CACACCAGCATACACAACACCAG AS: GGACACAGACAGAGACCAGAGC	NM_031197.2
Insr	S: CATGTGCAGGAATGGCTTGTT AS: TTCTGCGTTTTCTGCAGTGCTA	NM_010568.3
Irs1	S: AATCCTCAGGAGTTCATTGACTGAA AS: TTCCGGTGTCACAGTGCTTTC	NM_010570.4
Irs2	S: GGCCCGAACCTCAATAACAA AS: CCGCGCAACACGAAAAAG	NM_001081212.2
Nox2 (Mouse)	S: TGTGGTTGGGGCTGAATGTC AS: CTGAGAAAGGAGAGCAGATTTCG	NM_007807.5
Nox2 (Rat)	S: CCCTTTGGTACAGCCAGTGAAGAT AS: CAATCCCAGCTCCCACTAACATCA	NM_023965.1
Nox4 (Mouse)	S: GAAGGGGTTAAACACCTCTGC AS: ATGCTCTGCTTAAACACAATCCT	NM_015760.5
Nox4 (Rat)	S: TGGCCAACGAAGGGGTTAAA AS: GATCAGGCTGCAGTTGAGGT	NM_053524.1

Table 1: List of primers sequences

3.2.6 Immunoblot Analysis

Islets and cells were lysed in RIPA buffer after treatment with either palmitic acid conjugated with BSA or Recombinant Hhip (rHhip) protein (R&D Systems, Inc.). Twenty-microgram aliquots of protein were resolved on 10% bis-Tris-HCl-buffered (pH 6.4) polyacrylamide gels, transferred to polyvinylidene difluoride membranes, blocked in 5% powdered milk, and tris-buffer with Tween 20 for 3 h. Membranes were incubated overnight at 4°C, and primary antibodies were detected using appropriate secondary antibodies (either biotinylated antimouse or antirabbit) for 2 h at room temperature, and visualized using ECL.

3.2.7 Reagents and Chemicals

Antibodies used comprise anti-Hhip (5D11), glucagon, β-actin from Sigma-Aldrich Canada (Oakville, ON, Canada); anti-KI 67 from BD Bioscience (San Jose, CA, USA); anti-insulin (H-86) from Santa Cruz Biotechnology (Santa Cruz, CA, USA), and anti-mouse 8-OHdG from Abcam (Toronto, ON, CA). Mouse anti-Nox2 antibody (anti-gp91phox-Cter), acquired from Dr. Nathalie Grandvaux (CRCHUM) as described in [131]. Chemical reagents included small interfering RNA (siRNA) for Hhip from Life Technology, Inc., (Mississauga, ON, Canada); recombinant Hhip (rHhip) from R&D Systems, INC. (Burlington, ON, Canada); BSA (fatty acid free), and sodium palmitate (PA) from Sigma-Aldrich Canada. The semi-quantitation of the relative staining values was performed by NIH Image J software (Bethesda, MD). The images (N = 8-15) were analyzed and quantitated in a randomized and blinded fashion.

3.3 Statistical Analysis.

Groups of 8 to 12 mice were used for this study. *Ex vivo* and *in vitro* experiments, represent three to four separate experiments for each protocol. The values represented are mean ± SEM. Statistical significance between the experimental groups was analyzed by student's t-test, 1-way or 2-way ANOVA, followed by the Bonferroni test using Prism 5.0 software (GraphPad, San Diego, CA, USA). Probability levels of $*p \leq 0.05$; $**p \leq 0.01$; $***p \leq 0.001$were considered to be significant.

4.0 Results

4.1 Basal *in vivo* Metabolic Characteristics and Insulin Secretion

We compared the growth patterns of both male and female mice fed either ND, or HFD from the age of 6 (which was considered the baseline) until 14 weeks old, in a sex-independent manner (Figure 16a-16c, male; Figure 16d-16f, female). As expected, HFD resulted in increased body weight (BW), and percentage body fat in both sexes of $Hhip^{+/+}$ vs. $Hhip^{+/-}$ animals throughout the study period. There was a rapid weight increase within the first 6 weeks of the study (Figure 16a, male; Figure 16d, female), and similar BW gain patterns (Figure 16b, male; Figure 16e, female). However, the energy intake in male HFD-fed mice over time, seems to be greater than in female HFD-fed mice (Figure 16c, male; Figure 16f, female).

EchoMRI evaluation, further revealed that both male $Hhip^{+/+}$ and $Hhip^{+/-}$ mice had comparable levels of fat/lean mass both at the age of 6, or 14-week-old, in either ND, or HFD conditions (Figure 17).

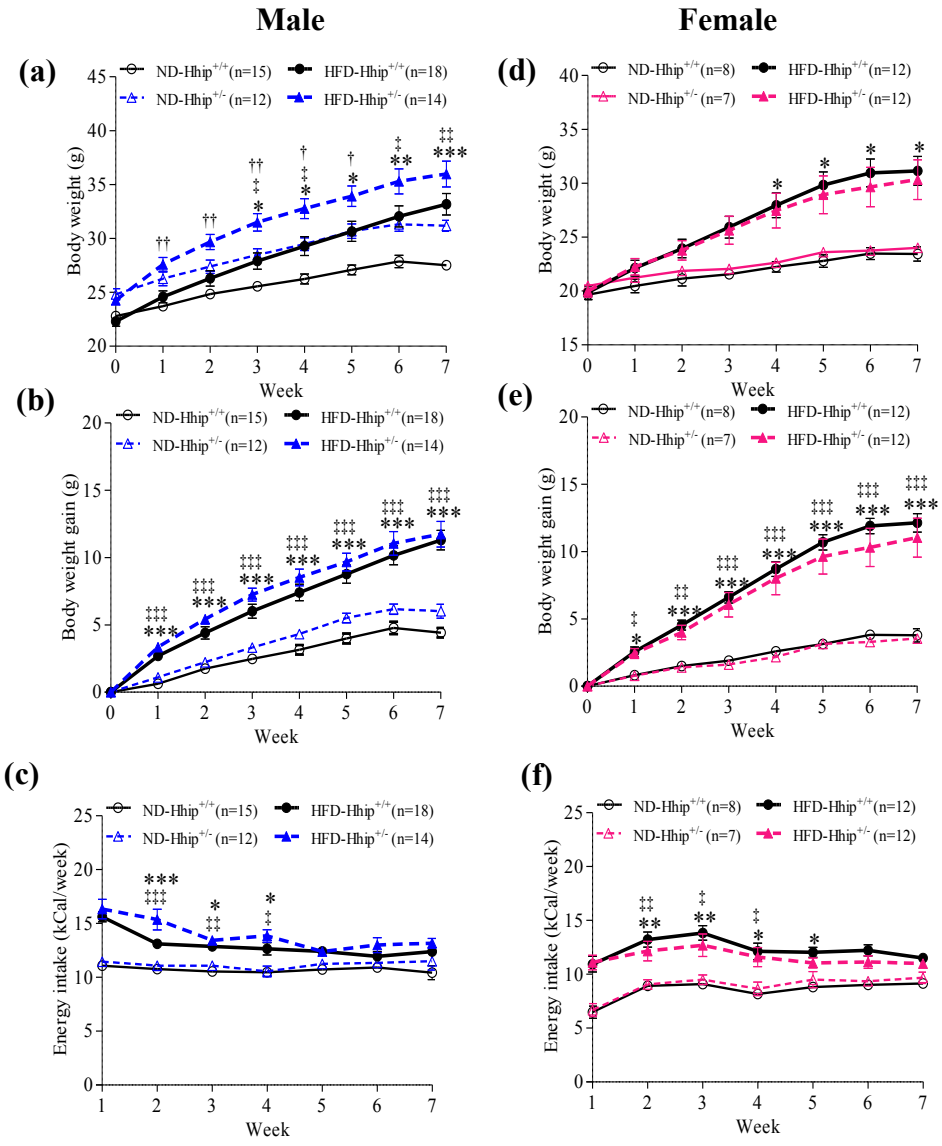

Figure 16: Physiological parameters in both male (a-c, ND-Hhip$^{+/+}$, n=15; ND-Hhip$^{+/-}$, n=12; HFD-Hhip$^{+/+}$, n=18; and HFD-Hhip$^{+/-}$, n=14) and female (d-f, ND-Hhip$^{+/+}$, n=8; ND-Hhip$^{+/-}$, n=7; HFD-Hhip$^{+/+}$, n=12; and HFD-Hhip$^{+/-}$, n=12) mice from the age of 6 to 14 weeks-old. (a, c) body weight (BW, g); (b, e) BW gain (g); (c, f) energy intake (kCal/week). Data shown as mean ± SEM; 1 way-ANOVA followed by Bonferroni's post hoc test. *$p \leq 0.05$; ** $p \leq 0.01$; *** $p \leq 0.001$ vs. ND-Hhip$^{+/+}$; $^{\#}p \leq 0.05$; $^{\#\#}p \leq 0.01$; $^{\#\#\#}p \leq 0.001$ vs. ND-Hhip$^{+/-}$; $^{\dagger}p \leq 0.05$; $^{\dagger\dagger}p \leq 0.01$; $^{\dagger\dagger\dagger}p \leq 0.001$, HFD-Hhip $^{+/+}$ vs. HFD-Hhip $^{+/-}$; NS, non-significant.

Male

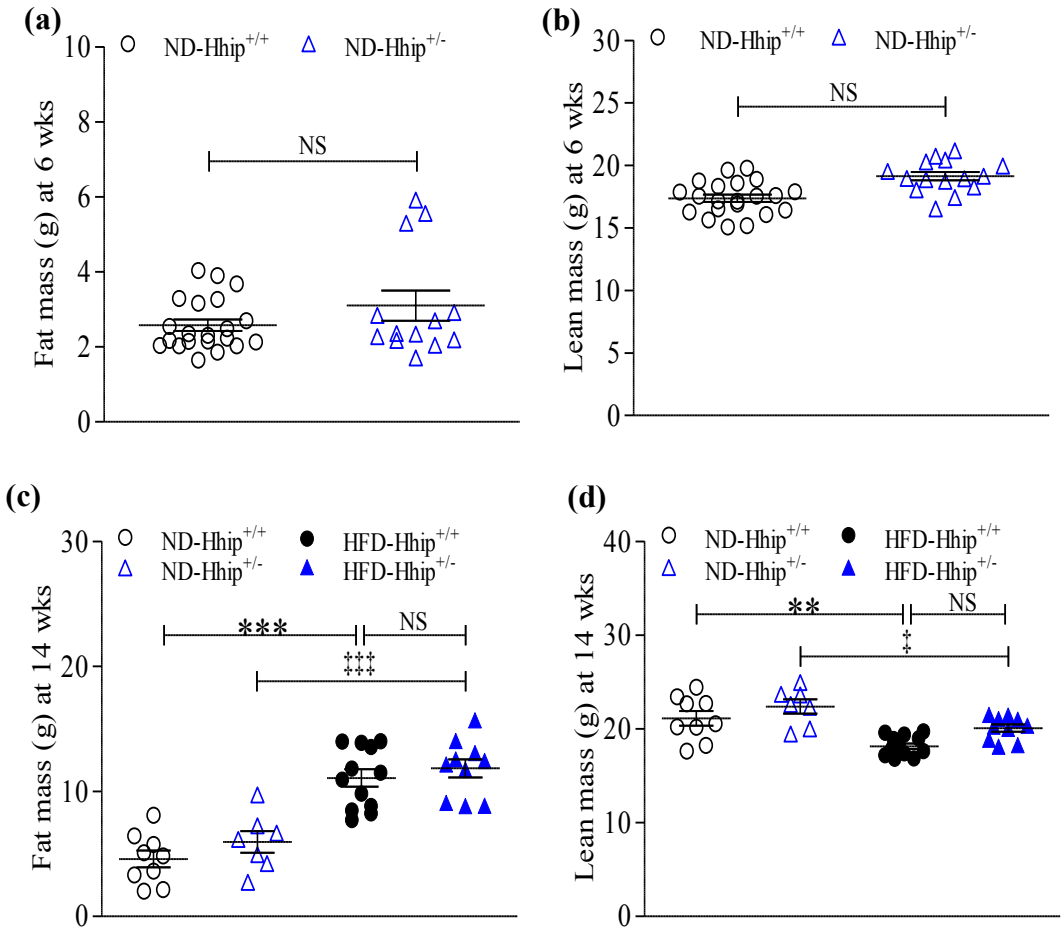

Figure 17: EchoMRI analysis in mice at the age of 6 (ND-Hhip$^{+/+}$, n=21; ND-Hhip$^{+/-}$, n=13) and 14 (ND-Hhip$^{+/+}$, n=9; ND-Hhip$^{+/-}$, n=7; HFD-Hhip$^{+/+}$, n=12; and HFD-Hhip$^{+/-}$, n=10) weeks-old. Data shown as mean ± SEM; 1 way-ANOVA followed by Bonferroni's post hoc test. *$p \leq 0.05$; ** $p \leq 0.01$; *** $p \leq 0.001$ vs. ND-Hhip$^{+/+}$; $^{\#}p \leq 0.05$; $^{\#\#}p \leq 0.01$; $^{\#\#\#}p \leq 0.001$ vs. ND-Hhip$^{+/-}$; $^{\dagger}p \leq 0.05$; $^{\dagger\dagger}p \leq 0.01$; $^{\dagger\dagger\dagger}p \leq 0.001$, HFD-Hhip $^{+/+}$ vs. HFD-Hhip $^{+/-}$; NS, non-significant.

Next, we analysed whether increased Hhip expression together with HFD challenge, might affect pancreatic β-cell function, by performing glucose tolerance tests. Intriguingly, after the 8-week period of HFD, both 14-weeks-old male, and female HFD-Hhip$^{+/+}$ mice developed pronounced glucose intolerance, and reduced glucose clearance accompanied by a significant impairment of *in vivo* glucose stimulated insulin secretion (Figure 18a, male; Figure 19a, female). This disorder of glucose intolerance is observed in pre-diabetic humans, and interestingly, this impaired IPGTT was specifically ameliorated in male HFD-Hhip$^{+/-}$ mice. No difference was observed in glucose tolerance between both male, and female ND-Hhip$^{+/+}$ and ND-Hhip$^{+/-}$mice. Quantification of the area under the curve of glucose clearance showed an approximate 30% reduction in male HFD-Hhip$^{+/-}$ mice compared to HFD-Hhip$^{+/+}$ (Figure 18b, male; Figure 19b, female). Thus, Hhip deficiency, ameliorated the metabolic phenotype of glucose intolerance detected in the cohort of HFD-Hhip$^{+/+}$ mice, further suggesting a negative correlation between Hhip levels and β-cell function.

To determine whether the glucose intolerance phenotype observed in HFD-Hhip$^{+/+}$ mice was due to a defect in pancreatic β-cells, we next analysed secreted insulin levels as a response to glucose. Measurements of circulating serum insulin in response to glucose stimuli showed that, male HFD-Hhip$^{+/-}$ compared to male HFD-Hhip$^{+/+}$ mice had significantly high levels of circulating plasma insulin (ng/ml), in total and/or in two insulin secretion phases (1st phase: 0-15 minutes; 2nd phase: 15-120 mins) (Figure 18c and 18d). Given that we observed a more exacerbated glucose tolerance phenotype, and significant hyperinsulinemia in HFD-fed male (Hhip$^{+/+}$ vs. Hhip$^{+/-}$) compared to HFD-fed female mice (Hhip$^{+/+}$ vs. Hhip$^{+/-}$) (Figure 19c and 19d), we therefore focused our analysis only on male mice for the rest of the studies.

Male

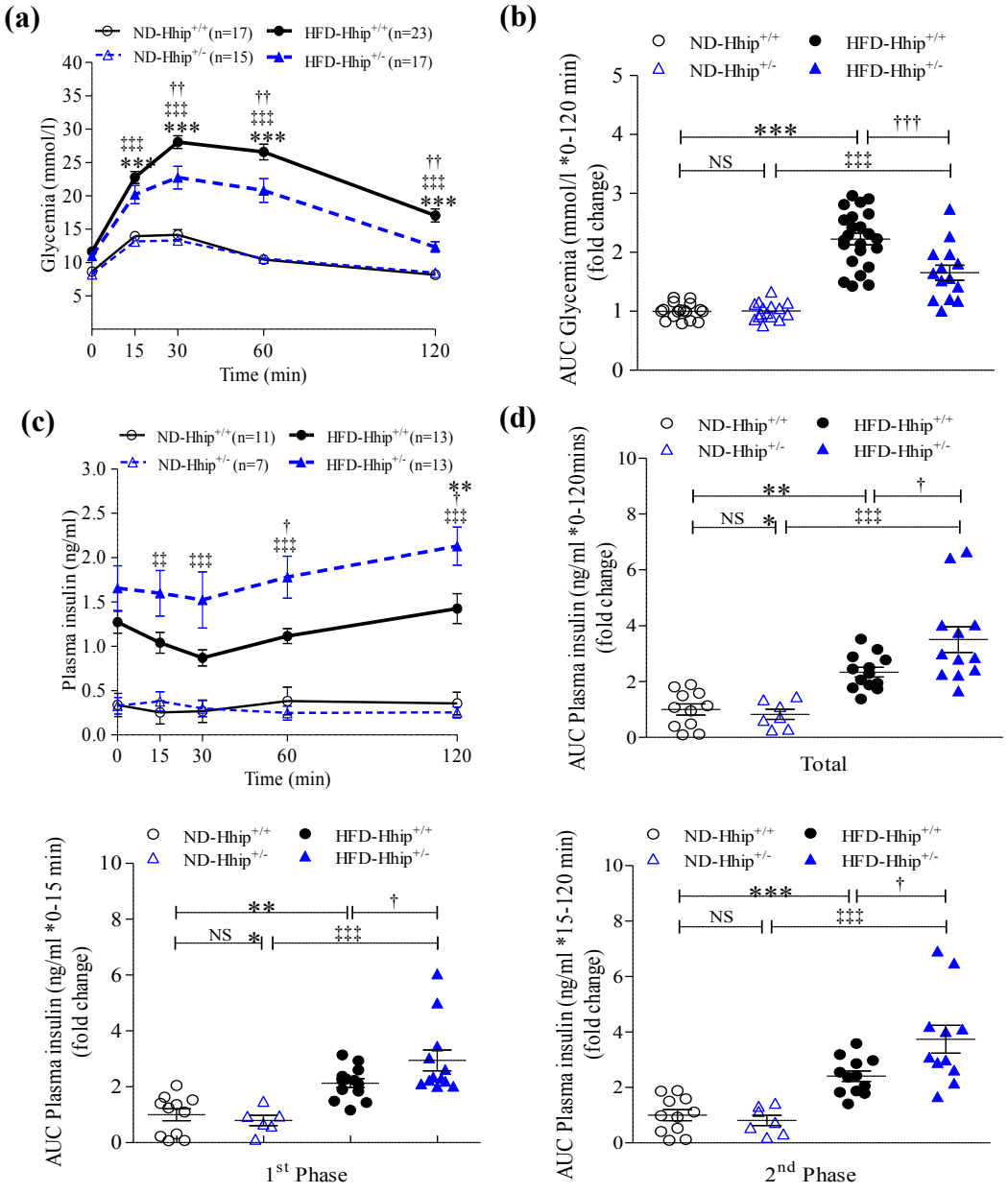

Figure 18: Metabolic parameters in male mice at the age of 14 weeks-old. (a) IPGTT (ND-Hhip$^{+/+}$, n=17; ND-Hhip$^{+/-}$, n=15; HFD-Hhip$^{+/+}$, n=23; and HFD-Hhip$^{+/-}$, n=17) and (b) IPGTT-area under the curve (AUC) quantification (0-120 mins); (c) plasma circulating insulin level (ng/ml), (ND-Hhip$^{+/+}$, n=8; ND-Hhip$^{+/-}$, n=7; HFD-Hhip$^{+/+}$, n=12; and HFD-Hhip$^{+/-}$, n=12) and (d) its AUC quantifications (total, 0-120 mins; 1st phase, 0-15 mins; 2nd phase, 15-120 mins). Data shown as mean ± SEM; 1 way-ANOVA followed by Bonferroni's post hoc test. *$p \leq 0.05$; ** $p \leq 0.01$; *** $p \leq 0.001$ vs. ND-Hhip$^{+/+}$; $^{\#}p \leq 0.05$; $^{\#\#}p \leq 0.01$; $^{\#\#\#}p \leq 0.001$ vs. ND-Hhip$^{+/-}$; $^{\dagger}p \leq 0.05$; $^{\dagger\dagger}p \leq 0.01$; $^{\dagger\dagger\dagger}p \leq 0.001$, HFD-Hhip $^{+/+}$ vs. HFD-Hhip $^{+/-}$; NS, non-significant.

Female

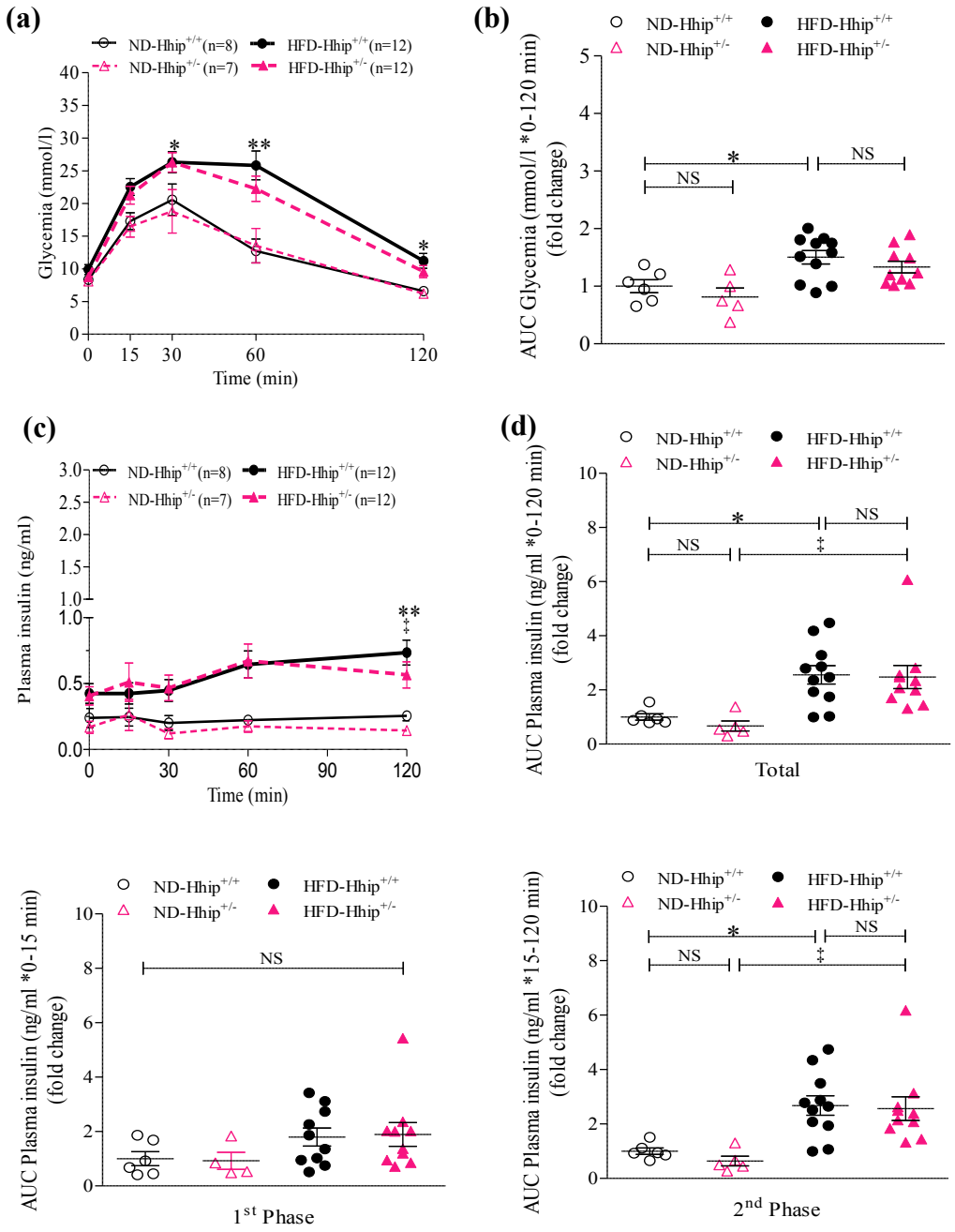

Figure 19: Metabolic parameters in female mice at the age of 14 weeks-old. (a) IPGTT (ND-Hhip$^{+/+}$, n=11; ND-Hhip$^{+/-}$, n=7; HFD-Hhip$^{+/+}$, n=13; and HFD-Hhip$^{+/-}$, n=13) and (b) IPGTT-area under the curve (AUC) quantification (0-120 mins); (c) plasma circulating insulin level (ng/ml), (ND-Hhip$^{+/+}$, n=6; ND-Hhip$^{+/-}$, n=5; HFD-Hhip$^{+/+}$, n=11; and HFD-Hhip$^{+/-}$, n=10) and (d) its AUC quantifications (total, 0-120 mins; 1st phase, 0-15 mins; 2nd phase, 15-120 mins). Data shown as mean ± SEM; 1 way-ANOVA followed by Bonferroni's post hoc test. *$p \leq 0.05$; ** $p \leq 0.01$; *** $p \leq 0.001$ vs. ND-Hhip$^{+/+}$; $^{\#}p \leq 0.05$; $^{\#\#}p \leq 0.01$; $^{\#\#\#}p \leq 0.001$ vs. ND-Hhip$^{+/-}$; $^{\dagger}p \leq 0.05$; $^{\dagger\dagger}p \leq 0.01$; $^{\dagger\dagger\dagger}p \leq 0.001$, HFD-Hhip $^{+/+}$ vs. HFD-Hhip $^{+/-}$; NS, non-significant.

To verify if pancreatic β-cells defect was accompanied by peripheral insulin resistance in HFD-Hhip$^{+/+}$ compared to HFD-Hhip$^{+/-}$ mice, we evaluated for potential whole-body defects in insulin sensitivity, by performing IPIST. Interestingly, we did not observe any significant changes in terms of IPIST in all four subgroups, hence, highlighting insulin sensitivity was still maintained (data not shown). Quantitative PCR (qPCR) analysis further revealed no changes in mRNA expression of genes involved in insulin response, such as IRS1, IRS2, InsR in isolated islets among the 4 subgroups of male mice (data not shown).

To understand whether the differences in response to glucose challenge of HFD-Hhip$^{+/+}$ compared to HFD-Hhip$^{+/-}$ might the result of diabetic complications, such as kidney damage, and hypertension, we analyzed the SBP of the mice in the four subgroups. Longitudinal SBP measurement (data not shown) was similar, and not significantly different among the four subgroups of mice (Hhip $^{+/+}$ vs Hhip $^{+/-}$; ND vs HFD). Accurate blood glucose level sensing is vital for proper β-cell function primarily involving the Glucose Transporter 2 (Glut2). Glut2 mRNA genes in isolated islets from both four subgroups did not reveal any changes in its expression levels (data not shown).

Next, we analyzed several pancreatic parameters including pancreatic mass (ratio of pancreas dry weight to BW), β-cell mass, and total islets numbers (data not shown) among the four subgroups (Hhip $^{+/+}$ vs Hhip $^{+/-}$; ND vs HFD). As a compensation mechanism after 8 weeks of HFD, we observed a modest trend in β-cell mass, and islet number increase, though not significantly different.

In summary, these results demonstrate that Hhip deficiency in β-cells led to the amelioration of impaired GSIS.

4.2 Pancreatic Hhip Expression and *ex vivo* Glucose Stimulated Insulin Secretion (GSIS) Independent of the Classical Hedgehog Signaling Pathway

Although Hhip is abundantly expressed in the developing pancreas [88], and in vascular endothelial cells [85], less is known about its basal expression patterns, and levels in mature islet cells (α and β-cells). Moreover, we questioned whether HFD could alter its expression profile in these islet cells, and what might be the subsequent impact on insulin secretion/action. Deletion of one Hhip allele resulted in approximately 50% reduction in Hhip protein in the islets. HFD feeding notably promoted Hhip protein expression in islets, with a more significant increase in HFD-Hhip$^{+/+}$ compared to HFD-Hhip$^{+/-}$ (Figure 20a).

Consistent with protein measurement, IF and IHC analysis also revealed increased Hhip expression in the islets of HFD-Hhip$^{+/+}$ mice (Figure 20b), with β-cells and not α-cells as the predominant target (revealed by co-localization with insulin (Figure 20c) and glucagon (Figure 20d).

Decreased serum insulin levels can result from impaired β-cell function, and to recapitulate the *in vivo* findings *ex vivo* and *in vitro*, we analyzed isolated islet from both Hhip$^{+/+}$ and Hhip$^{+/-}$ mice, as well as rat insulinoma β-cell line, to evaluate their ability to respond to glucose. As shown in Figure 21a, and 21b, both ND and HFD-Hhip$^{+/+}$ islets secreted significantly less insulin upon glucose challenge compared with ND and HFD-Hhip$^{+/-}$. In INS-1 832/13 cells *in vitro*, we further confirmed that transient transfection with siRNA-Hhip (50nM), further enhanced the stimulatory effects of high glucose (16.8mM) on GSIS (Figure 21c).

These findings implicate β-cell dysfunction as the cause of glucose intolerance in HFD-Hhip$^{+/+}$ compared to HFD-Hhip$^{+/-}$ mice. The reduction in GSIS was not associated with changes in gene expressions of *Pdx1*, *MafA, NeuroD1, Nkx6.1,* and *Neurogenin3* (*Ngn3)* in islets from all 4 subgroups (data not shown). Thus, Hhip expression, and levels did not affect critical β-cell markers, while maintaining a mature β-cell phenotype.

To further determine if Hhip was acting independently or through the classical Hh signaling pathway, we evaluated the gene expression levels of some of the classical player of this pathway, such as Shh, and Glis (Gli1, Gli2 and Gli3), in islets from all 4 subgroups. The expression pattern of the aforementioned were very low in the islets from the four subgroups (data not shown), demonstrating Hhip was acting independent of the Hh signalling pathway.

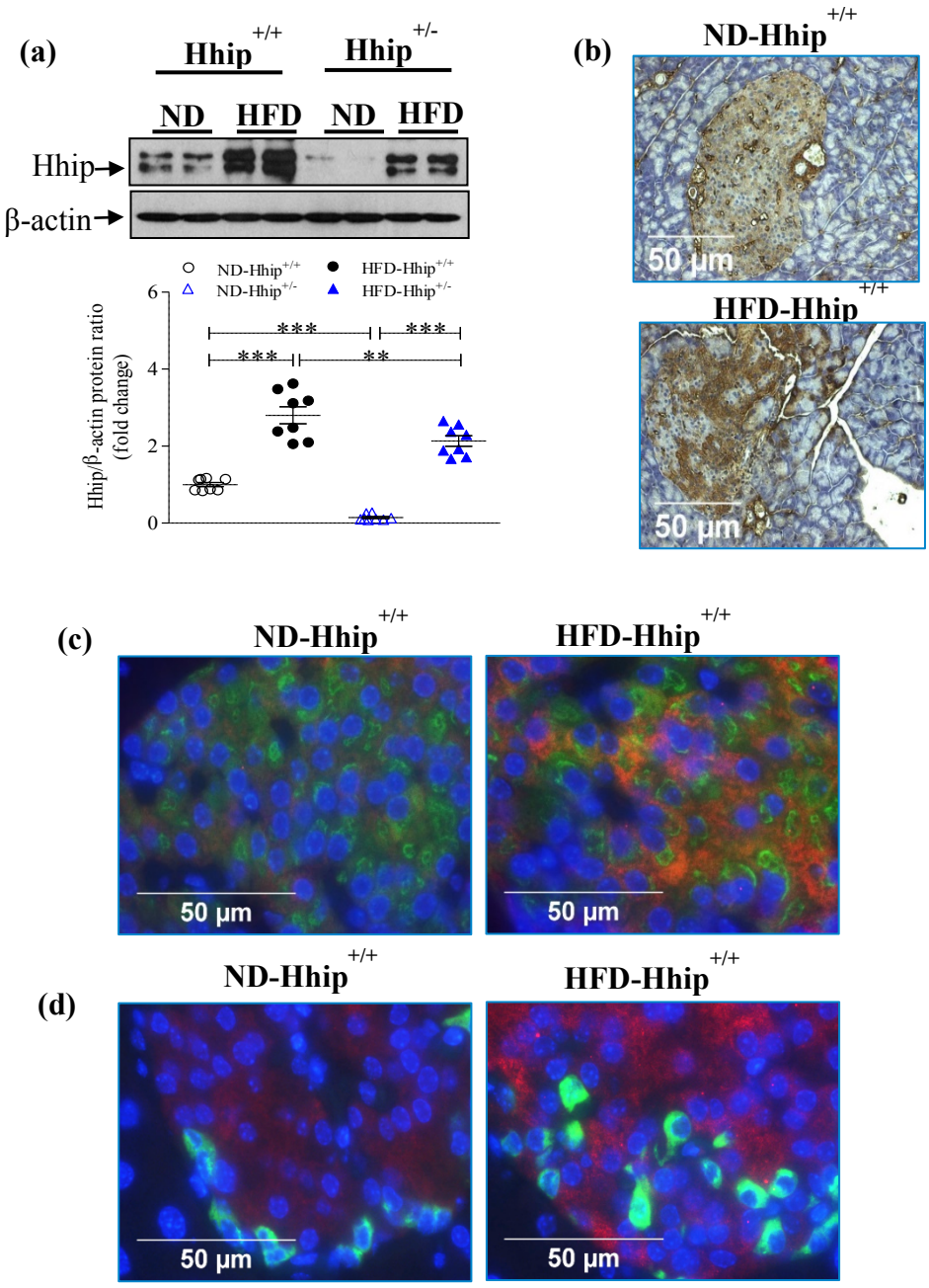

Figure 20: Pancreatic Hhip expression in the islets of male Hhip$^{+/+}$ mice (ND vs HFD) at 14 weeks-old (scale bar, 50µm); (a) WB (Hhip protein expression *ex vivo* -Three to four separate experiments); (b) Hhip-IHC staining; (c) Co-localization of IF-Hhip (red) and -insulin (green); (d) Co-localization of IF-Hhip (red) and -glucagon (green). Data shown as mean ± SEM; 1 way-ANOVA followed by Bonferroni's post hoc test. Data shown as mean ± SEM; 1 way-ANOVA followed by Bonferroni's post hoc test. *$p \leq 0.05$; *** $p \leq 0.001$ vs. ND-Hhip$^{+/+}$; ### $p \leq 0.001$ vs. ND-Hhip$^{+/-}$; †$p \leq 0.05$; ††$p \leq 0.01$, HFD-Hhip $^{+/+}$ vs. HFD-Hhip $^{+/-}$; NS, non-significant.

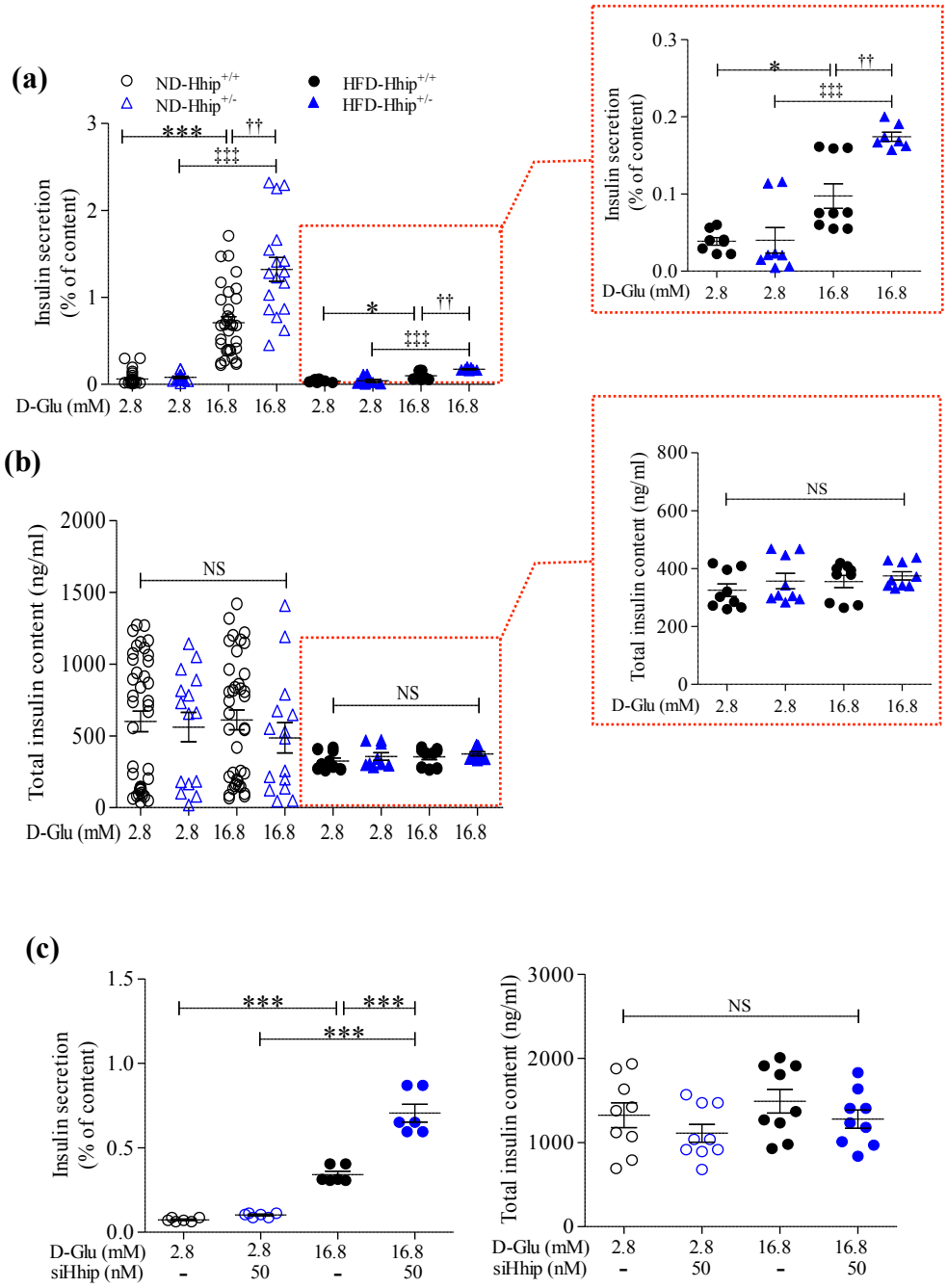

Figure 21: GSIS in isolated islets from male Hhip $^{+/+}$ vs Hhip $^{+/-}$ mice at 14 weeks-old under ND (a) and HFD (b) conditions (insulin secretion, % of total insulin content (ng/ml) measured in isolated islets cultured at 2.8 vs. 16.8 mM D-glucose medium). *p ≤0.05; *** $p \leq 0.001$ vs. ND-Hhip$^{+/+}$; $^{\#\#\#}$ $p \leq 0.001$ vs. ND-Hhip$^{+/-}$; $^{\dagger}p \leq 0.05$; $^{\dagger\dagger}p \leq 0.01$, HFD-Hhip $^{+/+}$ vs. HFD-Hhip $^{+/-}$; NS, non-significant. (c) siRNA-Hhip (50nM) effect on GSIS in INS-1 832/13 cells (insulin secretion, % of total insulin content (ng/ml) measured in INS-1 832/13 cells cultured at 2.8, or 16.8 mM D-glucose medium). *** $p \leq 0.001$ vs. INS-1 832/13 cells cultured in 2.8 mM D-glucose medium). NS, non-significant. Three to four separate experiments *ex vivo* and *in vitro*. Data shown as mean ± SEM; 1 way-ANOVA followed by Bonferroni's post hoc test.

4.3 β-Cell Analysis, Islet Integrity and Morphology

HFD has been shown to promote β-cell mass as an adaptation to insulin resistance, however, β-cell mass, and islet number did not significantly increase in either HFD-fed $Hhip^{+/+}$ or $Hhip^{+/-}$, although they trended higher than the cohort of mice maintained on ND. Numerous studies have delineated the importance of islet size, in relation to proper β-cell function. It has been reported that maintaining a heterogeneous population of islet sizes, as well as the organization of the β-cells within the islets could potentially affect their ability to efficiently secrete insulin.

To study whether the impaired GSIS observed in HFD-$Hhip^{+/+}$ compared to HFD-$Hhip^{+/-}$ mice was a result of the loss of islet size, and integrity, we analyzed the frequency distribution profile of islet sizes. This was done by measuring islet surface areas in a spectrum of 0-500 μm^2 to over 20000 μm^2 in mice from the 4 subgroups, under both ND and HFD conditions. Regardless of diet, $Hhip^{+/-}$ had more significant number of smaller islet population (<2000 μm^2), as compared to $Hhip^{+/+}$ mice, while $Hhip^{+/+}$ mice showed a significant right shift by having larger islet population (>2000 μm^2) in their pancreas (Figure 22a-22b). Double immunofluorescence analysis of both glucagon (marker for α-cells), and insulin (marker for β-cells), showed that the two islet populations had very different cellular arrangements with the β-cells of the small islets clustered in the center of the islets surrounded by α-cells at the periphery, whereas the larger islets presented an evenly distribution of both α and β-cells throughout the islets (Figure 22c) when compared to islets from both ND groups, which showed the α-cells at the periphery surrounding the β-cells in the core of the islet.

With the islet's integrity preserved in small islets compared to large islets, we hypothesized that small islets might have more insulin content than large islets per volume.

IHC staining with insulin demonstrated a stark difference in the intensity of insulin staining between the two-islet populations. In small islets, β-cells contained approximately the same level of insulin staining, whereas in large islets, insulin-containing β-cells located at the periphery of the islets contained approximately the same level of insulin while those found in the core had less insulin staining (Figure 23a). All images were compared within the same sections, to minimize variations in staining protocols.

To study if increased Hhip expression under HFD specifically in β-cells can promote pancreatic β-cells proliferation, we further analyzed Ki-67 immunostaining positive β-cells (marker for proliferation). All HFD-fed mice analyzed showed a significant increase in β-cells proliferation, HFD-Hhip$^{+/-}$ pancreas was highly proliferative compared to HFD-Hhip$^{+/+}$ (Figure 23b). Hence, our results demonstrate that, Hhip expression led to a compromise in islet hyperplasia, integrity, reduced insulin content and decreased β-cell proliferation.

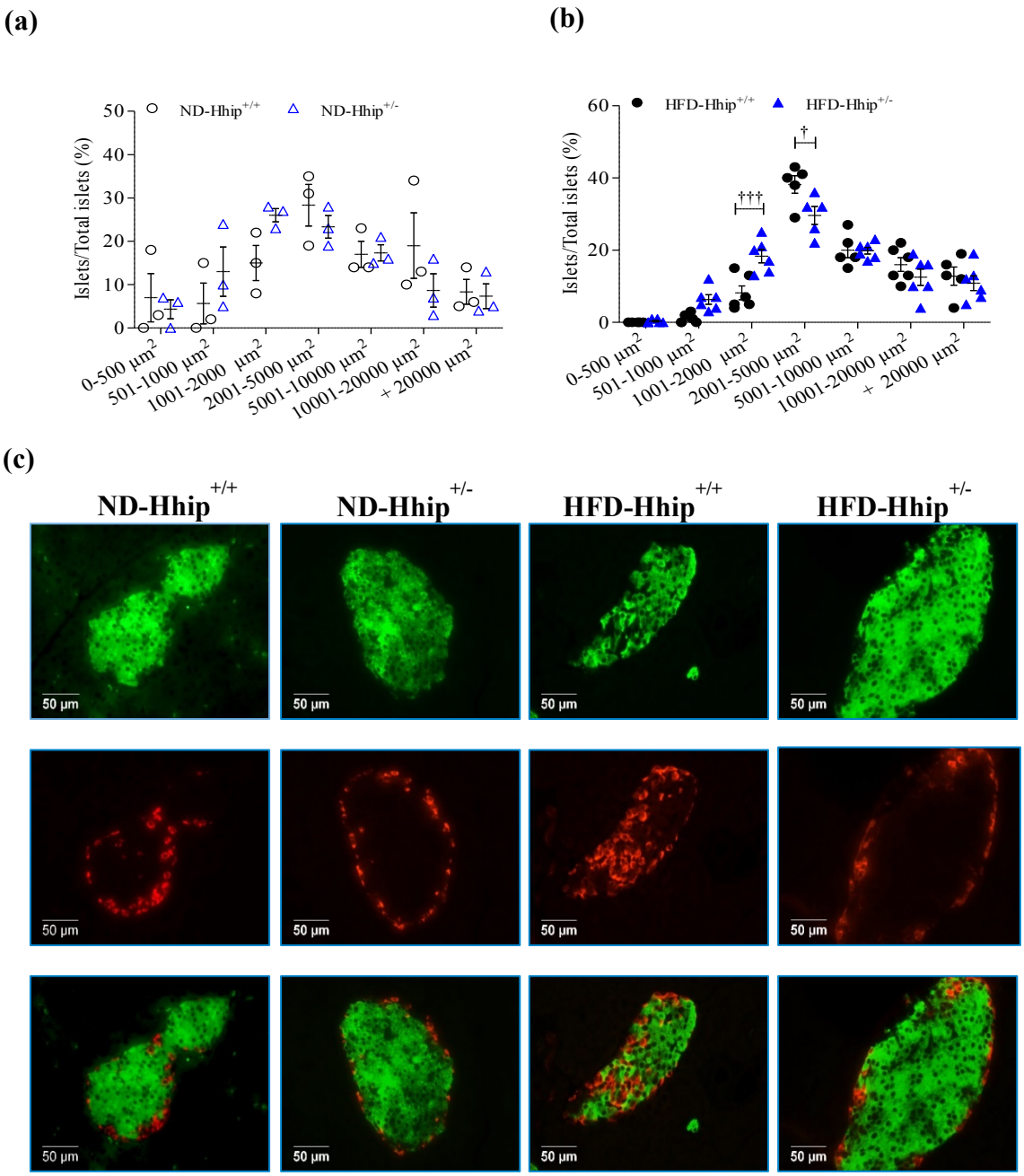

Figure 22: Islet analysis of male Hhip$^{+/+}$ and Hhip $^{+/-}$ mice (ND vs HFD) at 14 weeks-old. (a-b) Distribution profile of islet size (a, ND; b, HFD). [a, ND (ND-Hhip$^{+/+}$, n=3; ND-Hhip$^{+/-}$, n=3); b, HFD (HFD-Hhip$^{+/+}$, n=6; HFD-Hhip$^{+/-}$, n=6)]. Data shown as mean ± SEM; 2 way-ANOVA followed by Bonferroni's post hoc test. $^{\dagger}p \leq 0.05$; $^{\dagger\dagger\dagger}p \leq 0.001$, HFD-Hhip $^{+/+}$ vs. HFD-Hhip $^{+/-\dagger}p \leq 0.05$, Hhip $^{+/+}$ vs. Hhip $^{+/-}$; (c) Co-localization of IF-insulin (green) and –glucagon (red) staining, (scale bar, 50µm).

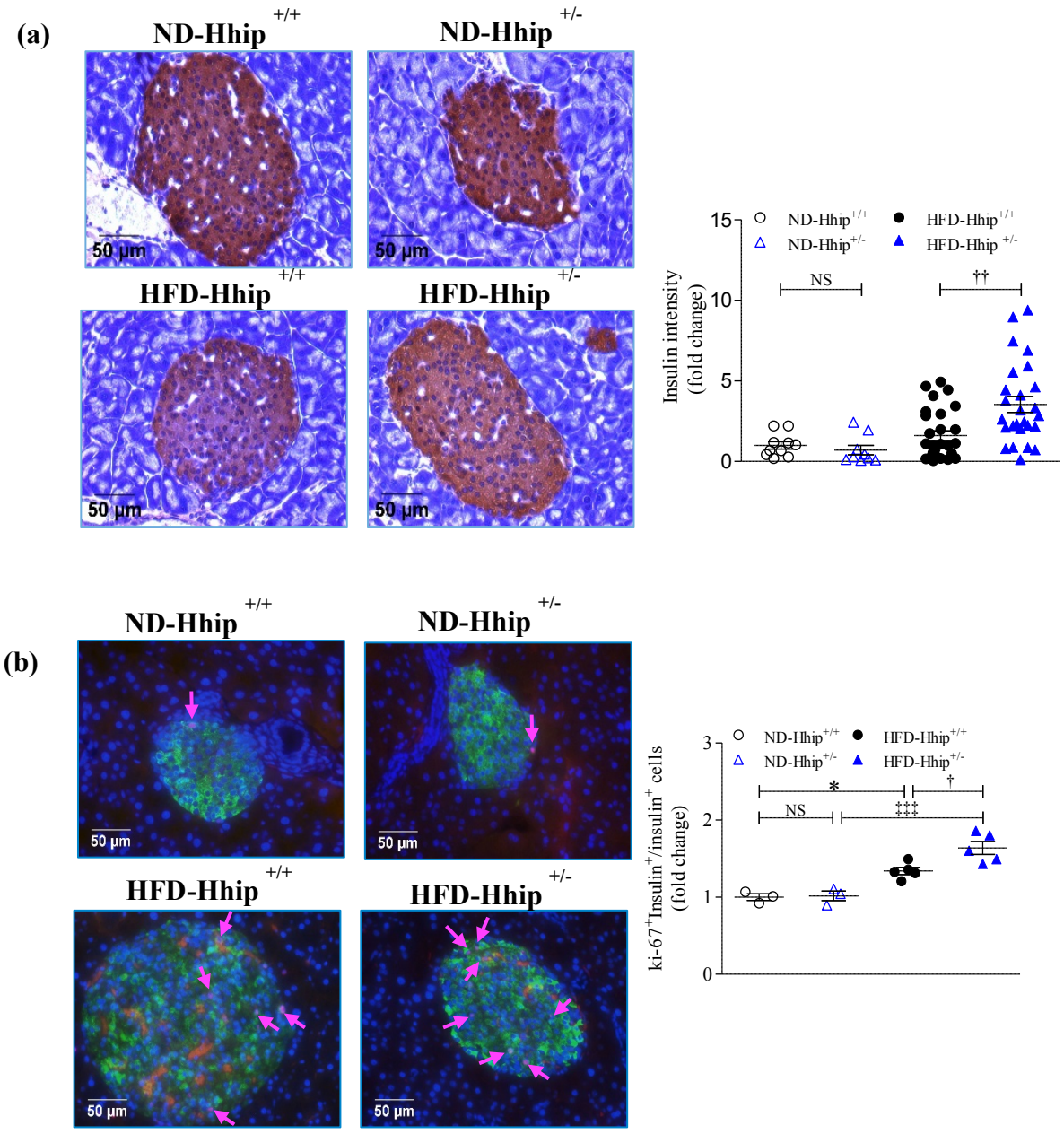

Figure 23: Islet analysis of insulin content and proliferation in male Hhip$^{+/+}$ and Hhip $^{+/-}$ mice (ND vs HFD) at 14 weeks-old. (a) Insulin-IHC (ND-Hhip$^{+/+}$, n=3; ND-Hhip$^{+/-}$, n=3; HFD-Hhip$^{+/+}$, n=5; and HFD-Hhip$^{+/-}$, n=5) and (b) IF-Ki67 staining (Ki67, red; insulin, green; DAPI, blue; Ki-67 positive nuclei, pink arrows) (ND-Hhip$^{+/+}$, n=3; ND-Hhip$^{+/-}$, n=3; HFD-Hhip$^{+/+}$, n=5; and HFD-Hhip$^{+/-}$, n=5) in the islets among 4 subgroups of male mice (Hhip $^{+/+}$ vs Hhip $^{+/-}$; ND vs HFD) at 14 week-old (scale bar, 50µm).

4.4 Oxidative Stress

Reduction in *in vivo,* and *ex vivo* GSIS in the islets of HFD-Hhip$^{+/+}$ mice vs. HFD-Hhip$^{+/-}$ mice was associated with significant increase in oxidative stress levels as determined by 8-OHdG positive staining (Figure 24), while no differences were observed between ND-Hhip$^{+/+}$ mice and ND-Hhip$^{+/-}$ mice. *In vitro*, rHhip dose-dependently decreased the numbers of insulin-positive cells (Figure 25a) and increased reactive oxygen production as measured by DHE-positive cells (Figure 25b), respectively.

To further address the possibility, and involvement of the NADPH oxidases pathway in response to HFD and Hhip expressions, we asked ourselves whether NADPH oxidases expressed in the pancreas are elevated in the islets. Interestingly, mRNA expression by qPCR of NADPH oxidases (NOX 1, 2 and 4 gene) from isolated mouse islets revealed that only NOX2 mRNA isoform was significantly increased in the islets of HFD-Hhip$^{+/+}$ mice vs. HFD-Hhip$^{+/-}$ mice (Figure 26a), while NOX1 and NOX4 mRNA were barely detectable in those islets. Co-immunofluorescence analysis confirmed this data, and further revealed that in contrast to HFD-Hhip$^{+/-}$, NOX2 and insulin double-positive cells were significantly higher in HFD-Hhip$^{+/+}$, specifically in β-cells (figure 26b).

In *in vitro* analysis with INS-1 832/13 cells, we could detect both NOX2 and NOX4 mRNA expression levels, but not NOX1 mRNA expression. As shown mechanistically, rHhip dose-dependently elevated NADPH activity (Figure 27a), and subsequently increase both NOX2 gene and protein expression levels (mRNA, Figure 27b; protein, Figure 27c), with no significant effect on both NOX4 gene and protein expression levels. In addition, 0.3mM BSA-PA conjugate stimulated NOX2 mRNA expression without affecting Nox4 mRNA expression (Figure 28a). Immunoblotting data further revealed that 0.3mM BSA-PA stimulated both Hhip

and NOX2 protein expression, which was aggravated when combined with rHhip (Figure 28b), resulting in a synergistic effect. Conversely, treatment with 0.3mM BSA-PA after transient transfection with siRNA-Hhip (Figure 28c) prevented both Hhip and NOX2 protein expression increase.

In summary, increased Hhip expression levels in HFD-Hhip$^{+/+}$ islets are associated with increase expression of NADPH activity, especially NOX2 isoform, resulting in inappropriate activation of oxidative stress, thereby comprising GSIS.

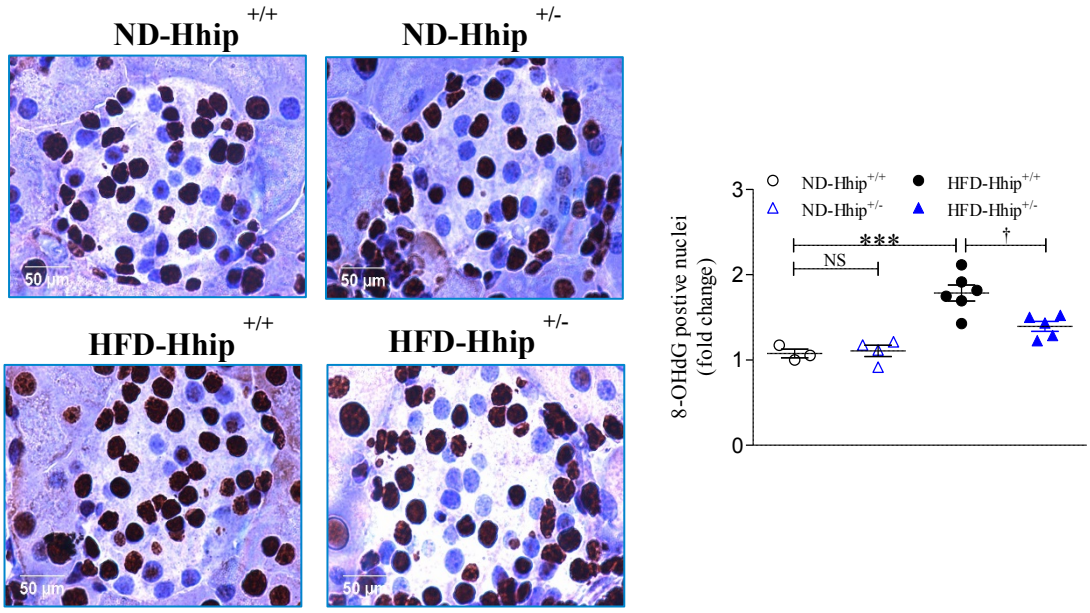

Figure 24: IHC *in vivo* of 8-OHdG-IHC staining (ND-Hhip$^{+/+}$, n=4; ND-Hhip$^{+/-}$, n=3; HFD-Hhip$^{+/+}$, n=6; and HFD-Hhip$^{+/-}$, n=5) in the islets among 4 subgroups of male mice (Hhip $^{+/+}$ vs Hhip $^{+/-}$; ND vs HFD) at 14 week-old (scale bar, 50µm). Semi-quantification of staining; Data shown as mean ± SEM; 1 way-ANOVA followed by Bonferroni's post hoc test. *$p \leq 0.05$; *** $p \leq 0.001$ vs. ND-Hhip$^{+/+}$; $^{\#\#\#}$ $p \leq 0.001$ vs. ND-Hhip$^{+/-}$; $^{\dagger}p \leq$ 0.05HFD-Hhip $^{+/+}$ vs. HFD-Hhip $^{+/-}$; NS, non-significant.

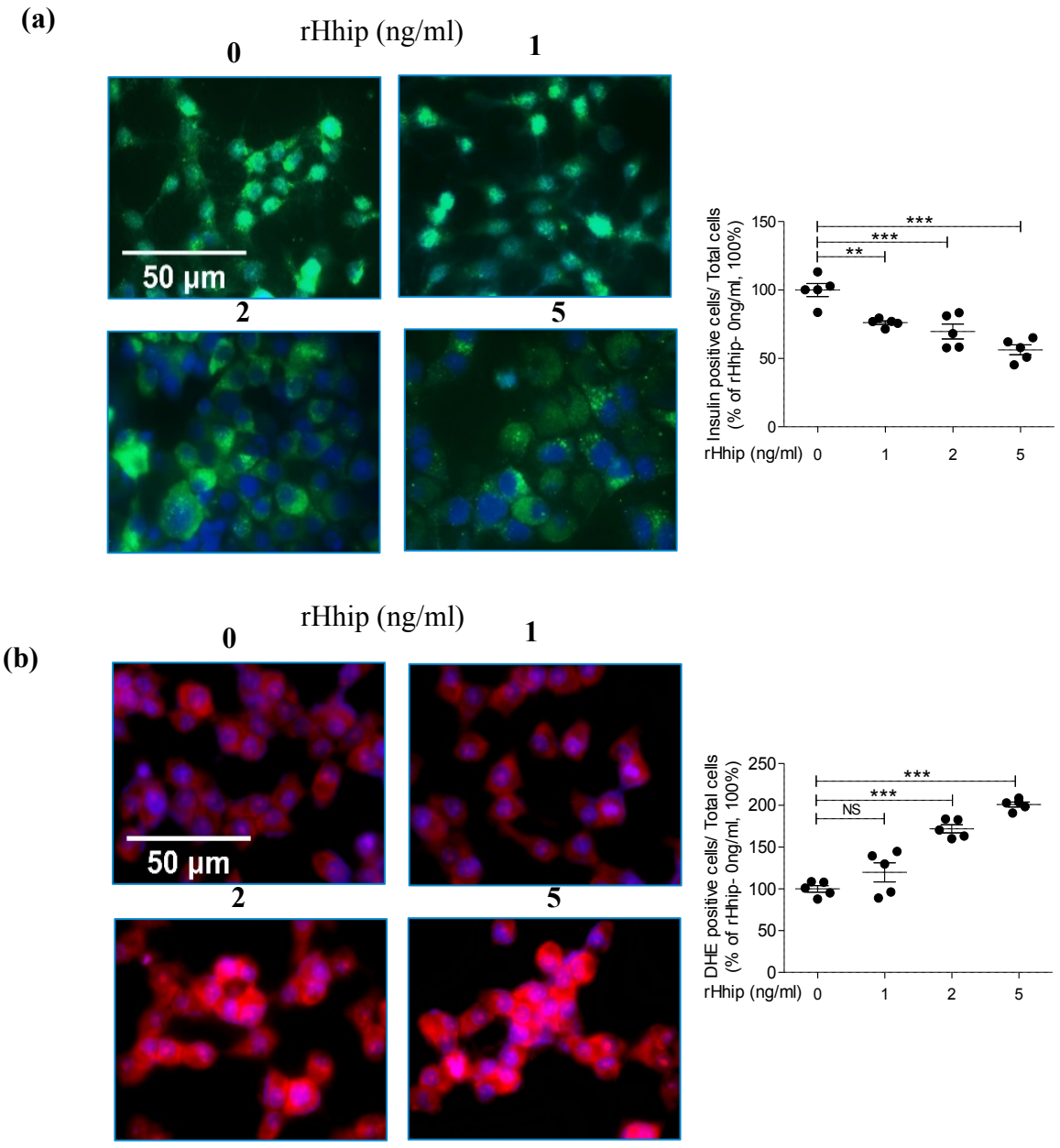

Figure 25: IF *in vitro*. (a) IF-Insulin staining (Insulin, green; DAPI, blue) and (b) DHE staining (DHE, red; DAPI, blue) (scale bar, 50µm); Semi-quantification. Four separate experiments; Data shown as mean ± SEM; 1 way-ANOVA followed by Bonferroni's post hoc test. *$p \leq 0.05$; **$p \leq 0.01$; ***$p \leq 0.001$; NS, non-significant vs INS-1 832/13 cells cultured in medium without rHhip (0ng/ml) (100%).

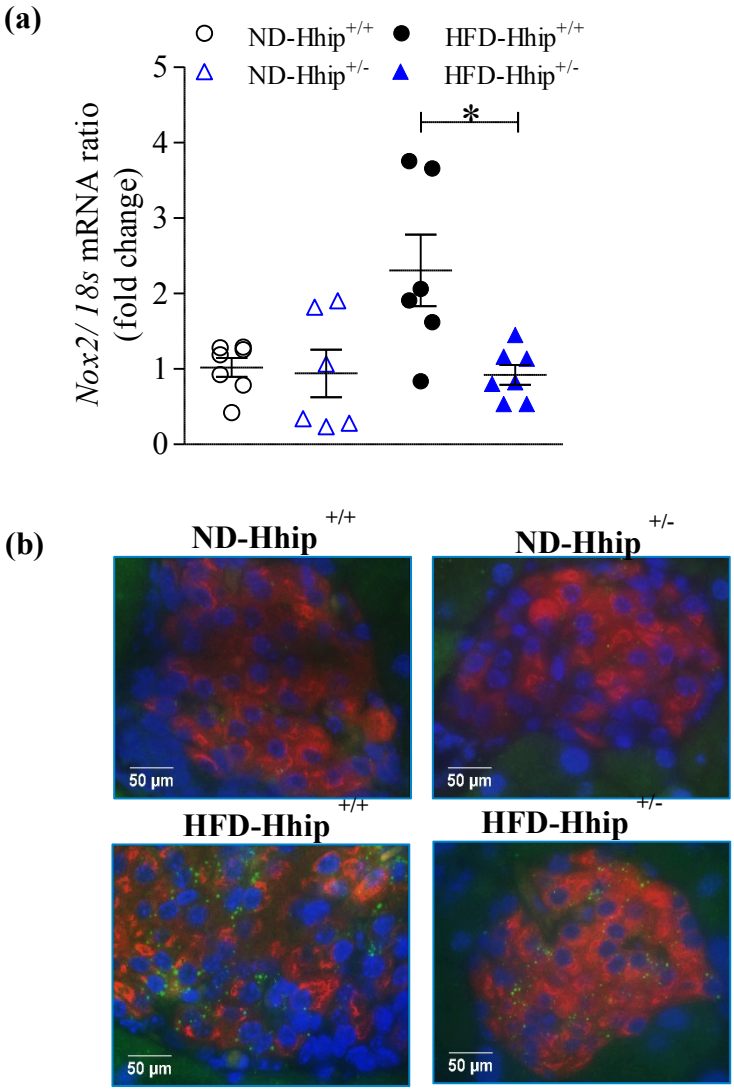

Figure 26: Nox2 gene expression *in vivo*. (a) qPCR –*Nox 2* mRNA expression (ND-Hhip$^{+/+}$, n=7; ND-Hhip$^{+/-}$, n=6; HFD-Hhip$^{+/+}$, n=6; and HFD-Hhip$^{+/-}$, n=7); Data shown as mean ± SEM; 1 way-ANOVA followed by Bonferroni's post hoc test; $^{\dagger}p \leq 0.05$, HFD-Hhip $^{+/+}$ vs. HFD-Hhip $^{+/-}$ male mice at 14-week-old; (b) IF-Nox2 staining (Nox2, green; Insulin, red; DAPI, blue) in the islets among 4 subgroups of male mice (Hhip $^{+/+}$ vs Hhip $^{+/-}$; ND vs HFD) at 14 week-old (scale bar, 50µm).

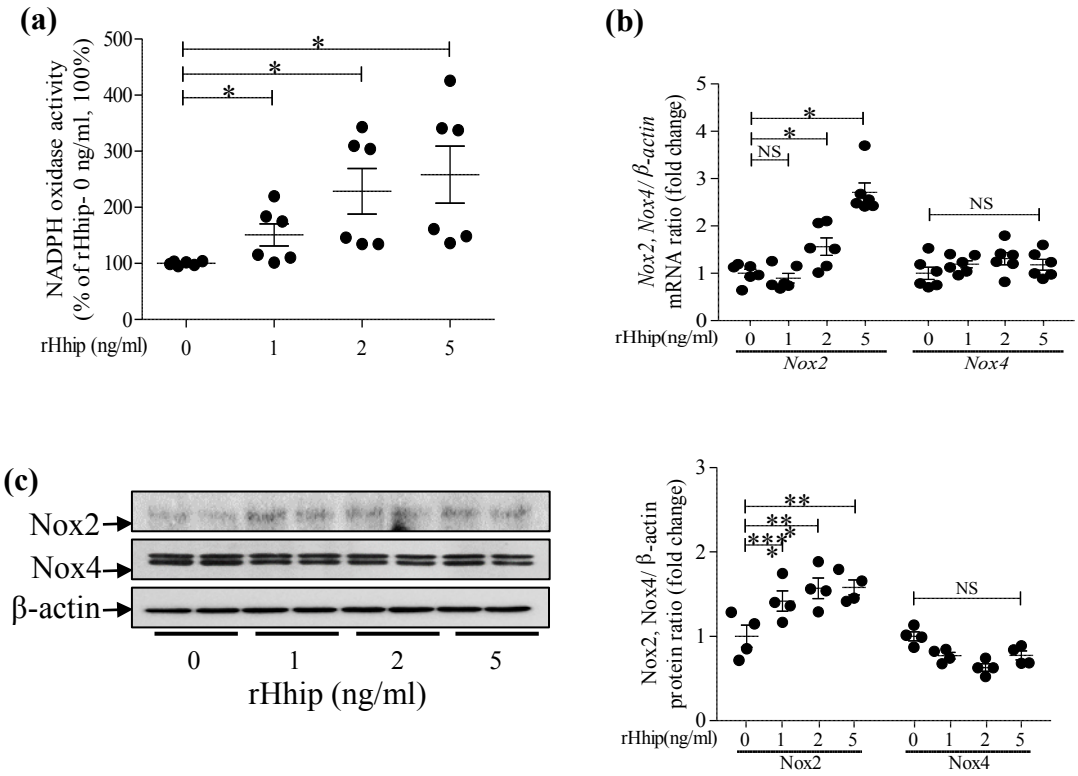

Figure 27: *In vitro* NADPH activity assay and Nox Expression. (a) NADPH activity activity in cells treated by rHhip (0-5ng/ml); (b) qPCR (*Nox2* and *Nox4* mRNA expression) in cells treated by rHhip (0-5ng/ml); (c) WB (Nox2 and Nox4 protein expression) in cells treated by rHhip (0-5ng/ml). Three to four separate experiments; Data shown as mean ± SEM; 1 way-ANOVA followed by Bonferroni's post hoc test;*$p \leq 0.05$; **$p \leq 0.01$; ***$p \leq 0.001$; NS, non-significant vs INS-1 832/13 cells.

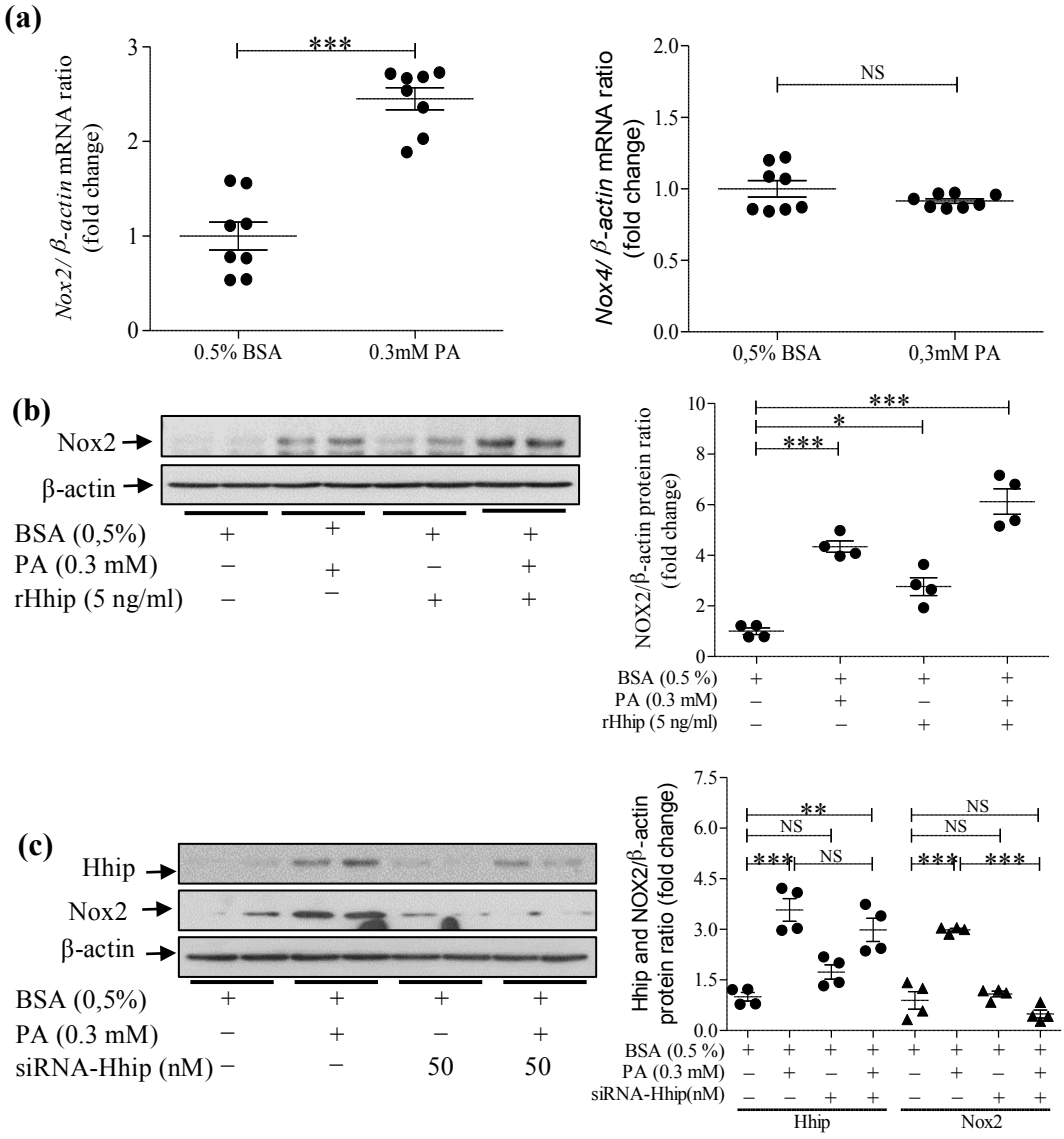

Figure 28: In vitro effect of PA and rHhip. (a) qPCR (0.3mM PA effect on *Nox2* and *Nox4* mRNA expression) in cells treated by PA. (b-c) WB (Nox 2 protein expression treated by either rHhip (b) or siRNA-Hhip (c)). Three to four separate experiments; Data shown as mean ± SEM; 1 way-ANOVA followed by Bonferroni's post hoc test *$p \leq 0.05$; **$p \leq 0.01$; ***$p \leq 0.001$; NS, non-significant vs INS-1 832/13 cells cultured in medium with 0.5% BSA (100%).

5.0 DISCUSSION

In the present study, we explored the pathophysiological function of Hhip in a mouse model with genetic reduction of Hhip, and to investigate its involvement in glucose homeostasis. While the importance of Hhip expression has been extensively investigated in murine pancreas organogenesis, and β-cell proliferation, its role in the adult pancreas has not been elucidated. A genome-wide diabetes profiling database, revealed that Hhip mRNA seems to be significantly up-regulated, specifically in the islets of diabetic ob/ob mice, but not in other tissues, such as liver, adipose, soleus, gastrocnemius, and hypothalamus (tissues involved in glucose uptake and insulin resistance), underscoring the specificity and importance of Hhip expression in murine T2DM islets. Obesity as a result of increase caloric intake, increases the risk of T2DM. Here, we have conducted a study to investigate the functional impact of Hhip expression in a model of diet induced-obesity mediated β-cell dysfunction in Hhip heterozygous mice ($Hhip^{+/-}$) vs. control littermates ($Hhip^{+/+}$), and to elucidate the underlying mechanism(s) *ex vivo* and *in vitro*. We demonstrated that, HFD feeding significatly increases Hhip gene expression levels in β-cells of $Hhip^{+/+}$ compared to $Hhip^{+/-}$, leading to impaired glucose tolerance, and hyperinsulinemia, as a compensatory response to insulin resistance. This phenotype was accompanied by a distortion in islet morphology, and architecture, without significant changes in both islet mass and number, and decreased GSIS by promoting pancreatic β-cell apoptosis, and oxidative stress via NOX2 gene expression.

$Hhip^{+/+}$ and $Hhip^{+/-}$ are indistinguishable from their control littermates [88]. As expected, eight weeks of HFD feeding successfully increased mouse BW over time independently of sex, and genotype. Both male, and female HFD-$Hhip^{+/+}$ mice exhibited impaired IPGTT with a significant compromise in *in vivo* GSIS, especially during the first 30

minutes after glucose administration. Interestingly, despite similarities in weight gain in both sexes, HFD-induced hyperinsulinemia, and metabolic changes was significantly increased in male compared to female (both $Hhip^{+/+}$ and $Hhip^{+/-}$) mice. The difference in the phenotype between the HFD-fed males, and females might be attributed to estrogen (female sex hormone), which has been suggested to protect against the development of metabolic syndrome, and the prevalence of obesity, insulin resistance, and T2DM by decreasing hepatic triglycerides (lipid homeostasis), improving energy expenditure, while favoring the loss of visceral white adipose tissue (HFD induced adipocyte hypertrophy) [132-136]. Since the animals used for this study were also relatively young (reproductive age), the observed pronounced metabolic changes in males was not surprising. As aforementioned, female mice used for this study are not a good model for DIO because of the age of the mice, and also because estrogen protects them against metabolic syndrome(s), thus, for the remainder of the study, we focused on male $Hhip^{+/+}$ and $Hhip^{+/-}$ animals, to elucidate the relevant mechanisms of Hhip.

There is accumulating evidence that high fat intake from HFD positively correlates with obesity, and insulin resistance, which is characterized by increased weight gain, impaired glucose tolerance, and accompanying hyperinsulinemia. These were all observed in both HFD-fed $Hhip^{+/+}$ and $Hhip^{+/-}$ male mice, indicating the possible development of insulin resistance. Systemic glucose tolerance is mostly impacted by both pancreatic β-cell function, estimated by both *in vivo* and *ex vivo* GSIS, and the pathophysiology of *in vivo* insulin sensitivity (inulin-stimulated glucose uptake by peripheral tissues as measured by IPTT) [52; 137]. Insulin has been shown to be involved in glucose uptake from circulation into peripheral insulin-responsive tissues (muscles, liver and fat). Whole-body response to exogenous insulin

during an IPITT challenge in our study demonstrated that glucose uptake by peripheral tissues was not compromised in both 4 subgroups fed both ND and HFD. Generally, insulin-mediated regulated glucose metabolism in peripheral tissues is through the IRS/PI3K/Akt signalling pathway, which plays a major role in the development and molecular mechanisms of obesity, insulin resistance, and T2DM. Recently, individuals with insulin resistance have been identified to have a corresponding decrease or absence in the expression of insulin receptor (IR), and insulin resistance-associated insulin receptor substrate-1 (IRS1) mutations [138-141]. Our data further revealed that HFD did not activate the expression of genes involved in insulin signaling such as IRS1, IRS2 and InsR in the four subgroups. This provides evidence that perhaps the observed phenotype of glucose intolerance observed in HFD-fed male Hhip$^{+/+}$ was predominantly due to impairment in glucose response as a result of pancreatic β-cell dysfunction, and not attributed to insulin sensitivity. In addition, systolic blood pressure measurements, further revealed mice in all four subgroups were normotensive, alluding the observed phenotype might be as a result of pancreatic β-cell dysfunction, as oppose to diabetic complications, such as kidney disease and hypertension, which has been shown to increase with the increase incidence of T2DM.

In vivo GSIS appeared to be a significantly compromised in HFD-Hhip$^{+/+}$ compared to HFD-Hhip$^{+/-}$, especially in the first 30 minutes following glucose administration, as evidenced from the circulating insulin measurement of both 1st and 2nd phases. This maybe as a result of several factors, including but not limited, to poor glucose sensing, inappropriate insulin production, and secretion. Glucose transporter isoform Glut2, is primarily responsible to catalyze the passive transport of glucose across the plasma membrane, especially in pancreatic β-cells, and is involved in GSIS. In diabetes, particularly in DIO or HFD-fed model, impaired

GSIS is associated with reductions in Glut2 expression, both at the mRNA and protein levels, as result of increases NEFA and lipotoxicity [142; 143]. Here, we did not observe any apparent changes of pancreatic islets Glut2 mRNA expression levels among all the four subgroups on either the ND or HFD, hinting that perharps pancreatic β-cell glucose transport might be normal. To recapitulate our *in vivo* observation *ex vivo*, static *ex vivo* analysis of GSIS in isolated islet from both ND and HFD fed mice also supports the enhanced insulin secretion *in vivo* profile from $Hhip^{+/-}$ compared to $Hhip^{+/+}$ from 2.8, to 16.8 mM. mRNA analysis of *Pdx1*, *MafA, NeuroD1, Nkx6.1,* and *Neurogenin3* (*Ngn3)* was not significantly different among the four, groups; implying maybe GSIS reduction in HFD-$Hhip^{+/+}$ compared to HFD-$Hhip^{+/-}$ was not associated with changes in gene expression levels of proteins involve in β-cell differentiation, and maturation. Furthermore, siRNA-Hhip in INS 832-13 cells (which responds to glucose over physiological ranges of glucose concentration), also resulted in an increase of GSIS in response to glucose challenge from 2.8 mM to 16.8 mM. These findings imply Hhip deficiency might directly preserve the capacity, and ability of GSIS in insulin secretion, hence highlighting β-cell malfunction as the main cause of glucose intolerance in HFD-$Hhip^{+/+}$ compared to HFD-$Hhip^{+/-}$ challenged mice.

As earlier mentioned, the traditional Hh signalling which was thought to be quiescent in adult tissues, has now been reported to be active in the mature pancreas, both in the areas of tissue maintenance, and function. The expression of the Hh ligands, especially Ihh, Ptc1, and Smo has been typically shown to be expressed in the β-cells of islets, and mainly colocalized with insulin [88; 117-119]. To further validate if Hhip deficiency's ability in preserving the capacity of GSIS in β-cells involved the classical Hedgehog signalling pathway, we analysed the mRNA expression of some of the key players of the pathway. Upon examining the

expression pattern of key player such as Shh and Glis (Gli 1, Gli 2 and Gli3), we found the expression pattern of the aforementioned were very low in the islets from the four subgroups, hence emphasizing the role of Hhip in preserving islet function in the current study might be independent of the classical hedgehog signaling pathway.

Emerging evidence indicates that both obese patients who develop T2DM, as well as HFD-challenged mice, all compensate for increased insulin demand as a result of insulin resistance, and metabolic overload by increasing their pancreatic β-cell mass. This increase is dependent on both the composition, and the timing of the diet. The increase in β-cell mass is a consequence of hypertrophy, and proliferation, which are major adaptations to insulin resistance, and also important in the maintenance of normoglycemia [26; 144-148]. As a compensatory response to HFD challenge, both $Hhip^{+/-}$ and $Hhip^{+/+}$ in our current model of 8 weeks HFD challenge responded by enhancing their pancreatic β-cell mass, displaying a visible trend, though not significantly different as compared to ND fed mice. This was similar to observations made by [146], which they showed that after 8 weeks on HFD, there was no significant difference in the β-cell mass in either control or mutant mice on HFD compared to animals of the same genotype fed chow. Although in their study, control mice on HFD trended higher than control mice on chow. As earlier explained, significant differences in pancreatic β-cell mass might require approximately close to or more than 10 weeks of HFD challenge [136]. Hence, to establish the metabolic function of Hhip in β-cell mass expansion in response to HFD, it might be interesting to prolong the duration of the stimulus (HFD insult). Similarly, HFD challenged $Hhip^{+/+}$ and $Hhip^{+/-}$ mice showed comparable parallel but not significant increase in islets numbers with no apparent difference between the two ND fed subgroups. Islets hyperplasia analysis from all four subgroups, reveals a shift of islets population to a

population of larger islets in both HFD fed subgroups. Interestingly, islets hyperplasia was significantly increased in HFD-fed $Hhip^{+/+}$ as compared to HFD-fed $Hhip^{+/-}$ mice underscoring the importance of Hhip deficiency in a disease model of DIO. In parallel, $Hhip^{-/-}$ null mice had a 45% reduction of pancreatic endocrine area, which was predominantly attributed to the loss of larger islets [88], thus suggesting that Hhip deficiency might protects against islets hyperplasia, both during development, nomal, and under disease conditions.

Islet size is a major determinant in islet insulin secretion, historically, small islets have been shown to secrete more insulin per volume than corresponding large islets even from the same pancreas [149]. Some of the observations advanced for these differences are either because there exist diffusion limitations, which hinder glucose from activating the pathway in the core of larger islets unlike in the smaller islets, or there exist inherent cellular differences within large and small islets resulting in a more effective activation of insulin pathway production by glucose in smaller islets compared to larger islets [150; 151]. Conversely, larger islets presented a more random arrangement, whereby there was invasion of the centralized β-cells core by α-cells, resulting in intermingling of both endocrine cell population, which was a common feature observed in our HFD-fed $Hhip^{+/+}$ compared to HFD-fed $Hhip^{+/-}$, thereby affecting their ability to effectively secrete insulin. Proportionally, β-cells population is inversely correlated to islets size, while α-cells population is directly correlated with islet size and this difference could account for the efficient GSIS observed in HFD-$Hhip^{+/-}$ compared to HFD-$Hhip^{+/+}$ hence explaining the phenotype of glucose intolerance. Due to a higher proportion of β-cells in smaller islets in $Hhip^{+/-}$, as compared to $Hhip^{+/+}$, we speculated that smaller islets might have more insulin content than larger islets. In fact, pancreatic sections stained, and analyzed for insulin staining intensity illustrated more intense insulin staining of

the smaller islet compared with the corresponding larger islet. Of all the islets analyzed, statistically the larger islets had less insulin when compared to smaller islets. Interestingly, this staining also reveals that the β-cells in the outer layer of the larger islets had significantly more insulin than the β-cells found in the islet core as was reported by [153]. These observations suggest that Hhip deficiency might improve insulin secretion, maintain islet size, morphology, integrity and architecture. This may play an essential role in islet survival, and function in disease conditions, such as improving GSIS alongside changes in islet size, and morphology, thereby enhancing efficient adult β-cell function.

The observation that Hhip deficiency ($Hhip^{+/-}$ as compared to $Hhip^{+/+}$) improves insulin secretion *in vivo, ex vivo and in vitro* is comparable with previous studies which showed that *in vitro* insulin secretion was enhanced by ectopic expression of Shh, using cultured insulinoma cells. This was achieved by increasing Hh signaling, even though it has been argued that although β-cell lines maintain some insulin production, and GSIS characteristics, they do not retain the fully differentiated state found in adult β-cells *in vivo* [154]. Mechanistically, the increase insulin secretion was mediated in part through the upregulation of pancreatic and duodenal homebox 1(Pdx1) expression involved mature β-cell maintenance. Moreover, treating insulinoma cells with cyclopamine (a steroidal alkaloid that specifically block cellular responses to vertebrate Hh signaling) resulted in Pdx1 and insulin transcription impairment, thereby suggesting β-cell regulation by Hh signalling was via Pdx1 promoter activation. Activation of insulin promoter by using an exogenous Hh signalling activator and its subsequent repression by an Hh antagonist highlights the insulin gene might be a potential target for Hh regulation in pancreatic β-cells [119; 155]. Even though *in vitro* systems might be different from *in vivo* systems, and despite the fact that cyclopamine unlike Hhip

(employed in our study) is not a physiological inhibitor, it was interesting to note that increased insulin production, and secretion is attributed to increase Hh signalling both in our study and in the above report. Indeed, we also found that Hhip expression was significantly increased in HFD-Hhip$^{+/+}$ islets compared to HFD-Hhip$^{+/-}$ and specifically co-localized with β-cells, and none with α-cells highlighting β-cells as the main target of HFD-induced Hhip expression. This echos the importance of regulating Hhip levels, and expression in T2DM.

Increased and prolonged HFD feeding has been reported to be responsible for pancreatic β-cell proliferation and apoptosis. The balance between proliferation and apoptosis has been shown to regulate β-cell volume, and this is very important in glucose homeostasis regulation [156; 159]. In obesity, and T2DM, β-cell proliferation has been shown to be the primary method by which β-cell mass increase in mice is achieved. Proliferation of islet cells can be demonstrated using proliferation markers, such as Ki-67.

In our study, HFD significantly up regulated proliferation in both HFD-fed subgroups with a more significant increase in HFD-Hhip$^{+/-}$ compared to Hhip-Hhip$^{+/+}$. Since the ability of β-cell to proliferate is important in maintaining β-cell mass, as well as compensating for insulin resistance, this advances the importance of Hhip gene expression in the aetiology of T2DM. Hhip gene expression has been shown to redirect cells towards apoptosis, fibrosis, and angiogenesis under conditions of oxidative stress, such as diabetes mellitus [85; 127; 158; 159]. We recently demonstrated that Hhip could directly elevate ROS generation, by interacting with NOX isoform(s) (*i.e.*, NOX 4 in the kidney), subsequently activating TGFβ1-signaling to result in renal cell fibrosis/apoptosis, with or without diabetic insult. Oxidative stress, which is a physiological condition enhanced by an imbalance between ROS and antioxidants induces modification of DNA, proteins, and promotes lipid peroxidation. This can

subsequently result in the production of (ROS), via NOX, and has been linked to insulin resistance, and β-cell dysfunction by impairing islet function at the level of insulin synthesis and secretion. Pancreatic β-cells are vulnerable to oxidative stress and ROS as a result of low antioxidant expression, and it is known that imbalances between increase ROS production and limited antioxidant enzyme expression and scavenging activities results in damages to β-cell's viability and secretory capacity [160; 161]. Therefore, it is important to evaluate ROS levels, and oxidative DNA damage in our HFD-fed model since they have been associated with diseases, such as DM. In this study, ROS levels and oxidative DNA damage measured by 8-OHdG, which is a by-product of the DNA base modification by ROS was gnificantly upregulated in the pancreas and islets of both HFD-fed subgroups. Moreover, enhanced ROS, and 8-OHdG levels was notably more elevated in HFD-Hhip$^{+/+}$ compared to HFD-Hhip $^{+/-}$, which correlated positively to the observed decrease in GSIS *in vivo,* as well as from islets isolates from HFD-Hhip$^{+/+}$.

In vitro, oxidative stress, and ROS were measured by DHE staining. rHhip dose-dependently decreased insulin-positive β-cells number; increased the number of DHE-positive cells and NADPH activity, respectively.

Together, these data suggested that HFD-increased Hhip gene expression, added to the imbalance between HFD induced ROS generation, and reduced antioxidant capacity might promote β-cell oxidative stress, thereby impairing GSIS and insulin secretion. Our data is consistent with other findings showing that elevated Hh signaling after overexpression of Shh reduced cytokine-induced apoptosis while treatment with cyclopamine increased cytokine-induced apoptosis in INS-1E cells and rat islets [122]. Interestingly, irrespective if the stress pathway is mediated by cytokines, which are associated with T1DM, or chronic high levels of

circulating glucose and lipids (glucolipotoxicity), and metabolic overload associated with T2DM, increase Hh signaling has been shown to counteract the corresponding apoptotic effects of these stimuli.

Hh signaling has also been reported to play a role in regulating cell proliferation and preventing apoptosis. Shh gene prevents apoptosis in the myocardium, inhibits H_2O_2-induced apoptosis in cultured neonatal cardiomyocytes, and protected germinal centre B cells against Fas-induced cell death [162-163]. In the pancreas, the NOX family represents one potential source of ROS in insulin-secreting cells, and they actively catalyse the transfer of electrons from NADPH to oxygen generating superoxide ions. Both human, rats, and mouse β-cells express membrane-associated catalytic components of NOX1, NOX2 and NOX4 with NOX2 identified as the most functional predominant pancreatic NOX isoform [38; 39; 164]. Among NOX isoforms, we detected *NOX 2* gene expression in both isolated islets and INS-1 832/13 cells; NOX 4 only in INS-1 832/13 cells; and *NOX1* neither islets nor INS-1 832/13 cells respectively, in accordance with other reports [38; 39]. In addition, only NOX2 gene expression was significantly stimulated in the islets of HFD-Hhip$^{+/+}$ mice, and the stimulation was ameliorated in the islets of HFD-Hhip$^{+/-}$ mice. Just like in human islets where NOX2 was shown to co-localize with insulin granules [98]. In our study, using IF staining, we also observed that NOX2 expression was significantly increased in β-cells of HFD-Hhip$^{+/+}$ mice. Moreover, isolated human islet from T2DM patients also demonstrated increased mRNA levels of the p22 subunit of NAD(P)H oxidase [165]. Notably, it is still unclear whether NOX2 gene has an impact on GSIS or not since both positive [38] and negative [166] results have been reported in NOX2 KO mice (C57/BL6) (JAX Laboratory, Bar Harbor, MA) as well.

Nevertheless, we further validated Hhip's impact on NOX2 gene expression *in vitro*. We found that rHhip directly stimulated NOX2 gene expression (mRNA and protein) in a dose-dependent manner; 0.3mM BSA-PA stimulated both Hhip and Nox2 protein expression that could be either aggravated or abolished by rHhip or siRNA-Hhip, respectively. Taken together, not only did we confirm the notion of NOX2 acting as the most predominant isoform, and therefore NOX2 elevates ROS production to antagonize GSIS in the regulation of insulin secretion [38], but we also established that a lower Hhip gene expression might protect islet integrity against HFD-mediated β-cell dysfunction; improve GSIS on maintaining sufficient levels of insulin secretion via ameliorating ROS-NOX2 gene expression. Clearly, β-cell specific gain- and/or loss-of-Hhip function/expression models would be merited to circumvent the potential pitfall of the current whole body Hhip-deficient model in future. Therefore, *in vivo* reduction in islet NOX2 gene, and protein expression, which eventually leads to decrease ROS generation, may constitute a positive pancreatic β-cell adaptive response with respects to increase metabolic fuels, as is the case in obesity, and T2DM.

6.0 Summary

As a summary of this Ph. D dissertation, we have shown that:

- Both male and female HFD-Hhip$^{+/+}$ mice developed pronounced glucose intolerance which was ameliorated in HFD-fed Hhip$^{+/-}$ male mice compared to HFD-fed Hhip$^{+/-}$ female mice.
- HFD feeding resulted in corresponding high levels of circulating plasma insulin, although the phenotype of hyperinsulinemia was significantly pronounced in both male (HFD-Hhip$^{+/+}$ and HFD-Hhip$^{+/-}$) than female (HFD-Hhip$^{+/+}$ and HFD-Hhip$^{+/-}$) mice. In response to HFD, the phenotype of hyperinsulinemia was more pronounced in HFD-Hhip$^{+/-}$ male mice compared to HFD-Hhip$^{+/+}$.
- HFD-Hhip$^{+/+}$ male mice had significantly larger islets, disoriented islet architecture, reduced insulin content and less proliferation which was significantly improved in HFD-Hhip$^{+/-}$ male mice.
- HFD-Hhip$^{+/+}$ male mice had significant apoptosis and oxidative stress mediated in part by *Nox2* as oppose to HFD-Hhip$^{+/-}$ male mice.

7.0 Conclusion

In conclusion, T2DM is a complex disease with increased incidence over the years, and this has been associated with immense social and economic burden. T2DM leads to a reduction in both the quality and life expectancy. Currently, treatments geared towards T2DM are mostly related to either relieving the symptoms or to manage the progression of the disease, but not aimed at the actual pathophysiology of the disease.

In our study, increased Hhip expression in adult pancreatic β-cell compromises *in vivo* glucose intolerance. Our finding indeed focuses on the pathophysiological role of Hhip and a novel pathway involved in pancreatic β-cell dysfunction. We observed that in response to HFD, pancreatic Hhip gene regulated *in vivo* and *ex vivo* insulin secretion in response to glucose by altering islet integrity and promoting NOX2 gene expression in β-cell. Hhip deficiency is critical in maintaining a cohort of healthy islets for efficient pancreatic β-cell function. Our mouse model of heterozygous Hhip knockout mimics changes observed in diabetic humans especially in T2DM, hence highlighting the importance, and relevance to human disease.

This dissertation presents a greater understanding of the biological activity of Hhip in the pancreas for both research and clinical applications. As a perspective, exploring a method to decrease/lower-down Hhip expression, and optimize Hh signaling may provide an opportunity to understand the mechanisms underlying the biological processes of this disease .This mght provide a new innovative way, and therapeutic strategy in the diagnosis, prevention, and optimize the success associated with treatment of T2DM.

8.0 Our Proposed Working Model

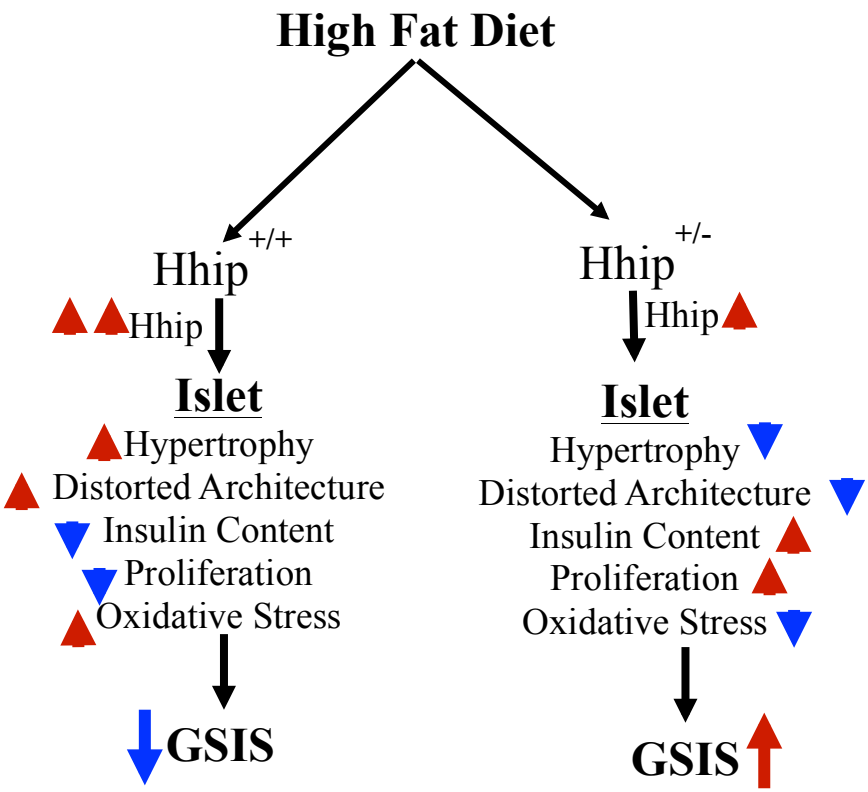

Figure 29: Proposed Working Model. In wild type ($Hhip^{+/+}$) mice, high fat diet promoted Hhip protein expression which led to islet hyperplasia, distorted islet architecture, increase oxidative stress while reducing islet proliferation and insulin content. This culminated in a significant reduction in GSIS. Conversely, in heterozygous ($Hhip^{+/-}$) mice, the increase in Hhip protein expression by high fat diet was ameliorated and this led to the maintenance of islet hyperplasia, architecture, increase islet proliferation and insulin content, favoring GSIS.

C. Unpublished Results

Hedgehog Interacting Protein Overexpression in Renal Proximal Tubules Accelerates Renal Dysfunction in Mice Fed with High Fat Diet

Henry Nchienzia[1], Shiao-Ying Chang[1], Min-Chun Liao[1], Xin-Ping Zhao[1], Isabelle Chenier [1], John S.D. Chan[1] and Shao-Ling Zhang [1§]

[1]Université de Montréal
Centre de recherche du Centre hospitalier de l'Université de Montréal (CRCHUM)
Tour Viger, 900 rue Saint-Denis, Montréal, QC, Canada H2X 0A9

[§] To whom correspondence should be addressed: Shao-Ling Zhang, Ph.D.
Tel: (514) 890-8000 ext. 15633
Fax: (514) 412-7204
Email: shao.ling.zhang@umontreal.ca

Key words: High Fat Diet, Hhip Gene Expression, Proximal Tubules, Kidney Dysfunction

Author Contribution

SLZ is the guarantor of this work, had full access to all study data, and takes responsibility for data integrity and the accuracy of data analysis. JSDC and SLZ were principal investigators and were responsible for the study conception and design. HN wrote the first draft of the manuscript, and SLZ drafted/reviewed/edited the manuscript. HN (Figures 31, 32, 33, and 34), SYC (Figures 30, 33e, 34, 35, 36 and 37), MCL (Figures 36), XPZ (36 and 37), IC (Figures 31, 32, 33e, design and discussion) and SLZ contributed to the experiments and collection of data. All authors were involved in the analysis and interpretation of data and contributed to the critical revision of the manuscript.

Abstract

Diabetes presents high risk factors associated with complications such as chronic kidney disease (CKD) characterized by a gradual loss in kidney function.

In this current study, we demonstrated how Hhip overexpression in renal proximal tubular cells contributes to early development of chronic kidney disease after 14 weeks of HFD. Mice in HFD fed groups showed significantly greater weight gain as compared to mice in ND fed groups. IPGTT revealed that HFD fed mice also developed glucose intolerance with no apparent changes in insulin sensitivity. HFD did not impact hypertension even though we had a modest trend of increase in perirenal fat deposit in the HFD fed subgroups. Renal function as measured by the glomerular filtration rate was normal in all four subgroups, indicating that neither HFD nor Hhip overexpression promoted renal hyperfiltration. Nonetheless, renal morphology revealed HFD kidneys had subclinical injury and presented signs of tubular vacuolization and damage compared to ND fed mice. This pathology of tubular damage and vacuolization was more pronounced in HFD-fed transgenic (Hhip-Tg) mice compared to non-Tg mice and this promoted mild tubular cell apoptosis and enhanced oxidative stress. In conclusion, HFD feeding-induced obesity led to detrimental effects on glucose tolerance and mild morphological changes in kidneys, characterized by the presence of osmotic nephrosis, increased renal oxidative stress and apoptosis which might be mediated by an increase in renal FABP4. This was exacerbated by the over-expression of Hhip in the renal proximal tubules.

1.0 INTRODUCTION

The kidneys are the main organs responsible for filtration and detoxification. A healthy kidney filters approximately 150 liters of blood while producing close to 3 liters of urine per day [167]. The nephron in the kidney is the main functional unit consisting of a renal corpuscle and tubule. The renal corpuscle is made up of the Bowman's capsule which surrounds the glomerulus [168]. The glomerular filtration rate (GFR) is an estimate of the filtration rate of the glomerulus per minute and it is considered as a standard marker for normal kidney function [169]. Immediately after the Bowman's capsule is the renal tubule. The first portion of the tubule is called the proximal convoluted tubule, which is responsible for the reabsorption of the most of the ultrafiltrate. Following the proximal convoluted tubules is the Loop of Henle which further allows for the reabsorption of water and ions such as calcium, sodium, potassium and chloride. After the loop of Henle are the distal convoluted tubules, which also reabsorbs ions (sodium, calcium, chloride) and regulate urine pH by secreting proteins while absorbing bicarbonate [168].

Diabetes presents high risk factors associated with complications such as chronic kidney disease (CKD) characterized by a gradual loss in kidney function [170]. The incidence of CKD is significantly escalating in many nations worldwide with an overall estimated prevalence of 8-16%, translating to approximately 500 million affected individuals [170 -171]. CKD often results in end stage renal disease (ESRD) which is currently a major public health concern [160]. The increased incidence of diabetic related kidney complications has been positively correlated with numerous factors including increasing rate of obesity, T2DM, hypertension and ageing making diabetes one of the leading causes of renal failure [173]. In both obese and obesity induced T2DM individuals, besides the adipose tissues, there is also

excess lipid accumulation in many organs including the kidneys, and this excess lipid eventually compromises organ function resulting in organ damage, including the kideys via a process known as lipotoxicity [174].

Renal tubules, which make up most of the kidneys, are prone to a variety of insults such as hypoxia, proteinuria and metabolic diseases. Proximal tubular cells have a high level of energy demand and most of the energy they use is produced by fatty acid oxidation, fatty acids yielding three times more adenosine triphosphate (ATP) than glucose [174; 175]. Recently, new findings support the fact that dysregulation of fatty acid oxidation followed by excess intracellular lipid accumulation profoundly affects the fate of tubular cells by promoting EMT, apoptosis, necrosis and eventually tubulointerstitial fibrosis (TIF) with increasing reactive oxygen species as a major contributing factor [176; 177]. Further data suggested fatty acids from high fat diet feeding increase renal CD36 and fatty acid–binding protein 4 (FABP4) expression and this synergistically contributes to lipotoxicity-mediated kidney injury [129].

Fatty-acid-binding protein 4 (FABP4) or adipocyte protein 2, a member of the FABP family of proteins (14-15 kDa proteins) is a fatty acid chaperone principally expressed in adipocytes and macrophages [178-179]. Besides the adipocytes and macrophages, FABP4 was found to be expressed in capillary endothelial cells and small veins in several tissues such as the heart and kidneys. FABP4 has been used as a potent clinical biomarker for metabolic and cardiovascular diseases such as obesity, hypertension, non-alcoholic fatty liver disease, ischemic heart disease, T2DM and insulin resistance in various cross-sectional and interventional studies [4]. Previous studies have reported increased FABP4 in the glomerulus, tubular cells and urine of patients with glomerular injury and also observed in the serum of

patients with acute and chronic renal dysfunction hence closely associating FABP4 with renal dysfunction [181- 183].

Hedgehog (Hh) signaling pathway is an evolutionarily conserved pathway that is essential in the regulation of embryogenesis and also in tissue homeostasis, discovered during an embryonic genetic screen that was aimed at understanding body segmentation in *Drosophilia melanogaster*. Hhip, a transmembrane glycoprotein, acts as a biological antagonist of the Hh pathway and is upregulated in response to Hh signaling via either canonical- or non-canonical Hh pathways. Hhip was actually discovered by screening a mouse cDNA expression library for proteins that could bind to all the Hh pathway ligands i.e., Sonic (Shh), Indian (Ihh), and Desert (Dhh). Hhip has been associated with organogenesis, and deregulation of Hhip expression results in developmental defects of the lungs, pancreas and skeleton. Although mostly quiescent in adult tissues, upregulation of Hhip is linked to many human diseases such as cancers, pancreatitis and chronic obstructive pulmonary disease.

2.0 Rationale and Background Knowledge

Publications from our lab showed that post weaning HFD feeding can accelerate kidney injury progression from dams in STZ-induced maternal diabetes mouse model [129]. We recently established that impaired nephrogenesis in kidneys of offsprings of our murine model of maternal diabetes was associated with upregulation of Hhip gene expression [128]. We further determined that hyperglycemia induced increased renal Hhip gene expression in adult murine kidneys of both Type 1 (Akita and STZ-induced) and Type 2 (db/db) diabetic models led to apoptosis of glomerular epithelial cells and promoted endothelial to mesenchymal transition (Endo-MT)- related renal fibrosis [127]. However, the pathophysiological role of Hhip in the kidney needs to be further elucidated in a model of non chronic diabetes.

3.0 Research Question/Aims/Objectives/Hypothesis

We hypothesized that ubiquitous renal Hhip in a model of HFD-induced obesity can exacerbate kidney dysfunction leading to chronic kidney disease. As an objective for the study, we will analyse the role of ubiquitous Hhip and the early mechanisms underlying the pathophysiology of renal dysfunction as a result of hyperglycemia associated with diet induced obesity by the over expression of Hhip in murine proximal tubules. This is important because there is a need for early detection of CKD so as to reduce the associated rates of morbidity, mortality and economic costs and the role of Hhip as a novel molecule associated with the pathogenesis of CKD could prove invaluable.

4.0 Animal Model

4.1 Generation of KAP-mHhip Transgenic (Hhip-Tg) Mice

To better understand and elucidate the role of ubiquitous Hhip in DM, specifically T2DM, we generated transgenic mice overexpressing mouse-Hhip (mHip) specifically in the renal proximal tubules (RPTC's) driven by the kidney-specific androgen-regulated protein (KAP) promoter. Mouse cDNA was cloned from mouse kidney fused with tags (FLAG at the 5' and Myc at the 3') and was inserted into a construct containing the KAP2 promoter (Figure 39a). The isolated KAP2-Myc-mHhip-FLAG transgene was subsequently microinjected into one-cell fertilized mouse embryos (Cyagen Biosciences, Santa Clara, CA). We obtained four positive Tg founders that were then crossed with WT C57BL/6 mice (Jackson Laboratories, C57BL/6J background) to generate F1 generation and confirm transgene transmission to the germline. Breeding was maintained by crossing heterozygous Tg mice to WT C57BL/6 mice. At 14 weeks of age (which represents a peak in testosterone levels, hence maximum transgene expression) male Hhip-Tg and non-Tg control littermates were euthanized and different organs were assayed to determine the tissue-specific expression of transgenic mHhip. By RT-PCR we determined that transgenic male mHhip mice expressed the Hhip transgene specifically in the kidney and more precisely in the proximal tubules. Hence, these data confirmed mHhip transgenic mice overexpress Hhip specifically in RPTC's as seen in Figure 39b. IF staining showed Hhip in Hhip-Tg compared to non-Tg mice specifically colocalized with aquaporin 1 (AQP1-used as a specific proximal tubule marker). This observation further validated our Hhip-Tg mouse model as depicted in Figure 39c.

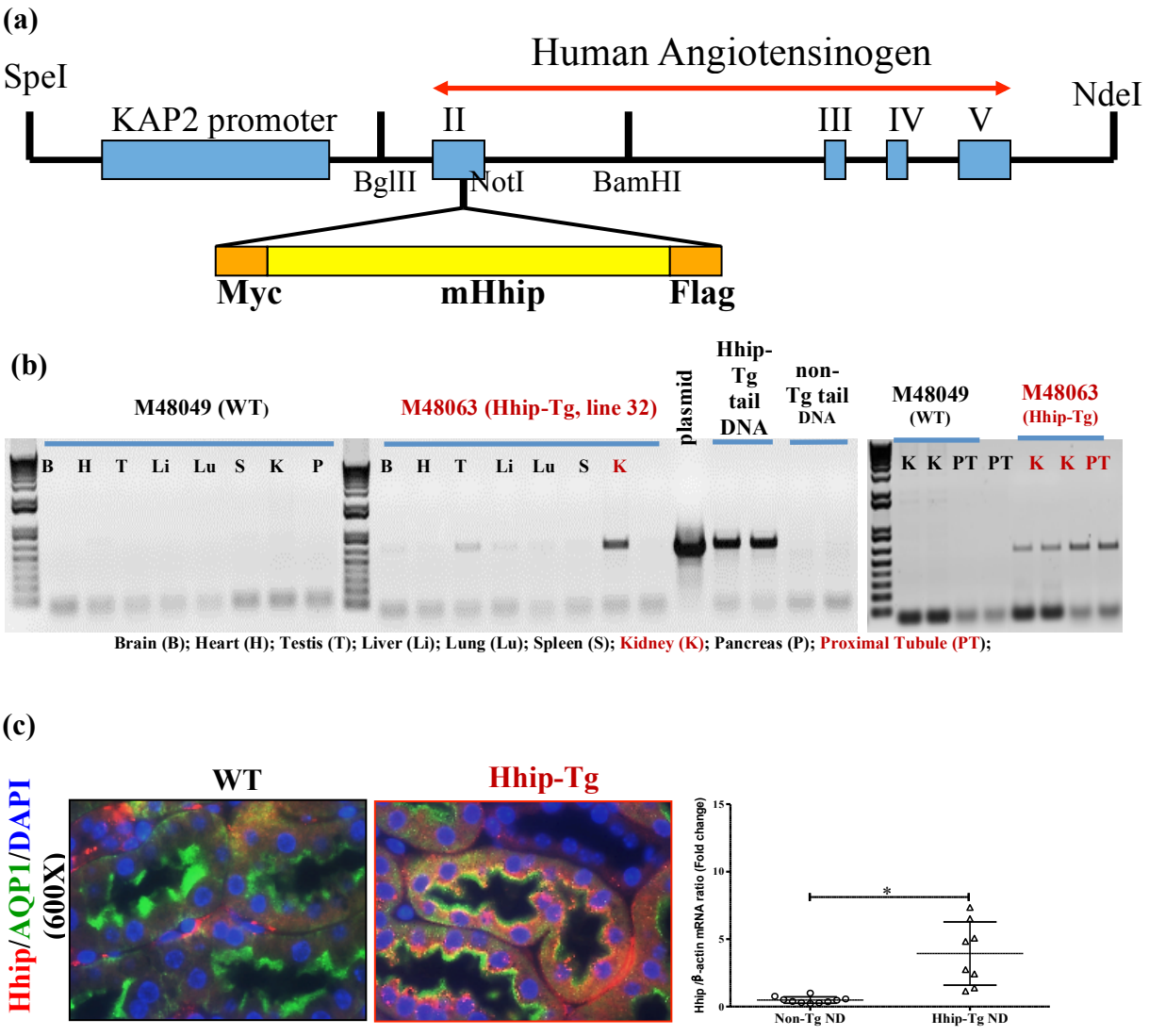

Figure 30: Generation of KAP-mHhip transgenic mice: (a) Schematic map of KAP2-Myc-mHhip-Flag construct; (b)RT-PCR analysis for tissue specific distribution of mHhip in male mHhip-Tg and non-Tg control littermates; (c) colocalisation of Hhip and AQP1 in the renal proximal tubule and Hhip proximal tubular mRNA expression.

5.0 Materials and Methods

5.1 The *in vivo* and *in vitro* Models

5.1.1 *In vivo* Models

Only male Hhip-Tg and non-Tg animal models were used for this current study. This is because the KAP promoter is driven by the male sex hormone androgen. Mice were housed under standard humidity and lighting conditions (12 h light–dark cycles) with free access to food and water ad libitum. 6 weeks old male (Hhip-Tg and non-Tg) mice were either fed normal chow (ND) (18% protein with 6.2% fat, 24% calories from protein, 18% fat and 58% carbohydrate) (Harland, Teklad, Montreal, Canada) or high fat (HFD) (20.5% protein with 36% fat, 14% calories from protein, 60% fat and 26% carbohydrate) (Bio-serv, Flemington, NJ) up to 20 weeks of age. After euthanasia at 20 weeks, kidneys were rapidly harvested, cleaned of all fat and weighed. Left kidney was immediately immersed in 4% formaldehyde and stored at 4°C for fixing. Tissues were subsequently embedded in paraffin after successful dehydration in ethanol for either immunohistochemistry (IHC) and/or immunofluorescence (IF). Part of the right kidney was decapsulated and processed for RPTC isolation by Percoll gradient [182-185] while the other half was snap frozen in OCT. Animal care and procedures were approved by the Institutional committee for the protection of animals of the of the Centre de Recherche du Centre Hospitalier de l'Université de Montréal (CRCHUM).

5.2 Biological, Metabolic Parameters and Physiological Measurements

5.2.1 Biological and Metabolic Parameters

Body weight (BW, g) and energy intake (kCal/week, calculated from daily food intake measured every morning of food change) were monitored weekly throughout the course of the experimental study.

Intraperitoneal glucose tolerance test (IPGTT) and intraperitoneal insulin tolerance test (IPITT) were performed according to a standard protocol with 6- and 4- hours fasting period at the age of 20 weeks respectively as reported elsewhere [129].

In brief, for IPGTT, 3 µl of tail blood was used to measure fasting blood glucose with a portable glucometer and glucose test strips using an Accu-Chek Performa glucose meter (Roche Diagnostics, Laval, Canada). Animals subsequently received 2 g/kg body weight sterilized and filtered glucose by intraperitoneal (ip) injection and blood glucose was measured at 15, 30, 60, 90 and 120 mins from tail blood post injection.

For IPITT, fasting blood glucose was measured as above. Animals also received an ip injection of 1Unit/kg filtered-sterilized insulin (Eli Lilly Canada, Toronto, Canada), and blood glucose was measured as described above at 15, 30, 60 and 90 mins respectively post injection.

Systolic blood pressure (SBP) was monitored using the tail-cuff method with a BP-2000 Blood Pressure Analysis System (Visitech System Inc., Apex, NC) as reported [108]. Acclimatization of animals to SBP measurement was done starting at 19 weeks of age which served as a 1-week pre-training period (SBP measured thrice weekly), followed by actual SBP measurements thrice a week at 20 weeks of age.

The fluorescein isothiocyanate-inulin clearance method was used to measure the glomerular filtration rate (GFR) in live mice as reported elsewhere [129] and recommended by the Diabetic Complications Consortium (http://www.diacomp.org/).

5.2.4 Histological Analysis and RT-PCR

Renal morphology was analyzed by periodic acid–Schiff (PAS) and hematoxylin and eosin (HE) staining.

In vivo oxidative stress was assessed by dihydroethidium (Sigma-Aldrich, Oakville, Canada) staining in frozen kidney sections as reported previously reported [120]. Paraffin embedded kidney sections were used to evaluate *in vivo* apoptosis by BAX. Some of the sections were further subjected to TUNEL assay to visualize apoptotic cells (green) followed by DAPI staining (TUNEL kit, Roche Diagnostics). Nuclei that were both labelled with TUNEL and DAPI were considered as TUNEL positive cells.

The antibodies used included BAX (Santa Cruz Biotechnologies, Santa Cruz, CA); FAPB4 antibody (R&D Systems, Burlington, Canada). The semi-quantitation of the relative staining values was performed by NIH Image J software (Bethesda, MD). The images (N = 6–8 per animal) were analyzed and quantitated in a randomized and blinded fashion.

For IHC, slides were further using the ab64261-Rabbit specific HRP/DAB (ABC) detection kit according to the manufacturer's instructions (Abcam, Cambridge, MA, USA)

Real-time quantitative qPCR (Fast SYBR green mastermix kit and the 7500 Fast real-time PCR system; Applied Biosystems, Foster City, CA, USA) was used to quantify the mRNA levels of various genes in isolated RPTC's. qPCR primer sequences are listed in Table 2.

Table 2: Primers sequences

Gene	Primer Sequences	Reference Sequence
IL-10 (Mouse)	S: GCTCTTACTGACTGGCATGAG AS:CGCAGCTCTAGGAGCATGTG	NM_010548.2
MCP-1 (Mouse)	S: TTAAAAACCTGGATCGGAACCAA AS:GCATTAGCTTCAGATTTACGGGT	NM_011333.3
Hif1-α (Mouse)	S: ACCTTCATCGGAAACTCCAAAG AS: CTGTTAGGCTGGGAAAAGTTAGG	NM_001313919.1
IL1-β (Mouse)	S: GCAACTGTTCCTGAACTCAACT AS: ATCTTTTGGGGTCCGTCAACT	NM_008361.4

Table 2: List of primers sequences

5.2.5 Statistical Analysis.

Groups of 8 to 12 mice were used for this study. *Ex vivo* and *in vitro* experiments, represent three to four separate experiments for each protocol. The values represented are mean ± SEM. Statistical significance between the experimental groups was analyzed by student's t-test, 1-way or 2-way ANOVA, followed by the Bonferroni test using Prism 5.0 software (GraphPad, San Diego, CA, USA). Probability levels of $*p \leq 0.05$; $**p \leq 0.01$; $***p \leq 0.001$were considered to be significant.

6.0 Results

6.1 Physiological Measurements

6.1.1 Body Weight Progression

To investigate the effect of diet on renal function of mice transgenic for Hhip, HFD was introduced to one half of the experimental animals (both Hhip-Tg and non-Tg) while the other half was maintained on ND from 6-20 weeks of age. Mice body weight and food consumption was measured weekly. Base line body weight was comparable between both Hhip-Tg and non-Tg mice before the introduction of the diet. As expected, weight gain by both HFD fed Hhip-Tg and non-Tg mice was comparable and significantly greater compared to ND fed mice as from week 3 after introducing the diet till the end of the 14-week period. This weight gain profile was maintained until the end of the study as seen in Figure 31. Hence this data shows that over-expression Hhip in the proximal tubule does not influence weight gain.

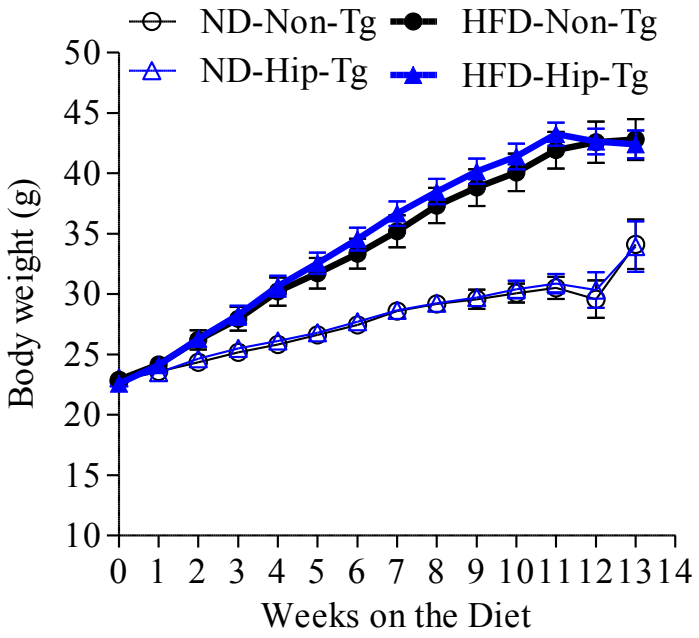

Figure 31: Physiological parameter of both Hhip-Tg and non-Tg mice mice from the age of 6 to 20 weeks old. BW (g) progression. (ND-non-Tg, n=8; ND-Hhip-Tg, n=9; HFD non-Tg, n=13; and HFD-Hhip-Tg, n=15). Data shown as mean ± SEM; 1 way-ANOVA followed by Bonferroni's post hoc test.

6.1.2 Physiological and Metabolic Parameters of Hhip Overexpression in Response to HFD – IPGTT, IST, SBP and GFR

Figure 32 displays the metabolic characteristics of the mice at 20weeks. Fasted blood glucose levels at baseline after 6hours fasting were not significantly different between Hhip-Tg and non-Tg mice across the diets even though HFD fed mice were mildly hyperglycemic as seen in the elevated baseline fasted blood glucose levels.

HFD is known to induce hyperglycemia accompanied by impaired glucose intolerance. To characterize this impact, systemic glucose intolerance was measured by IPGTT and irrespective of the genotype, HFD promoted glucose intolerance in both HFD fed Hhip-Tg and non-Tg mice. Even though HFD fed Hhip-Tg and non-Tg mice had a slight trend of insulin insensitivity compared to ND fed Hhip-Tg and non-Tg mice, they still maintained whole body insulin sensitivity as shown in IPITT data (Figure 32a and 32b). These data highlight the fact that both Hhip-Tg and non-Tg HFD fed mice were susceptible to obesity induced glucose intolerance and not insulin resistance as compared to Hhip-Tg and non-Tg ND fed mice. Therefore, the overexpression of Hhip in mouse proximal tubules does not affect systemic metabolic changes and peripheral responses to insulin.

(a)

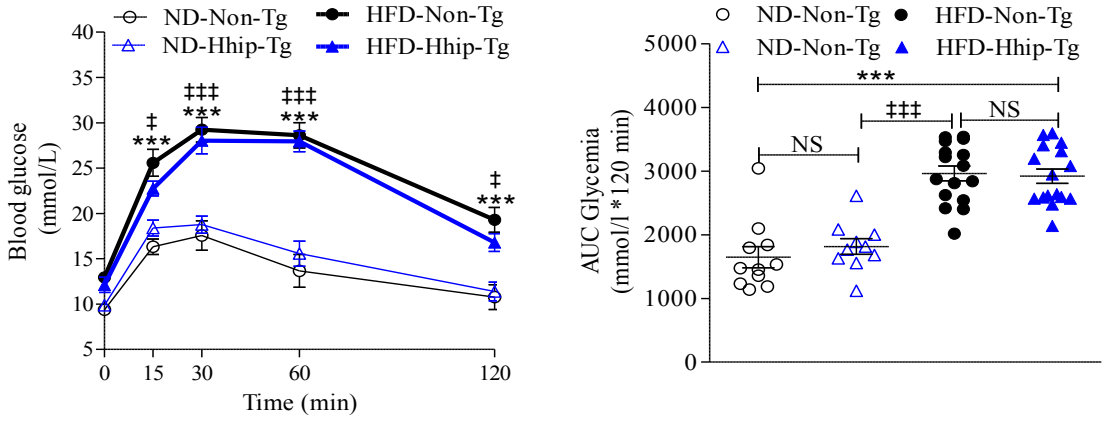

(b)

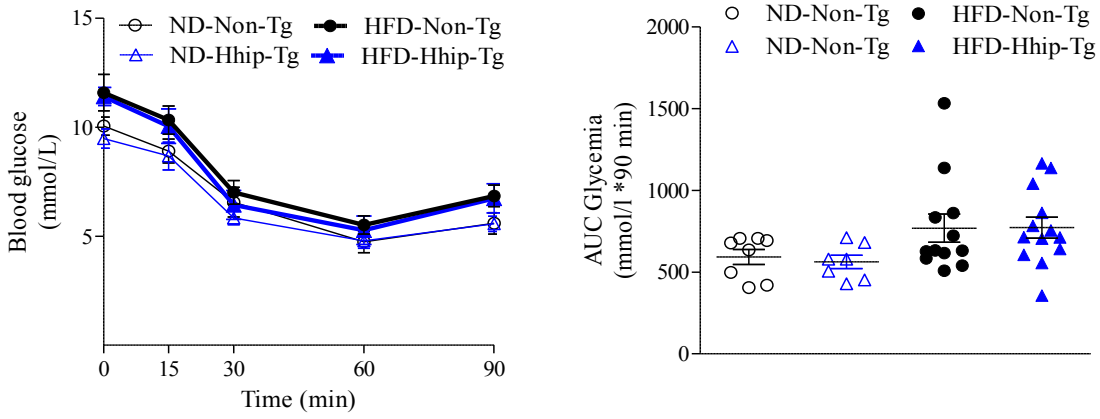

Figure 32: Physiological parameters in male KAP-Hhip-Tg and non-Tg male at age of 20 weeks old. (a) IPGTT (a: ND-non-Tg, n=10; ND-Hhip-Tg, n=10; HFD-non-Tg, n=15; and HFD-Hhip-Tg, n=16); and IPGTT-area under the curve (AUC) quantification (0-120 mins); (b) IST (b: ND-non-Tg, n=10; ND-Hhip-Tg, n=10; HFD-non-Tg, n=15; and HFD-Hhip-Tg, n=16) and IST-area under the curve (AUC) quantification (0-90 mins) . Data shown as mean ± SEM; 1 way-ANOVA followed by Bonferroni's post hoc test. *p ≤0.05; ** p ≤ 0.01; *** p ≤ 0.001 vs. ND-Non-Tg; #p ≤0.05; ## p ≤ 0.01; ### p ≤ 0.001 vs. ND-Hhip-Tg; NS, non-significant.

To further determine if HFD feeding induces changes in systolic blood pressure (SBP), we monitored SBP by the tail cuff method at 20 weeks of age. This analysis revealed no significant changes in SBP among all four subgroups irrespective of the diet, even though both HFD fed Hhip-Tg and non-Tg mice showed a slightly lower SBP (Figure 33a).

Perirenal fat which has been shown to be implicated in the pathogenesis of CKD and hypertension (Figure 33b) was not significantly different between the mice in all four subgroups although HFD fed Hhip-Tg and non-Tg mice trended higher than the ND fed Hhip-Tg and non-Tg mice.

To determine the impact of the diet on kidney masses, both right and left kidneys were averaged to the tibia length (used as an estimate of overall animal growth). This assessment showed that kidney size from both ND and HFD fed Hhip-Tg and non-Tg was similar among all 4 subgroups (Figure 33c-33d).

Glomerular filtration rate (GFR), as a measure of kidney function, further revealed no changes in kidney function regardless of the diet and also independent if the mice was transgenic for Hhip or not (Figure 33e).

Therefore, from the above data, over expressing Hhip in the RPTC did not promote the incidence of hypertension, renal hyperfiltration nor compromised kidney function.

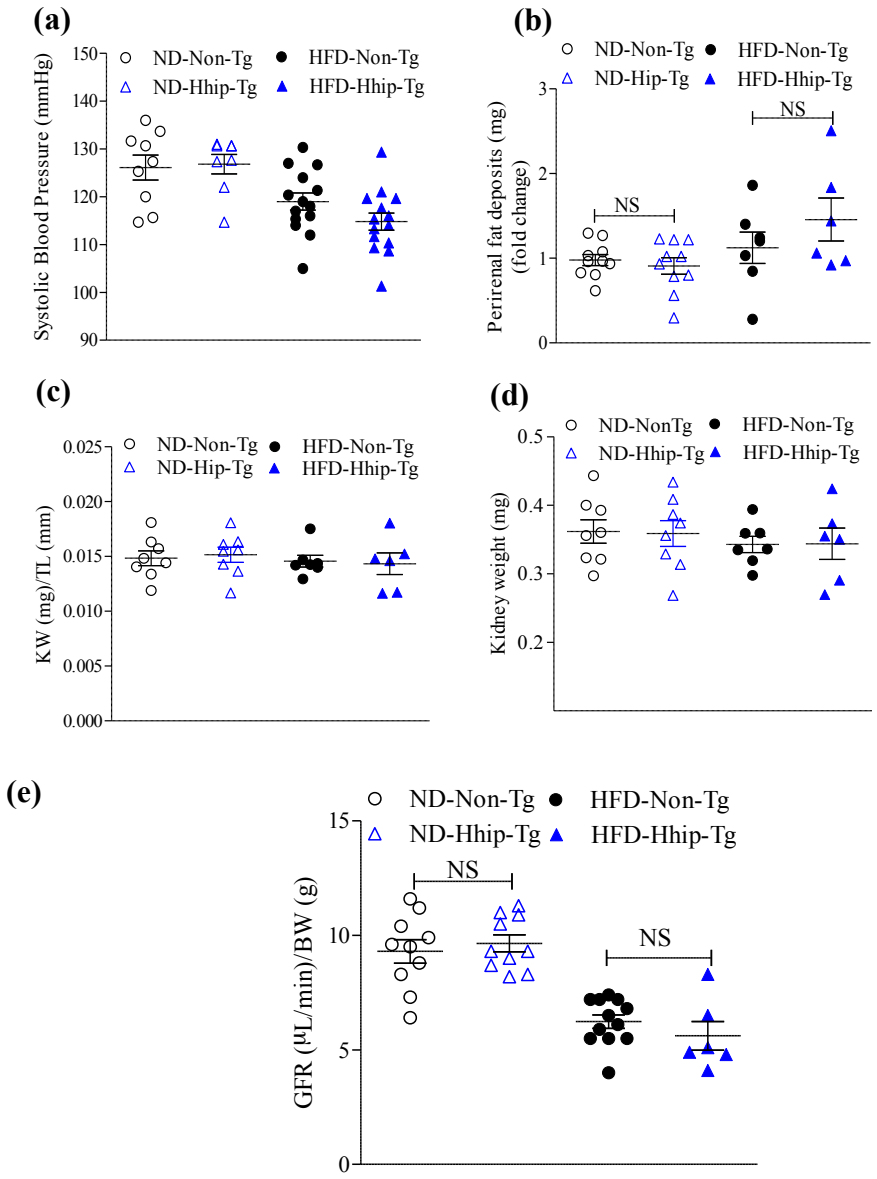

Figure 33: Metabolic parameters in male KAP-Hhip-Tg and non-Tg male at age of 20 weeks old. (a) SBP measurement (ND-non-Tg, n=9; ND-Hhip-non-Tg, n=8; HFD-non-Tg, n=14 and HFD-Hhip-Tg, n=14); (b) Perirenal fat deposits (mg); (c) Kidney weight; (d) Kidney weight/Tibial length ratio; (e) Glomerular filtration rate normalized to BW. (ND-non-Tg, n=9; ND-Hhip-non-Tg, n=10; HFD-non-Tg, n=6 and HFD-Hhip-Tg, n=6). Data shown as mean ± SEM; 1 way-ANOVA followed by Bonferroni's post hoc test. *p ≤0.05; ** p ≤ 0.01; *** p ≤ 0.001 vs. ND-Non-Tg; #p ≤0.05; ## p ≤ 0.01; ### p ≤ 0.001 vs. ND-Hhip-Tg; NS, non-significant.

6.1.3 Hhip Overexpression and HFD Do not Compromise Renal Morphology

We next evaluated the potential effect of HFD feeding on the development of renal injury. Renal morphology of the kidneys from all four subgroups were comprehensively studied by both periodic-acid Schiff (PAS) and hematoxylin and eosin (HE) staining as shown in Figure 34. In the kidney sections of both HFD subgroups, PAS staining (Figure 34) revealed evidence of HFD enhanced tubule dilation and vacuolization, a condition known as osmotic nephrosis. This observation was significantly exacerbated in HFD fed Hhip-Tg mice compared to non-Tg mice. This was further accompanied by increased cell sloughing inside the tubular lumen alongside missing or ruptured brush border. There was no difference in both ND fed Hhip-Tg and non-Tg mice. Consisted with PAS staining, HE staining further confirmed the pronounced tubular vacuolization observed in HFD fed Hhip-Tg mice as compared to HFD fed non-Tg mice. Even though HFD promoted structural changes in the form of vacuolization in both HFD fed subgroups, these changes appeared more severe in HFD fed Hhip-Tg mice compared to HFD fed non-Tg mice. These results indicate that overexpressing Hhip in the proximal tubules can potentially compromise kidney morphology.

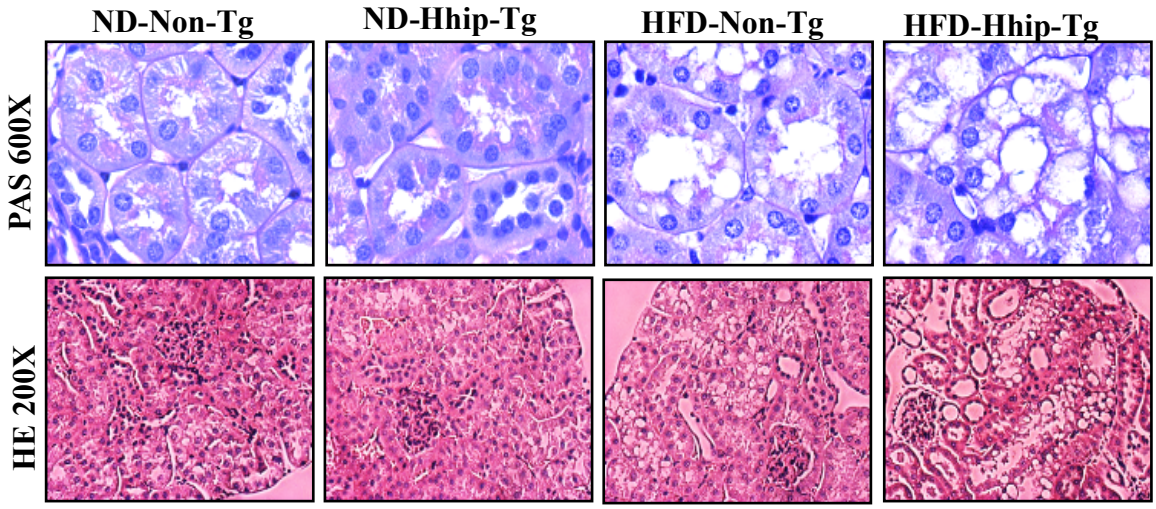

Figure 34: PAS and HE *in vivo* staining in the kidney among 4 subgroups of male mice at 20 weeks-old.

6.1.4 Hhip Overexpression and HFD-Induced Obesity Do not Induce Renal Lipid Accumulation but Promotes FAPB4 Deposition

FABP4 has been shown to regulate renal interstitial cell apoptosis and play important roles in both renal inflammation and lipid metabolism. We assessed FABP4 gene expression in the renal cortex by IHC (Figure 35). Interestingly, our IHC analysis showed HFD increased renal FAPB4 expression in both HFD fed groups compared to ND fed groups. This increase in FABP4 was more obvious in HFD fed Hhip-Tg mice compared to HFD fed non-Tg mice. Protein expression was increased in HFD non-Tg while mRNA showed an increase in Tg-ND compared to other subgroups.

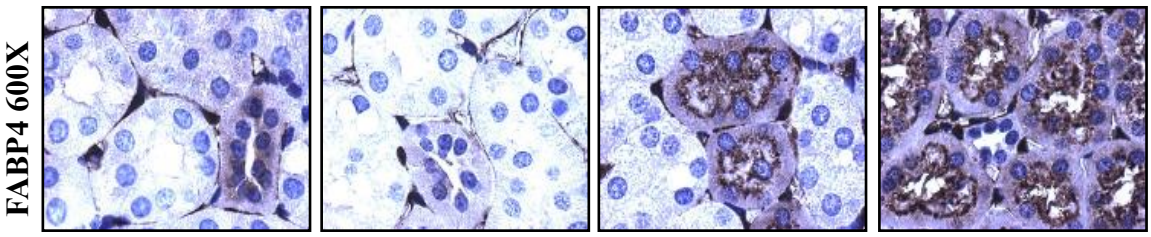

Figure 35: IHC in vivo. FABP4 staining in the kidney among 4 subgroups of male mice at 20 weeks-old.

6.1.5 Hhip Overexpression and HFD Induced Obesity Do not Result in Inflammation

Numerous studies have associated renal inflammation with the progression of diet induced obesity renal disorder in most animal models, we therefore evaluated the renal gene expression of some inflammatory markers in the current model. Under our experimental condition, gene levels of IL-1β, IL-10 and Hif 1α were all unchanged, irrespective of the diet and/ or transgene as seen in Figure 36.

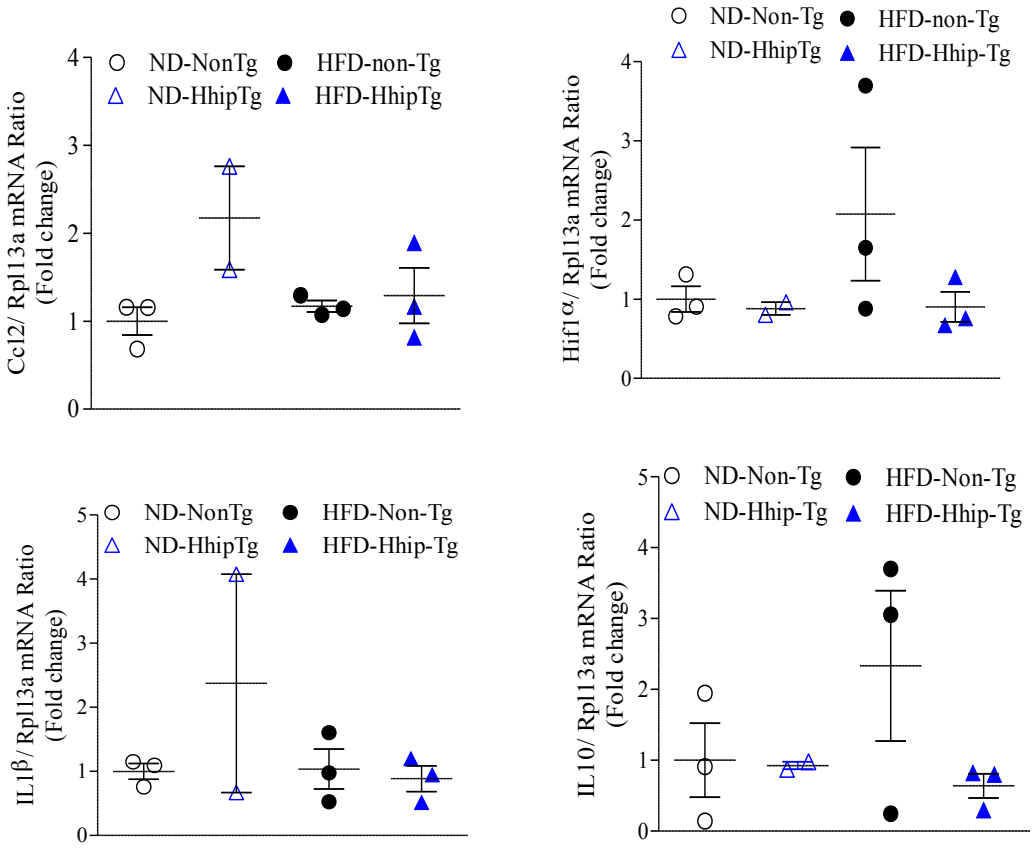

Figure 36: qPCR-mRNA expression of Ccl2, Hhif1α, IL 1β and IL 10 genes (vs Rpl 13a mRNA ratio) in isolated proximal tubules among the 4 subgroups of male mice, (ND-non-Tg, n=3; ND-Hhip-non-Tg, n=2; HFD-non-Tg, n=3 and HFD-Hhip-Tg, n=3). Data shown as mean ± SEM; 1 way-ANOVA followed by Bonferroni's post hoc test.

6.1.6 Hhip Overexpression and HFD-Induced Obesity Promote Renal Oxidative Stress and Apoptosis

HFD has been positively correlated with renal oxidative stress and apoptosis. The presence of high concentrations of polyunsaturated fatty acids in the kidneys, which can be easily oxidized in the presence of reactive oxygen species, makes the kidneys more susceptible to oxidative stress. Renal oxidative stress measured by dihydroethidium staining (whereby superoxide anion $O_2^{\cdot -}$ oxidizes the non-fluorescent dihydroethidium to fluorescent ethidium) revealed evidence of elevated oxidative stress in both HFD fed Hhip-Tg and non-Tg mice compared to ND fed mice figure 37. This was further enhanced in HFD fed Hhip-Tg mice. IHC further revealed that under HFD, BAX (a pro-apoptotic protein) positive staining was significantly increased specifically in the proximal tubules (Figure 37). Kidney sections were further subjected to TUNEL assay to analyze apoptotic cells and IF staining showed that HFD promotes tubular cells apoptosis. In line with oxidative stress, the increase in both BAX protein deposits and TUNEL positive cell increase was more pronounced in the proximal tubules of HFD fed Hhip-Tg mice as compared to non-Tg mice as seen in Figure 37.

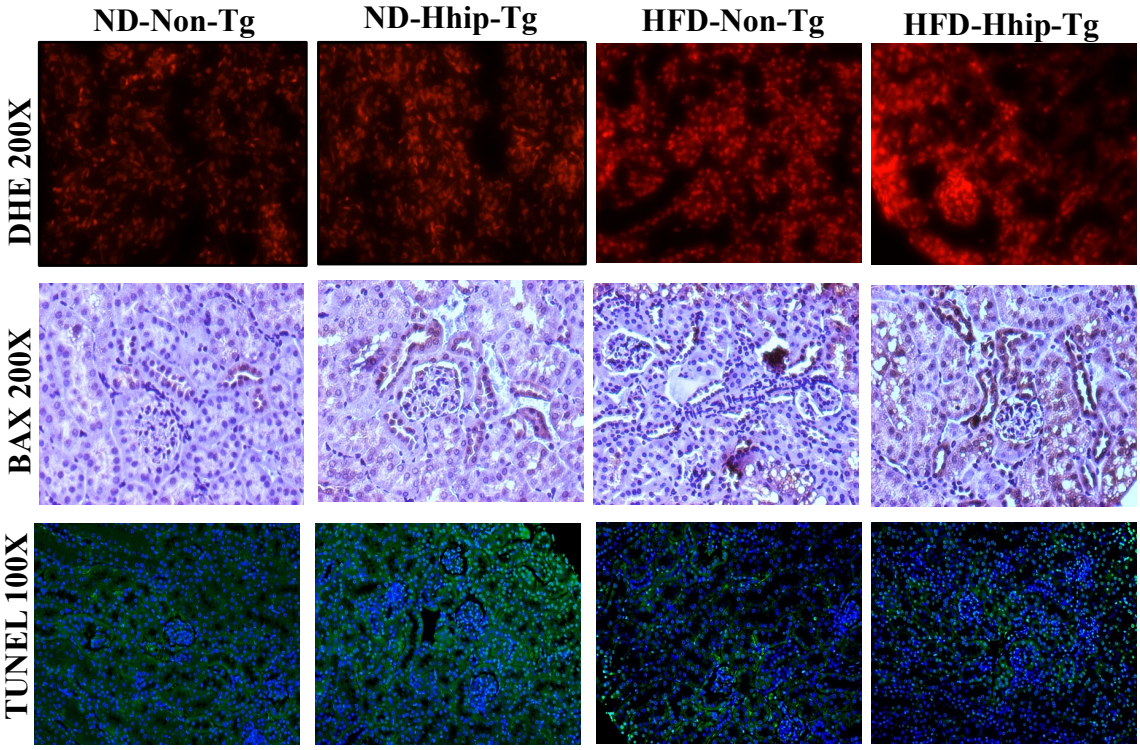

Figure 37: In vivo assessment of renal oxidative stress and apoptosis in the kidney among 4 subgroups of male mice at 20 weeks-old.

Discussion

HFD in rodent studies has been shown to induce a myriad of major symptoms compatible to human metabolic syndrome such as obesity, hypertension, glucose intolerance, insulin resistance as well as renal injury. The present study aimed to investigate both the morphological and functional response of kidneys transgenic for Hhip to HFD in the absence of frank hyperglycemia. To investigate the role of Hhip and provide evidence of Hhip as a major player in CKD *in vivo*, we generated mice overexpressing mHhip in renal proximal tubules. Our findings in this study provide evidence that both Hhip-Tg and non-Tg mice showed mild features of metabolic syndrome such as obesity, glucose intolerance and mild insulin resistance in response to HFD in the absence of frank hyperglycemia. HFD did not impact hypertension even though we had a modest trend of increase in perirenal fat deposit in the HFD fed subgroups. Accompanying these changes, renal function as measured by the glomerular filtration rate was normal in all four subgroups, indicating that neither HFD nor Hhip overexpression promoted renal hyperfiltration. Nonetheless, despite normal renal function, renal morphology revealed HFD kidneys had subclinical injury and presented signs of tubular vacuolization and damage compared to ND fed mice. This pathology of tubular damage and vacuolization was more pronounced in HFD-fed Hhip-Tg mice compared to non-Tg mice and this promoted mild tubular cell apoptosis and enhanced oxidative stress.

We demonstrated that feeding HFD to both Hhip-Tg and non-Tg mice for a period of 14 weeks led to a greater increase in body weight relative to the ND fed mice. This observed increase in body weight was comparable between Hhip-Tg and non-Tg mice. This observation that the mice used in this study are a reliable strain for the experimental study of diet induced

obesity. Hence over expressing Hhip in the proximal tubules does not compromise the ability of both Hhip-Tg and non-Tg mice to gain weight when challenged with HFD. In addition, body weight increases in both HFD fed Hhip-Tg and non-Tg mice resulted in significant glucose intolerance. Even though HFD feeding has been positively correlated with increased obesity induced glucose intolerance and insulin resistance, interestingly from our results, we did not observe any frank obesity-induced insulin resistance as measured by IPITT, similar to results reported by Glastras et al, who showed offsprings of diabetic dams given STZ and fed HFD, despite their increased body weight adiposity and hyperglycemia, were not insulin resistant [186].

Obesity, type 2 diabetes and the accumulation of perirenal fat especially in obese human subjects and most animal models of HFD studies, has been shown to increase the incidence of hypertension by compressing both the lymphatic and venous vessels leading to increased hydrostatic pressure and renin-angiotensin-aldosterone (RAAS) system activation. [187-190]. However, in this study, HFD did not provoke the incidence of hypertension even though we found a modest but not significant increase in perirenal fat deposits in our HFD fed group compared to the ND fed groups. Our data is consistent with that presented by Aliou et al who also showed that male mice from both control and diabetic dams were normotensive after 16 weeks on HFD [129]. A similar observation was also made by Fernandes et al who also reported that Sprague Dawley rats were normotensive after 24 weeks on the HFD [191]. Kidney mass measurements also revealed that kidney weights from mice from the four subgroups were similar even when normalized with tibial length (which is a measure of animal growth). These findings suggest that over expression of Hhip in the proximal tubules has no effect on systemic blood pressure and kidney size nor does it affect overall growth. There is

accumulating evidence that obesity and diabetes compromise kidney function as measured by GFR in both Akita [192], db/db [193] and STZ injected mice [128], however, contrary to these results, we did not observe any disturbances in kidney function in our present model under HFD. Our data is consistent with findings made by Aliou et al who also showed that HFD feeding in male offspring of diabetic dams did not affect kidney function compared to control mice [129]. Likewise, Glastras et al also showed that low dose STZ combined with HFD had little effect on the renal outcome at 24 weeks HFD [186]. A possible explanation for the lack of impact in kidney function in this current model of DIO may be because we did not observe frank hyperglycemia or overt obesity which have both been shown to promote renal hyperfiltration. Further analysis of proximal tubular cell size and volume (data not shown) also showed no tubular hyperfiltration among the four subgroups. Taking into account the above, the lack of impact on kidney function might help explain why a major parameter such as blood pressure was unaffected in all four subgroups.

Despite no observed significant changes in kidney function by HFD feeding as estimated by GFR, renal morphology assessment by both PAS and HE showed signs of morphological damage in the kidneys of HFD fed mice. This morphological condition is characterized by tubular dilation, tubular swelling and the presence of vacuoles in both the convoluted and straight parts of the renal proximal tubules and known as osmotic nephrosis. This is evidence by the presence of non-specific intracytoplasmic vacuoles, tubular injury, and missing or ruptured brush border accompanied by cell sloughing [194-197]. This condition was present mainly in the HFD fed subgroups which was more dramatic in HFD fed Hhip-Tg compared to the non-Tg mice. Even though the presence of osmotic nephrosis does not directly impact proximal tubular function in particular, nor kidney function as a whole,

however if progressive, osmotic nephrosis can potentially lead to the development of severe kidney injury or end stage kidney failure, especially in patients with other kidney injuries such as diabetes or under hypoxic conditions. Hence, from our PAS data, we can conclude that over expression of Hhip in the proximal tubules in addition to HFD can promote the occurrence of osmotic nephrosis which might eventually compromise kidney function.

Obesity has been shown to upregulate the incidence of renal oxidative stress and inflammation [191; 186]. In addition to the above observed structural changes, we observed enhanced HFD-induced renal oxidative stress which was significantly increased in HFD fed Hhip-Tg compared to non-Tg mice, even though there were no obvious pathological changes. Simultaneously, there was an increased accumulation of BAX protein specifically in the proximal tubules of HFD fed mice compared to ND fed mice. While this increase was observed in both HFD subgroups, it was more prominent in HFD fed Hhip-Tg compared to non-Tg mice. Likewise, IF staining also showed an increase TUNEL positive cells in HFD fed Hhip-Tg mice compared to non-Tg fed mice. Although there is no obvious kidney damage or loss of function in the current model, these data would indicate the presence of increased oxidative stress as measured by DHE, an increase in the deposit of a pro-apoptotic protein, BAX, as well as an increase TUNEL positive cells which could potentially mean over expressing Hhip in renal proximal tubules might increase the probability of the occurrence of CKD in the face of continuous HFD feeding. The above findings will be extended *in vitro* to provide a mechanistic explanation by employing the use of an immortalized proximal tubule cell line and treating them with palmitic acid and glucose to mimic the circulating increase in fatty acids associated with HFD.

A strong association has been established by many studies between HFD feeding and renal inflammation [198]. However, in this study, HFD feeding for 14 weeks did not promote renal inflammation as seen from the gene expression of inflammation related factors such IL-1β, HIF-1α and MCP-1 in isolated proximal tubules. These results are similar with observations made by Fernandes et al who reported that both HFD fed Sprague Dawley rats and C57BL/6 mice were obese without significant renal inflammation [191]. Yang et al also showed that HFD feeding in mice alone resulted in obesity and hyperlipidemia but no systemic inflammation [198]. These findings suggest that in the absence of frank hyperglycemia and overt obesity in a DIO model of kidney injury, Hhip overexpression in the proximal tubule does not promote inflammation induced-renal injury. This might have to be further confirmed at the protein level by way of western blot, by measuring the plasma levels of some inflammatory makers (TNFα, IL-6) and by also analyzing the whole kidney cortex. It will also be interesting to verify and confirm these findings *in vitro* by use of immortalized proximal tubule cell line.

In the early stages of CKD and DN, there is increased accumulation of macrophages in the kidney as a result of increased oxidative stress and chronic inflammation. These events have been shown to subsequently induce the expression of serum FABP4 [199-201]. From our study, using IHC analysis we observed a significant HFD-induced FAPB4 deposition in the kidney cortex. Interestingly, FABP4 deposition was restricted to the proximal tubules and these deposits were more significant in HFD fed Hhip-Tg compared to non-Tg mice. As reported by Aliou et al increased renal FABP4 might be involved in renal dysfunction and injury in HFD-fed mice, thus suggesting that FAPB4 might be implicated in HFD induced ROS generation which might eventually impair kidney function and lead to CKD [129]. The

aforementioned observation will have to be confirmed both at the gene and protein levels. Renal lipid accumulation in this model will also have to be assessed by Oil Red O staining since fat infiltration in a model of diet induced obesity has been associated with CKD.

In conclusion, the main findings in this study are that HFD feeding induces obesity which led to detrimental effects on glucose tolerance, mild morphological changes in kidneys characterized by the presence of osmotic nephrosis, increased renal oxidative stress, and apoptosis which might be mediated by increased renal FABP4. Of interest, this observation was exacerbated by the over expression of Hhip in the renal proximal tubules, hence implicating Hhip as a major player in this scenario. Even though the observed renal changes were mild, progressive HFD feeding together with the over expression of Hhip in the renal proximal tubule can synergistically lead to the potential incidence of kidney dysfuntion. The findings of this current study complement our previous study where we show that heightened Hhip expression in kidneys of both genetic models of T1DM and T2DM may mediate glomerular endothelial fibrosis and apoptosis [128].

Thesis General Discussion and Conclusion

Adaptation to modern life style, with increased consumption of high caloric food together with increased rates of physical inactivity favors the incidence of obesity associated with morbidity and mortality [202-203]. Obesity has been shown to play a very important role in the etiology of T2DM [204-205]. Previously considered as an adult disease, recently it has been established that the incidence of T2DM in young adults is on the rise [206-207].

In this thesis, we studied the role of Hhip in the etiology of T2DM, as well as its implication in diabetic complications, especially diabetic nephropathy. In order to better understand and elucidate the role of Hhip, we used a model of diet induced obesity (DIO) by feeding high fat diet to C57BL/6 mice either deficient for Hhip (whole body knockout) or overexpressing Hhip (tissue specific overexpression). As opposed to genetically altered model, such as the db/db model, a major advantage of using the HFD model with the C57BL/6 genetic background is that the mice have been shown to have a good response to high fat diet by exhibiting a myriad of symptoms associated with metabolic disorders, which closely resembles the metabolic disorders observed in humans. Hence, this provides an avenue to investigate life style alterations in relation to T2DM without genetic modification, elucidate the role of Hhip in the etiology of this disease, and possible intervention strategies.

Conclusion from Article 1

The results presented in Chapter 2 (article 1) of this thesis clearly demonstrate how whole-body knockout of Hhip plays a very important role in regulating insulin secretion by promoting beta cell proliferation, and preventing beta cell apoptosis via increased nitrate oxidase (NOX2) without affecting weight gain (appetite). Thus, our results collectively show how Hhip can potentially regulate the fate of pancreatic beta cells in T2DM, and in the face of hyperglycemia. In this chapter (article 1), mice were maintained on the HFD for 8 weeks, which puts us in the prediabetic window of obesity, and here we showed how Hhip deficiency ($Hhip^{+/-}$) promotes beta cell compensatory/secretory responses during prediabetes, thereby preventing the onset of insulin resistance, and the eventual progression to T2DM as compared to wild type animals ($Hhip^{+/+}$). While it is well established that insulin secretion is compromised in islets of T2DM patients and HFD fed mouse models [208-209], this study highlights the functional contribution of Hhip deficiency in improving glucose homeostasis by enhancing insulin secretion in this disease state. Thus, this study presents a better model to study prediabetic stages and beta cell compensatory responses providing us with a window of opportunity for primary interventions. Even though much is still not known with respect to the role of Hhip and T2DM, our findings presented in this chapter highlight the role of Hhip in maintaining islet integrity, improving insulin secretory capacity, and ameliorating glucose tolerance. Therefore, targeting Hhip might offer a novel therapeutic molecule to consider in the development of anti-diabetic drugs targeted towards T2DM.

Insulin resistance in its target tissues (fat, liver and muscles) is central to the development of T2DM, and forms the pathophysiological basis of obesity-induced T2DM [210]. One of the limitations of this study is the use of a whole-body knockout in which case

we could not clearly distinguish the contribution of each of the above organs in the observed phenotype. This could be circumvented by using an inducible tissue specific knock out model. An inducible system is required because Hhip is very important for organogenesis, hence can only be knocked out after birth in targeted tissues. Also, the use of HFD in mice in mimicking systemic metabolic syndrome is greatly impacted by the genetic background, with mice on the C57BL/6 more prone to develop obesity and obesity induced-T2DM [211-212]. Likewise incidence of obesity- induced T2DM also varies within the human population, studies have identified populations such as Blacks, Hispanics and Native Americans as high-risk populations [213-215]. Another limitation of this study is acknowledged in the use of mice on a mixed genetic background of C57BL/6, Swiss-Webster and 129, respectively. In this case it is difficult to account for the contribution of each background to the development of the observed phenotype of systemic metabolic syndrome. Therefore, back crossing the line to a pure background (preferably C57BL/6) might help identify the role of the background vis a vis the observed phenotype. In attempting to elucidate the role of GSIS in vivo, we faced the difficulty of clearly demonstrating the first phase GSIS effect on insulin secretion. This might be one of many reasons such as the mice being on a mixed background or maybe because we did not evaluate early time points in insulin secretion, such as 5 and 10 mins, respectively. Backcrossing to a pure background and considering earlier time points might help clarify this challenge. In order to elucidate the effect of HFD in Hhip female mice, it might be interesting to extend the study with female mice beyond the reproductive age of the animal (where the estrogen levels are low), so as to mimic human disease condition(s) in post-menopausal women.

Conclusion from Article 2

Obesity induced T2DM is strongly associated with the development of kidney dysfuntion and as an extension of chapter 2 (article 1), we further investigated the role of Hhip overexpression in diet-induced obesity related to renal damage. Reports have shown that diabetic complications might sometime exist in prediabetic stages, and the development of diabetic complications, as well as deterioration in glycemic control, are linked as people progress from prediabetes to T2DM [216-217] . In order to test this hypothesis, we placed C57BL/6 mice specifically overexpressing Hhip in their renal proximal tubules for 14 weeks on HFD. Our findings so far from this study demonstrate that HFD induced metabolic detrimental effects, such as glucose intolerance, independent of Hhip overexpression. Even though we did not observe a distinct decline in kidney function, kidney pathology analysis revealed mild subclinical changes including increased tubular vacuolization known as osmotic nephrosis with an upregulation of oxidative stress markers, pro-apoptotic markers, FABP4 protein deposition (specifically in the proximal tubules) as well as the onset of tubular cell death assessed by TUNEL positive staining. Clearly from our data, we observe that these adverse events were all synergistically increased by Hhip overexpression in the proximal tubules of Hhip-Tg and HFD feeding compared to just HFD feeding alone in non-Tg mice. This design was effective because it provided a better insight to the contribution of Hhip under obese conditions. Thus, our data demonstrates how Hhip in the face of obesity-induced T2DM can predispose the kidneys to the development of kidney dysfunction. This highlights Hhip as a potential targeted molecule in the early development of kidney dysfuntion and may enable

intervention studies in order to prevent the progression of kidney damage, and consequently reduce the complications of kidney dysfunction and subsequently end stage renal disease.

There are some limitations that are recognized in this study. While C57BL/6 mice are known to be obesity prone and a good model for diet-induced obesity studies, reports have also shown that they are resistant to HFD-induced renal dysfunction [219-221]. As reason advanced for this, some studies suggest that HFD alone mimics only early stages of T2DM, specifically the prediabetic phase since the animals never fully develop beta cell failure, and hence frank hyperglycemia as observed in advances stages of T2DM in human patients [41]. As a consequence, maybe that is why in this model we did not observe any significant changes in kidney function as measured by GFR as opposed to genetic models of both T1DM (Akita) [192] and T2DM (db/db) [193]. We could either increase the duration of HFD from 14 to 32 weeks as reported by Glastrass et al [186], where they showed that HFD plus the addition of one dose of STZ was insufficient to induce chronic kidney damage after 24 weeks suggesting the duration of the high fat diet be extended to 32 weeks. Also, SBP in this study was measured by tail cuff as opposed to telemetry and to capture the effect of DIO on SBP, we could use a more reliable method like telemetry.

As a general conclusion, this thesis highlights the role of Hhip, and Hhip inhibition in the context of T2DM. This may provide an interesting and unique therapeutic approach since collectively our results demonstrate Hhip can potentially regulate organ function such as pancreas and kidneys in T2DM.

D. REFERENCES

[1] Da Silva Xavier G (2018) The cells of the islets of langerhans. Journal of clinical medicine 7:54
[2] White JR (2014) A brief history of the development of diabetes medications. Diabetes spectrum 27:82-86
[3] Lakhtakia R (2013) The history of diabetes mellitus. Sultan Qaboos Univ Med J 13:368-370
[4] Das AK, Shah S (2011) History of diabetes: from ants to analogs. J Assoc Physicians India 59 Suppl: 6-7
[5] Ahmed AM (2002) History of diabetes mellitus. Saudi Med J 23:373-378
[6] Wasson C, Kelly A, Ninan D, Tran Q (2019) Diabetes Mellitus (DM). In: Anonymous Absolute Obstetric Anesthesia Review. Springer, pp. 97-99
[7] Mendes O, Koetzner L, Chen J (2018) Nutraceutical Impact on the Pathophysiology of Diabetes Mellitus. In: Anonymous Nutritional and Therapeutic Interventions for Diabetes and Metabolic Syndrome (Second Edition). Elsevier, pp. 329-341
[8] Zimmet P, Alberti K, Shaw J (2001) Global and societal implications of the diabetes epidemic. Nature 414:782
[9] Graham ML, Schuurman H (2015) Validity of animal models of type 1 diabetes, and strategies to enhance their utility in translational research. Eur J Pharmacol 759:221-230
[10] Cho N, Shaw J, Karuranga S, et al. (2018) IDF Diabetes Atlas: Global estimates of diabetes prevalence for 2017 and projections for 2045. Diabetes Res Clin Pract 138:271-281
[11] Guariguata L, Whiting DR, Hambleton I, Beagley J, Linnenkamp U, Shaw JE (2014) Global estimates of diabetes prevalence for 2013 and projections for 2035. Diabetes Res Clin Pract 103:137-149
[12] Atlas D (2006) International diabetes federation. Press Release, Cape Town, South Africa 4
[13] Murray CJ, Lopez AD (2013) Measuring the global burden of disease. N Engl J Med 369:448-457
[14] Cai X, McGinnis JF (2016) Diabetic Retinopathy: Animal Models, Therapies, and Perspectives. Journal of Diabetes Research 2016
[15] American Diabetes Association (2019) 2. Classification and Diagnosis of Diabetes: Standards of Medical Care in Diabetes-2019. Diabetes Care 42:S13-S28
[16] Baynes H (2015) Classification, pathophysiology, diagnosis and management of diabetes mellitus. J diabetes metab 6:1-9

[17] Skyler JS, Bakris GL, Bonifacio E, et al. (2017) Differentiation of Diabetes by Pathophysiology, Natural History, and Prognosis. Diabetes 66:241-255
[18] Agardh E, Allebeck P, Hallqvist J, Moradi T, Sidorchuk A (2011) Type 2 diabetes incidence and socio-economic position: a systematic review and meta-analysis. Int J Epidemiol 40:804-818
[19] Kahn SE, Hull RL, Utzschneider KM (2006) Mechanisms linking obesity to insulin resistance and type 2 diabetes. Nature 444:840
[20] Janochova K, Haluzik M, Buzga M (2019) Visceral fat and insulin resistance--what we know? Biomedical Papers of the Medical Faculty of Palacky University in Olomouc 163
[21] Parasuraman S, Wen LE (2015) Animal Model for Obesity-An Overview. Systematic Reviews in Pharmacy 6:9
[22] Barness LA, Opitz JM, Gilbert-Barness E (2007) Obesity: genetic, molecular, and environmental aspects. American Journal of Medical Genetics Part A 143:3016-3034
[23] Mokdad AH, Marks JS, Stroup DF, Gerberding JL (2005) Correction: actual causes of death in the United States, 2000. JAMA 293:293-294
[24] Al-Goblan AS, Al-Alfi MA, Khan MZ (2014) Mechanism linking diabetes mellitus and obesity. Diabetes Metab Syndr Obes 7:587-591
[25] Ye J (2013) Mechanisms of insulin resistance in obesity. Frontiers of medicine 7:14-24
[26] Prentki M, Nolan CJ (2006) Islet beta cell failure in type 2 diabetes. J Clin Invest 116:1802-1812
[27] Cobb J, Eckhart A, Motsinger-Reif A, Carr B, Groop L, Ferrannini E (2016) alpha-Hydroxybutyric Acid Is a Selective Metabolite Biomarker of Impaired Glucose Tolerance.
[28] https://www.endocrineweb.com/conditions/type-2-diabetes/insulin-resistance-causes-symptoms.
[29] https://www.medicalnewstoday.com/articles/305567.php. Diabetes Care 39:988-995
[30] Vaag A (2008) To be predisposed to insulin resistance and type 2 diabetes. J Physiol (Lond) 586:2421-2421
[31] Chung ST, Chacko SK, Sunehag AL, Haymond MW (2015) Measurements of Gluconeogenesis and Glycogenolysis: A Methodological Review. Diabetes 64:3996-4010
[32] Hatting M, Tavares CD, Sharabi K, Rines AK, Puigserver P (2018) Insulin regulation of gluconeogenesis. Ann N Y Acad Sci 1411:21-35
[33] Cernea S, Dobreanu M (2013) Diabetes and beta cell function: from mechanisms to evaluation and clinical implications. Biochemia medica: Biochemia medica 23:266-280
[34] Kim J, Yoon K (2011) Glucolipotoxicity in pancreatic β-cells. Diabetes & metabolism journal 35:444-450
[35] Sezer H (2017) Insulin resistance, obesity and lipotoxicity. In: Anonymous Obesity and Lipotoxicity. Springer, pp. 277-304
[36] Poitout V, Amyot J, Semache M, Zarrouki B, Hagman D, Fontés G (2010) Glucolipotoxicity of the pancreatic beta cell. Biochimica et Biophysica Acta (BBA)-Molecular and Cell Biology of Lipids 1801:289-298
[37] Huang Q, You W, Li Y, et al. (2018) Glucolipotoxicity-Inhibited miR-299-5p Regulates Pancreatic beta-Cell Function and Survival. Diabetes 67:2280-2292
[38] Newsholme P, Morgan D, Rebelato E, et al. (2009) Insights into the critical role of NADPH oxidase (s) in the normal and dysregulated pancreatic beta cell. Diabetologia 52:2489-2498

[39] Li N, Li B, Brun T, et al. (2012) NADPH oxidase NOX2 defines a new antagonistic role for reactive oxygen species and cAMP/PKA in the regulation of insulin secretion. Diabetes 61:2842-2850
[40] Newsholme P, Rebelato E, Abdulkader F, Krause M, Carpinelli A, Curi R (2012) Reactive oxygen and nitrogen species generation, antioxidant defenses, and β-cell function: a critical role for amino acids. J Endocrinol 214:11-20
[41] Gerber PA, Rutter GA (2017) The role of oxidative stress and hypoxia in pancreatic beta-cell dysfunction in diabetes mellitus. Antioxidants & redox signaling 26:501-518
[42] Alfar EA, Kirova D, Konantz J, Birke S, Mansfeld J, Ninov N (2017) Distinct levels of reactive oxygen species coordinate metabolic activity with beta-cell mass plasticity. Scientific Reports 7:3994
[43] Graciano MF, Valle M, Kowluru A, Curi R, Carpinelli A (2011) Regulation of insulin secretion and reactive oxygen species production by free fatty acids in pancreatic islets. Islets 3:213-223
[44] Yagishita Y, Fukutomi T, Sugawara A, et al. (2014) Nrf2 protects pancreatic beta-cells from oxidative and nitrosative stress in diabetic model mice. Diabetes 63:605-618
[45] Pi J, Zhang Q, Fu J, et al. (2010) ROS signaling, oxidative stress and Nrf2 in pancreatic beta-cell function. Toxicol Appl Pharmacol 244:77-83
[46] Guichard C, Moreau R, Pessayre D, Epperson TK, Krause KH (2008) NOX family NADPH oxidases in liver and in pancreatic islets: a role in the metabolic syndrome and diabetes? Biochem Soc Trans 36:920-929
[47] Nakayama M, Inoguchi T, Sonta T, et al. (2005) Increased expression of NAD (P) H oxidase in islets of animal models of Type 2 diabetes and its improvement by an AT1 receptor antagonist. Biochem Biophys Res Commun 332:927-933
[48] Robertson RP, Zhou H, Zhang T, Harmon JS (2007) Chronic oxidative stress as a mechanism for glucose toxicity of the beta cell in type 2 diabetes. Cell Biochem Biophys 48:139-146
[49] Sakuraba H, Mizukami H, Yagihashi N, Wada R, Hanyu C, Yagihashi S (2002) Reduced beta-cell mass and expression of oxidative stress-related DNA damage in the islet of Japanese Type II diabetic patients. Diabetologia 45:85-96
[50] Li N, Li B, Brun T, et al. (2012) NADPH oxidase NOX2 defines a new antagonistic role for reactive oxygen species and cAMP/PKA in the regulation of insulin secretion. Diabetes 61:2842-2850
[51] Nakayama M, Inoguchi T, Sonta T, et al. (2005) Increased expression of NAD (P) H oxidase in islets of animal models of Type 2 diabetes and its improvement by an AT1 receptor antagonist. Biochem Biophys Res Commun 332:927-933
[52] Hansen L, Pedersen O (2005) Genetics of type 2 diabetes mellitus: status and perspectives. Diabetes, Obesity and Metabolism 7:122-135
[53] King A, Bowe J (2016) Animal models for diabetes: understanding the pathogenesis and finding new treatments. Biochem Pharmacol 99:1-10
[54] Al-Awar A, Kupai K, Veszelka M, et al. (2016) Experimental diabetes mellitus in different animal models. Journal of diabetes research 2016
[55] Glastras SJ, Chen H, Teh R, et al. (2016) Mouse models of diabetes, obesity and related kidney disease. PloS one 11:e0162131
[56] Barrett P, Mercer JG, Morgan PJ (2016) Preclinical models for obesity research. Dis Model Mech 9:1245-1255

[57] Williams LM, Campbell FM, Drew JE, et al. (2014) The development of diet-induced obesity and glucose intolerance in C57BL/6 mice on a high-fat diet consists of distinct phases. PLoS One 9:e106159
[58] Buettner R, Schölmerich J, Bollheimer LC (2007) High-fat diets: modeling the metabolic disorders of human obesity in rodents. Obesity 15:798-808
[59] Sampath S, Karundevi B (2014) Effect of troxerutin on insulin signaling molecules in the gastrocnemius muscle of high fat and sucrose-induced type-2 diabetic adult male rat. Mol Cell Biochem 395:11-27
[60] Burchfield JG, Kebede MA, Meoli CC, et al. (2018) High dietary fat and sucrose results in an extensive and time-dependent deterioration in health of multiple physiological systems in mice. J Biol Chem 293:5731-5745
[61] Pennington KA, van der Walt N, Pollock KE, Talton OO, Schulz LC (2017) Effects of acute exposure to a high-fat, high-sucrose diet on gestational glucose tolerance and subsequent maternal health in mice. Biol Reprod 96:435-445
[62] King A (2017) Animal Models of Type 1 and Type 2 Diabetes Mellitus. In: Anonymous Animal Models for the Study of Human Disease (Second Edition). Elsevier, pp. 245-265
[63] Wang B, Charukeshi Chandrasekera P, J Pippin J (2014) Leptin-and leptin receptor-deficient rodent models: relevance for human type 2 diabetes. Current diabetes reviews 10:131-145
[64] Katsuda Y, Ohta T, Shinohara M, Bin T, Yamada T (2013) Diabetic mouse models. Open Journal of Animal Sciences 3:334
[65] Ellenbroek JH, Töns HA, de Graaf N, et al. (2013) Topologically heterogeneous beta cell adaptation in response to high-fat diet in mice. PLoS One 8:e56922
[66] http://columbiasurgery.org/pancreas/pancreas-and-its-functions.
[67] Li R, Yu L, Zhang X, Zhou X, Wang M, Zhao H (2015) Distribution of islet hormones in human adult pancreatic ducts. Digestion 91:174-179
[68] Steiner DJ, Kim A, Miller K, Hara M (2010) Pancreatic islet plasticity: interspecies comparison of islet architecture and composition. Islets 2:135-145
[69] Li N, Yang Z, Li Q, et al. (2018) Ablation of somatostatin cells leads to impaired pancreatic islet function and neonatal death in rodents. Cell death & disease 9:682
[70] Zhu S, Russ HA, Wang X, et al. (2016) Human pancreatic beta-like cells converted from fibroblasts. Nature communications 7:10080
[71] Zhu S, Russ HA, Wang X, et al. (2016) Human pancreatic beta-like cells converted from fibroblasts. Nature communications 7
[72] Kobayashi M, Yamato E, Tanabe K, Tashiro F, Miyazaki S, Miyazaki J (2016) Functional Analysis of Novel Candidate Regulators of Insulin Secretion in the MIN6 Mouse Pancreatic β Cell Line. PloS one 11:e0151927
[73] Asfari M, Janjic D, Meda P, Li G, Halban PA, Wollheim CB (1992) Establishment of 2-mercaptoethanol-dependent differentiated insulin-secreting cell lines. Endocrinology 130:167-178
[74] Hohmeier HE, Mulder H, Chen G, Henkel-Rieger R, Prentki M, Newgard CB (2000) Isolation of INS-1-derived cell lines with robust ATP-sensitive K+ channel-dependent and -independent glucose-stimulated insulin secretion. Diabetes 49:424-430
[75] Skelin M, Rupnik M, Cencic A (2010) Pancreatic beta cell lines and their applications in diabetes mellitus research. ALTEX 27:105-113

[76] McCluskey JT, Hamid M, Guo-Parke H, McClenaghan NH, Gomis R, Flatt PR (2011) Development and functional characterization of insulin-releasing human pancreatic beta cell lines produced by electrofusion. J Biol Chem 286:21982-21992
[77] Hectors TL, Vanparys C, Pereira-Fernandes A, Martens GA, Blust R (2013) Evaluation of the INS-1 832/13 cell line as a beta-cell based screening system to assess pollutant effects on beta-cell function. PloS one 8:e6003
[78] Zawalich WS, Zawalich KC (1996) Regulation of insulin secretion by phospholipase C. Am J Physiol 271:E409-16
[79] Jensen PB, Knop FK, Chen G, Hohmeier HE, Mulder H, Newgard CB (2001) Identification of genes involved in glucose-stimulated insulin secretion. DIABETES-NEW YORK- 50:S134-S134
[80] Meda P, Schuit F (2013) Glucose-stimulated insulin secretion: the hierarchy of its multiple cellular and subcellular mechanisms. Diabetologia 56:2552-2555
[81] Komatsu M, Takei M, Ishii H, Sato Y (2013) Glucose-stimulated insulin secretion: A newer perspective. Journal of diabetes investigation 4:511-516
[82] Nüsslein-Volhard C, Wieschaus E (1980) Mutations affecting segment number and polarity in Drosophila. Nature 287:795
[83] Silapunt S, Chen L, Migden MR (2016) Hedgehog pathway inhibition in advanced basal cell carcinoma: latest evidence and clinical usefulness. Therapeutic advances in medical oncology 8:375-382
[84] Bishop B, Aricescu AR, Harlos K, O'Callaghan CA, Jones EY, Siebold C (2009) Structural insights into hedgehog ligand sequestration by the human hedgehog-interacting protein HHIP. Nature structural & molecular biology 16:698-703
[85] Olsen CL, Hsu P, Glienke J, Rubanyi GM, Brooks AR (2004) Hedgehog-interacting protein is highly expressed in endothelial cells but down-regulated during angiogenesis and in several human tumors. BMC Cancer 4:1
[86] Hibsher D, Epshtein A, Oren N, Landsman L (2016) Pancreatic mesenchyme regulates islet cellular composition in a patched/hedgehog-dependent manner. Scientific reports 6:38008
[87] Low JA, de Sauvage FJ (2010) Clinical experience with Hedgehog pathway inhibitors. Journal of Clinical Oncology 28:5321-5326
[88] Kawahira H, Ma NH, Tzanakakis ES, McMahon AP, Chuang PT, Hebrok M (2003) Combined activities of hedgehog signaling inhibitors regulate pancreas development. Development 130:4871-4879[81] Lau J, Kawahira H, Hebrok M (2006) Hedgehog signaling in pancreas development and disease. Cellular and Molecular Life Sciences CMLS 63:642-652
[89] Carballo GB, Honorato JR, de Lopes, Giselle Pinto Farias (2018) A highlight on Sonic hedgehog pathway. Cell Communication and Signaling 16:11
[90] Lau J, Kawahira H, Hebrok M (2006) Hedgehog signaling in pancreas development and disease. Cellular and Molecular Life Sciences CMLS 63:642-652
[91] Hebrok M, Kim SK, St Jacques B, McMahon AP, Melton DA (2000) Regulation of pancreas development by hedgehog signaling. Development 127:4905-4913
[92] Gupta S, Takebe N, LoRusso P (2010) Targeting the Hedgehog pathway in cancer. Therapeutic advances in medical oncology 2:237-250
[93] Rubin LL, de Sauvage FJ (2006) Targeting the Hedgehog pathway in cancer. Nature reviews Drug discovery 5:1026

[94] Hooper JE, Scott MP (2005) Communicating with hedgehogs. Nature reviews Molecular cell biology 6:306
[95] Liu Y, Cao X, Jiang J, Jia J (2007) Fused-Costal2 protein complex regulates Hedgehog-induced Smo phosphorylation and cell-surface accumulation. Genes Dev 21:1949-1963
[96] Chamoun Z, Mann RK, Nellen D, et al. (2001) Skinny hedgehog, an acyltransferase required for palmitoylation and activity of the hedgehog signal. Science 293:2080-2084
[97] Gallet A, Rodriguez R, Ruel L, Therond PP (2003) Cholesterol modification of hedgehog is required for trafficking and movement, revealing an asymmetric cellular response to hedgehog. Developmental cell 4:191-204
[98] Ingham PW, McMahon AP (2001) Hedgehog signaling in animal development: paradigms and principles. Genes Dev 15:3059-3087
[99] Briscoe J, Thérond PP (2013) The mechanisms of Hedgehog signalling and its roles in development and disease. Nature reviews Molecular cell biology 14:416
[100] Panáková D, Sprong H, Marois E, Thiele C, Eaton S (2005) Lipoprotein particles are required for Hedgehog and Wingless signalling. Nature 435:58
[101] Bolanos-Garcia VM, Miguel RN (2003) On the structure and function of apolipoproteins: more than a family of lipid-binding proteins. Prog Biophys Mol Biol 83:47-68
[102] Olofsson SO, Asp L, Boren J (1999) The assembly and secretion of apolipoprotein B-containing lipoproteins. Curr Opin Lipidol 10:341-346
[103] Eugster C, Panáková D, Mahmoud A, Eaton S (2007) Lipoprotein-heparan sulfate interactions in the Hh pathway. Developmental cell 13:57-71
[104] Jia J, Tong C, Jiang J (2003) Smoothened transduces Hedgehog signal by physically interacting with Costal2/Fused complex through its C-terminal tail. Genes Dev 17:2709-2720
[105] Hebrok M (2003) Hedgehog signaling in pancreas development. Mech Dev 120:45-57
[106] Klieser E, Swierczynski S, Mayr C, et al. (2016) Differential role of Hedgehog signaling in human pancreatic (patho-) physiology: An up to date review. World J Gastrointest Pathophysiol 7:199-210
[107] Apelqvist Å, Ahlgren U, Edlund H (1997) Sonic hedgehog directs specialised mesoderm differentiation in the intestine and pancreas. Current Biology 7:801-804
[108] di Magliano MP, Hebrok M (2003) Hedgehog signalling in cancer formation and maintenance. Nature Reviews Cancer 3:903-911
[109] Kawahira H, Scheel DW, Smith SB, German MS, Hebrok M (2005) Hedgehog signaling regulates expansion of pancreatic epithelial cells. Dev Biol 280:111-121
[110] Kayed H, Kleeff J, Esposito I, et al. (2005) Localization of the human hedgehog-interacting protein (Hip) in the normal and diseased pancreas. Molecular Carcinogenesis: Published in cooperation with the University of Texas MD Anderson Cancer Center 42:183-192
[111] Yao Z, Han L, Chen Y, et al. (2018) Hedgehog signalling in the tumourigenesis and metastasis of osteosarcoma, and its potential value in the clinical therapy of osteosarcoma. Cell death & disease 9:701
[112] Chuang PT, Kawcak T, McMahon AP (2003) Feedback control of mammalian Hedgehog signaling by the Hedgehog-binding protein, Hip1, modulates Fgf signaling during branching morphogenesis of the lung. Genes Dev 17:342-347

[113] Tada M, Kanai F, Tanaka Y, et al. (2008) Down-regulation of hedgehog-interacting protein through genetic and epigenetic alterations in human hepatocellular carcinoma. Clin Cancer Res 14:3768-3776
[114] Bak M, Hansen C, Friis Henriksen K, Tommerup N (2001) The human hedgehog-interacting protein gene: structure and chromosome mapping to 4q31.21-->q31.3. Cytogenet Cell Genet 92:300-303
[115] Chuang P, McMahon AP (1999) Vertebrate Hedgehog signalling modulated by induction of a Hedgehog-binding protein. Nature 397:617
[116] Nielsen SK, Møllgård K, Clement CA, et al. (2008) Characterization of primary cilia and Hedgehog signaling during development of the human pancreas and in human pancreatic duct cancer cell lines. Developmental dynamics: an official publication of the American Association of Anatomists 237:2039-2052
[117] Kayed H, Kleeff J, Osman T, Keleg S, Büchler MW, Friess H (2006) Hedgehog signaling in the normal and diseased pancreas. Pancreas 32:119-129
[118] Thomas MK, Rastalsky N, Lee JH, Habener JF (2000) Hedgehog signaling regulation of insulin production by pancreatic beta-cells. Diabetes 49:2039-2047
[119] Thomas MK, Lee JH, Rastalsky N, Habener JF (2001) Hedgehog Signaling Regulation of Homeodomain Protein Islet Duodenum Homeobox-1 Expression in Pancreatic β-Cells 1. Endocrinology 142:1033-1040
[120] Bailey JM, Mohr AM, Hollingsworth MA (2009) Sonic hedgehog paracrine signaling regulates metastasis and lymphangiogenesis in pancreatic cancer. Oncogene 28:3513
[121] Ma X, Sheng T, Zhang Y, et al. (2006) Hedgehog signaling is activated in subsets of esophageal cancers. International journal of cancer 118:139-148
[122] Umeda H, Ozaki N, Mizutani N, et al. (2010) Protective effect of hedgehog signaling on cytokine-induced cytotoxicity in pancreatic beta-cells. Exp Clin Endocrinol Diabetes 118:692-698
[123] http://diabetes.wisc.edu/search.ph
[124] Evangelista M, Tian H, de Sauvage FJ (2006) The hedgehog signaling pathway in cancer. Clin Cancer Res 12:5924-5928
[125] Smelkinson M (2017) The Hedgehog signaling pathway emerges as a pathogenic target. Journal of developmental biology 5:14
[126] Petrova R, Joyner AL (2014) Roles for Hedgehog signaling in adult organ homeostasis and repair. Development 141:3445-3457
[127] Zhao X, Chang S, Liao M, et al. (2018) Hedgehog Interacting Protein Promotes Fibrosis and Apoptosis in Glomerular Endothelial Cells in Murine Diabetes. Scientific reports 8:5958
[128] Zhao X, Liao M, Chang S, et al. (2014) Maternal diabetes modulates kidney formation in murine progeny: the role of hedgehog interacting protein (HHIP). Diabetologia 57:1986-1996
[129] Aliou Y, Liao M, Zhao X, et al. (2016) Post-weaning high-fat diet accelerates kidney injury, but not hypertension programmed by maternal diabetes. Pediatr Res 79:416
[130] Jacqueminet S, Briaud I, Rouault C, Reach G, Poitout V (2000) Inhibition of insulin gene expression by long-term exposure of pancreatic β cells to palmitate is dependent on the presence of a stimulatory glucose concentration. Metab Clin Exp 49:532-536
[131] Soucy-Faulkner A, Mukawera E, Fink K, et al. (2010) Requirement of NOX2 and reactive oxygen species for efficient RIG-I-mediated antiviral response through regulation of MAVS expression. PLoS pathogens 6:e1000930

[132] Dakin RS, Walker BR, Seckl JR, Hadoke PW, Drake AJ (2015) Estrogens protect male mice from obesity complications and influence glucocorticoid metabolism. Int J Obes 39:1539
[133] Handgraaf S, Riant E, Fabre A, et al. (2013) Prevention of obesity and insulin resistance by estrogens requires ERalpha activation function-2 (ERalphaAF-2), whereas ERalphaAF-1 is dispensable. Diabetes 62:4098-4108
[134] Pettersson US, Waldén TB, Carlsson P, Jansson L, Phillipson M (2012) Female mice are protected against high-fat diet induced metabolic syndrome and increase the regulatory T cell population in adipose tissue. PloS one 7:e46057
[135] Barros RP, Gustafsson J (2011) Estrogen receptors and the metabolic network. Cell metabolism 14:289-299
[136] Shi H, Clegg D (2009) Sex differences in the regulation of body weight. Physiol Behav 97:199-204
[137] Kennedy AJ, Webb CD, Hill AA, Gruen ML, Jackson LG, Hasty AH (2013) Loss of CCR5 results in glucose intolerance in diet-induced obese mice. American Journal of Physiology-Heart and Circulatory Physiology
[138] Escribano O, Beneit N, Rubio-Longas C, Lopez-Pastor A, Gomez-Hernandez A (2017) The role of insulin receptor isoforms in diabetes and its metabolic and vascular complications. Journal of diabetes research 2017
[139] Foti D, Chiefari E, Fedele M, et al. (2005) Lack of the architectural factor HMGA1 causes insulin resistance and diabetes in humans and mice. Nat Med 11:765
[140] Whitehead JP, Humphreys P, Krook A, et al. (1998) Molecular scanning of the insulin receptor substrate 1 gene in subjects with severe insulin resistance: detection and functional analysis of a naturally occurring mutation in a YMXM motif. Diabetes 47:837-839
[141] Taylor SI, Accili D, Imai Y (1994) Insulin resistance or insulin deficiency. Which is the primary cause of NIDDM? Diabetes 43:735-740
[142] Salimi M, Zardooz H, Khodagholi F, Rostamkhani F, Shaerzadeh F (2016) High-fat diet with stress impaired islets' insulin secretion by reducing plasma estradiol and pancreatic GLUT2 protein levels in rats' proestrus phase. J Physiol Pharmacol 67:653-666
[143] Thorens B (2015) GLUT2, glucose sensing and glucose homeostasis. Diabetologia 58:221-232
[144] Gupta D, Jetton TL, LaRock K, et al. (2017) Temporal characterization of beta cell-adaptive and -maladaptive mechanisms during chronic high-fat feeding in C57BL/6NTac mice. J Biol Chem 292:12449-12459
[145] Mosser RE, Maulis MF, Moullé VS, et al. (2015) High fat diet-induced beta cell proliferation occurs prior to insulin resistance in C57Bl/6J male mice. American Journal of Physiology-Heart and Circulatory Physiology
[146] Golson ML, Misfeldt AA, Kopsombut UG, Petersen CP, Gannon M (2010) High Fat Diet Regulation of beta-Cell Proliferation and beta-Cell Mass. Open Endocrinol J 4:10.2174/1874216501004010066
[147] Peyot ML, Pepin E, Lamontagne J, et al. (2010) Beta-cell failure in diet-induced obese mice stratified according to body weight gain: secretory dysfunction and altered islet lipid metabolism without steatosis or reduced beta-cell mass. Diabetes 59:2178-2187
[148] Ahrén J, Ahrén B, Wierup N (2010) Increased β-cell volume in mice fed a high-fat diet: a dynamic study over 12 months. Islets 2:353-356
[149] Striegel DA, Hara M, Periwal V (2015) The beta cell in its cluster: stochastic graphs of beta cell connectivity in the islets of Langerhans. PLoS computational biology 11:e1004423

[150] Huang H, Stehno-Bittel L (2015) Differences in insulin biosynthesis pathway between small and large islets do not correspond to insulin secretion. Islets 7:e1129097
[151] Fujita Y, Takita M, Shimoda M, et al. (2011) Large human islets secrete less insulin per islet equivalent than smaller islets in vitro. Islets 3:1-5
[152] Huang H, Novikova L, Williams SJ, Smirnova IV, Stehno-Bittel L (2011) Low insulin content of large islet population is present in situ and in isolated islets. Islets 3:6-13
[153] Farhat B, Almelkar A, Ramachandran K, et al. (2013) Small human islets comprised of more β-cells with higher insulin content than large islets. Islets 5:87-94
[154] Landsman L, Parent A, Hebrok M (2011) Elevated Hedgehog/Gli signaling causes beta-cell dedifferentiation in mice. Proc Natl Acad Sci U S A 108:17010-17015
[155] Thomas MK, Rastalsky N, Lee JH, Habener JF (2000) Hedgehog signaling regulation of insulin production by pancreatic beta-cells. Diabetes 49:2039-2047
[156] Beaudry JL, D'souza AM, Teich T, Tsushima R, Riddell MC (2013) Exogenous glucocorticoids and a high-fat diet cause severe hyperglycemia and hyperinsulinemia and limit islet glucose responsiveness in young male Sprague-Dawley rats. Endocrinology 154:3197-3208
[157] Ahrén J, Ahrén B, Wierup N (2010) Increased β-cell volume in mice fed a high-fat diet: a dynamic study over 12 months. Islets 2:353-356
[158] Nie D, Wu Q, Zheng P, et al. (2016) Endothelial microparticles carrying hedgehog-interacting protein induce continuous endothelial damage in the pathogenesis of acute graft-versus-host disease. American Journal of Physiology-Cell Physiology
[159] Zeng X, Goetz JA, Suber LM, Scott Jr WJ, Schreiner CM, Robbins DJ (2001) A freely diffusible form of Sonic hedgehog mediates long-range signalling. Nature 411:716
[160] Ježek P, Dlasková A, Plecitá-Hlavatá L (2012) Redox homeostasis in pancreatic cells. Oxidative medicine and cellular longevity 2012
[161] Kajimoto Y, Kaneto H (2004) Role of oxidative stress in pancreatic β-cell dysfunction. In: Anonymous Mitochondrial Pathogenesis. Springer, pp. 168-176
[162] Kusano KF, Pola R, Murayama T, et al. (2005) Sonic hedgehog myocardial gene therapy: tissue repair through transient reconstitution of embryonic signaling. Nat Med 11:1197
[163] Sacedon R, Diez B, Nunez V, et al. (2005) Sonic hedgehog is produced by follicular dendritic cells and protects germinal center B cells from apoptosis. J Immunol 174:1456-1461
[164] Bedard K, Krause K (2007) The NOX family of ROS-generating NADPH oxidases: physiology and pathophysiology. Physiol Rev 87:245-313
[165] Marchetti P, Lupi R, Lorenzetti M, et al. (1998) Pancreatic glucagon damages isolated human islet function. 2:397
[166] de Souza AH, Santos LR, Roma LP, Bensellam M, Carpinelli AR, Jonas J (2017) NADPH oxidase-2 does not contribute to β-cell glucotoxicity in cultured pancreatic islets from C57BL/6J mice. Mol Cell Endocrinol 439:354-362[167] Bleyer A (2014) Urine output and residual kidney function in kidney failure.
[168] https://www.medicalnewstoday.com/articles/305488.php.
[169] https://www.kidney.org/atoz/content/gfr.
[170] George C, Mogueo A, Okpechi I, Echouffo-Tcheugui JB, Kengne AP (2017) Chronic kidney disease in low-income to middle-income countries: the case for increased screening. BMJ Glob Health 2:e000256-2016-000256. eCollection 2017

[171] Jha V, Garcia-Garcia G, Iseki K, et al. (2013) Chronic kidney disease: global dimension and perspectives. The Lancet 382:260-272
[172] Liyanage T, Ninomiya T, Jha V, et al. (2015) Worldwide access to treatment for end-stage kidney disease: a systematic review. The Lancet 385:1975-1982
[173] Ayodele OE, Alebiosu CO (2010) Burden of chronic kidney disease: an international perspective. Advances in chronic kidney disease 17:215-224
[174] Jao T, Nangaku M, Wu C, et al. (2019) ATF6α downregulation of PPARα promotes lipotoxicity-induced tubulointerstitial fibrosis. Kidney Int
[175] Liu B, Tang T, Lv L, Lan H (2018) Renal tubule injury: a driving force toward chronic kidney disease. Kidney Int 93:568-579
[176] Kang HM, Ahn SH, Choi P, et al. (2015) Defective fatty acid oxidation in renal tubular epithelial cells has a key role in kidney fibrosis development. Nat Med 21:37
[177] Ross M (2015) Defective fatty acid oxidation in renal tubular epithelial cells has a key role in kidney fibrosis development. Kidney Int 87:490-491
[178] Obajdin J, Cotter M, Snelling S, et al. (2018) Fatty-acid binding protein 4 (FABP4) as a potential preclinical biomarker of drug-induced kidney injury. Toxicological Sciences 166:441-450
[179] Furuhashi M, Saitoh S, Shimamoto K, Miura T (2014) Fatty acid-binding protein 4 (FABP4): pathophysiological insights and potent clinical biomarker of metabolic and cardiovascular diseases. Clinical Medicine Insights: Cardiology 8:CMC. S17067
[180] Furuhashi M, Saitoh S, Shimamoto K, Miura T (2014) Fatty acid-binding protein 4 (FABP4): pathophysiological insights and potent clinical biomarker of metabolic and cardiovascular diseases. Clinical Medicine Insights: Cardiology 8:CMC. S17067
[181] Okazaki Y, Furuhashi M, Tanaka M, et al. (2014) Urinary excretion of fatty acid-binding protein 4 is associated with albuminuria and renal dysfunction. PLoS One 9:e115429
[182] Lo CS, Chang SY, Chenier I, et al. (2012) Heterogeneous nuclear ribonucleoprotein F suppresses angiotensinogen gene expression and attenuates hypertension and kidney injury in diabetic mice. Diabetes 61:2597-2608
[183] Abdo S, Lo C, Chenier I, et al. (2013) Heterogeneous nuclear ribonucleoproteins F and K mediate insulin inhibition of renal angiotensinogen gene expression and prevention of hypertension and kidney injury in diabetic mice. Diabetologia 56:1649-1660
[184] Ghosh A, Abdo S, Zhao S, et al. (2017) Insulin inhibits Nrf2 gene expression via heterogeneous nuclear ribonucleoprotein F/K in diabetic mice. Endocrinology 158:903-919
[185] Ghosh A, Zhao S, Lo C, et al. (2019) Heterogeneous Nuclear Ribonucleoprotein F Mediates Insulin Inhibition of Bcl2-Modifying Factor Expression and Tubulopathy in Diabetic Kidney. Scientific reports 9:6687
[186] Glastras SJ, Chen H, Tsang M, et al. (2017) The renal consequences of maternal obesity in offspring are overwhelmed by postnatal high fat diet. PLoS One 12:e0172644
[187] Ma S, Zhu X, Eirin A, et al. (2016) Perirenal fat promotes renal arterial endothelial dysfunction in obese swine through tumor necrosis factor-α. J Urol 195:1152-1159
[188] Ricci MA, Scavizzi M, Ministrini S, De Vuono S, Pucci G, Lupattelli G (2018) Morbid obesity and hypertension: The role of perirenal fat. The Journal of Clinical Hypertension 20:1430-1437
[189] Chughtai HL, Morgan TM, Rocco M, et al. (2010) Renal sinus fat and poor blood pressure control in middle-aged and elderly individuals at risk for cardiovascular events. Hypertension 56:901-906

[190] De Pergola G, Campobasso N, Nardecchia A, et al. (2015) Para-and perirenal ultrasonographic fat thickness is associated with 24-hours mean diastolic blood pressure levels in overweight and obese subjects. BMC cardiovascular disorders 15:108
[191] Fernández-Sánchez A, Madrigal-Santillán E, Bautista M, et al. (2011) Inflammation, oxidative stress, and obesity. International journal of molecular sciences 12:3117-3132
[192] Chang J, Gurley SB (2012) Assessment of diabetic nephropathy in the Akita mouse. In: Anonymous Animal Models in Diabetes Research. Springer, pp. 17-29
[193] Tesch GH, Lim AK (2010) Recent insights into diabetic renal injury from the db/db mouse model of type 2 diabetic nephropathy. American Journal of Physiology-Renal Physiology 300:F301-F310
[194] Matsushita K, Takasu S, Kuroda K, et al. (2018) Mechanisms Underlying Exacerbation of Osmotic Nephrosis Caused by Pre-existing Kidney Injury. Toxicological Sciences 165:420-430
[195] Kiss N, Hamar P (2016) Histopathological evaluation of contrast-induced acute kidney injury rodent models. BioMed research international 2016
[196] Dickenmann M, Oettl T, Mihatsch MJ (2008) Osmotic nephrosis: acute kidney injury with accumulation of proximal tubular lysosomes due to administration of exogenous solutes. American Journal of Kidney Diseases 51:491-503
[197] Chowdhury S, Lecomte V, Erlich J, Maloney C, Morris M (2016) Paternal high fat diet in rats leads to renal accumulation of lipid and tubular changes in adult offspring. Nutrients 8:521
[198] Yang P, Xiao Y, Luo X, et al. (2017) Inflammatory stress promotes the development of obesity-related chronic kidney disease via CD36 in mice. J Lipid Res 58:1417-1427
[199] Cabre A, Lazaro I, Girona J, et al. (2007) Fatty acid binding protein 4 is increased in metabolic syndrome and with thiazolidinedione treatment in diabetic patients. Atherosclerosis 195:e150-e158
[200] Trojnar M, Patro-Małysza J, Kimber-Trojnar Ż, Leszczyńska-Gorzelak B, Mosiewicz J (2019) Associations between Fatty Acid-Binding Protein 4–A Proinflammatory Adipokine and Insulin Resistance, Gestational and Type 2 Diabetes Mellitus. Cells 8:227
[201] Yeung DC, Xu A, Tso AW, et al. (2009) Circulating levels of adipocyte and epidermal fatty acid-binding proteins in relation to nephropathy staging and macrovascular complications in type 2 diabetic patients. Diabetes Care 32:132-134
[202] Diabetes Canada Clinical Practice Guidelines Expert Committee, Punthakee Z, Goldenberg R, Katz P (2018) Definition, Classification and Diagnosis of Diabetes, Prediabetes and Metabolic Syndrome. Can J Diabetes 42 Suppl 1:S10-S15
[203] Goldenberg R, Punthakee Z (2013) Definition, classification and diagnosis of diabetes, prediabetes and metabolic syndrome. Canadian journal of diabetes 37:S8-S11
[204] Wang S, Ma W, Yuan Z, et al. (2016) Association between obesity indices and type 2 diabetes mellitus among middle-aged and elderly people in Jinan, China: a cross-sectional study. BMJ Open 6:e012742-2016-012742
[205] Al-Goblan AS, Al-Alfi MA, Khan MZ (2014) Mechanism linking diabetes mellitus and obesity. Diabetes Metab Syndr Obes 7:587-591
[206] Lascar N, Brown J, Pattison H, Barnett AH, Bailey CJ, Bellary S (2018) Type 2 diabetes in adolescents and young adults. The Lancet Diabetes & Endocrinology 6:69-80
[207] Xu G, Liu B, Sun Y, et al. (2018) Prevalence of diagnosed type 1 and type 2 diabetes among US adults in 2016 and 2017: population based study. BMJ 362:k1497

[208] Guillausseau P, Meas T, Virally M, Laloi-Michelin M, Médeau V, Kevorkian J (2008) Abnormalities in insulin secretion in type 2 diabetes mellitus. Diabetes Metab 34:S43-S48
[209] Meas T, GUILLAUSSEAU P (2011) Abnormalities in Insulin Secretion in Type 2 Diabetes Mellitus. Metabolic Syndrome :53
[210] Gonzalez A, Merino B, Marroquí L, et al. (2013) Insulin hypersecretion in islets from diet-induced hyperinsulinemic obese female mice is associated with several functional adaptations in individual β-cells. Endocrinology 154:3515-3524
[211] Rossmeisl M, Rim JS, Koza RA, Kozak LP (2003) Variation in type 2 diabetes--related traits in mouse strains susceptible to diet-induced obesity. Diabetes 52:1958-1966
[212] West DB, Boozer CN, Moody DL, Atkinson RL (1992) Dietary obesity in nine inbred mouse strains. Am J Physiol 262:R1025-32
[213] Barroso I, Gurnell M, Crowley V, et al. (1999) Dominant negative mutations in human PPARγ associated with severe insulin resistance, diabetes mellitus and hypertension. Nature 402:880
[214] King H, Rewers M (1993) Global estimates for prevalence of diabetes mellitus and impaired glucose tolerance in adults. WHO Ad Hoc Diabetes Reporting Group. Diabetes Care 16:157-177
[215] Walston J, Silver K, Bogardus C, et al. (1995) Time of onset of non-insulin-dependent diabetes mellitus and genetic variation in the β3-adrenergic–receptor gene. N Engl J Med 333:343-347
[216] Mykkanen L, Haffner SM, Kuusisto J, Pyorala K, Laakso M (1994) Microalbuminuria precedes the development of NIDDM. Diabetes 43:552-557
[217] Nelson R, Tan M, Beck G, et al. (1999) Changing glomerular filtration with progression from impaired glucose tolerance to type II diabetes mellitus. Diabetologia 42:90-93
[218] Barrière DA, Noll C, Roussy G, et al. (2018) Combination of high-fat/high-fructose diet and low-dose streptozotocin to model long-term type-2 diabetes complications. Scientific reports 8:424
[219] Uil M, Scantlebery AM, Butter LM, et al. (2018) Combining streptozotocin and unilateral nephrectomy is an effective method for inducing experimental diabetic nephropathy in the 'resistant'C57Bl/6J mouse strain. Scientific reports 8:5542
[220] Schlondorff D (2010) Choosing the right mouse model for diabetic nephropathy. Kidney Int 77:749-750
[221] Wicks SE, Nguyen T, Breaux C, Kruger C, Stadler K (2016) Diet-induced obesity and kidney disease–In search of a susceptible mouse model. Biochimie 124:6